

Hulu-Med: A Transparent Generalist Model towards Holistic Medical Vision-Language Understanding

Songtao Jiang^{1,2}, Yuan Wang^{1,2}, Sibo Song³, Tianxiang Hu^{1,2}, Chenyi Zhou¹, Bin Pu⁴, Yan Zhang¹, Zhibo Yang³, Yang Feng⁵, Joey Tianyi Zhou⁶, Jin Hao⁷, Zijian Chen⁸, Ruijia Wu⁹, Tao Tang¹⁰, Junhui Lv¹¹, Hongxia Xu¹¹, Hongwei Wang¹, Jun Xiao¹, Bin Feng², Fudong Zhu², Kenli Li⁴, Weidi Xie^{12,✉}, Jimeng Sun^{8,✉}, Jian Wu^{1,11,✉}, and Zuozhu Liu^{1,2,11,✉}

¹College of Computer Science and Technology, Zhejiang University-University of Illinois Urbana-Champaign Institute, Zhejiang University, Hangzhou 310027, Zhejiang, China.

²Stomatology Hospital, School of Stomatology, Zhejiang University School of Medicine, Zhejiang University, Hangzhou 310016, Zhejiang, China.

³Alibaba Inc, Hangzhou 310023, China.

⁴College of Computer Science and Electronic Engineering, Hunan University, Changsha 410082, China.

⁵Angelalign Technology Inc., Shanghai 200082, China.

⁶CFAR & IHPC, Agency for Science, Technology and Research, 138632, Singapore.

⁷Department of Orthodontics, Shanghai Ninth People's Hospital, College of Stomatology, Shanghai Jiao Tong University School of Medicine, Shanghai 200011, China.

⁸Siebel School of Computing and Data Science, University of Illinois Urbana-Champaign, Urbana, IL 61801, USA.

⁹Antai College of Economics and Management, Shanghai Jiao Tong University, Shanghai 200030, China.

¹⁰China Mobile Group Zhejiang Company Limited, Hangzhou 310016, Zhejiang, China.

¹¹Zhejiang Key Laboratory of Medical Imaging Artificial Intelligence, Haining 314400, Zhejiang, China.

¹²School of Artificial Intelligence, Shanghai Jiao Tong University, Shanghai 200030, China.

✉Corresponding author

ABSTRACT

Real-world clinical decision-making requires integrating heterogeneous data, including medical text, 2D images, 3D volumes, and videos, while existing AI systems fail to unify all these signals, limiting their utility. In this paper, we introduce **Hulu-Med**, a transparent, generalist medical Vision–Language Model (VLM) designed to unify language-only, 2D/3D vision–language, and video understanding within a single architecture. Hulu-Med is trained on a curated corpus of 16.7 million samples, comprising exclusively public or synthetic data, spanning 12 major anatomical systems and 14 medical imaging modalities. Hulu-Med employs a medical-aware token-reduction strategy that prunes redundant visual tokens, achieving up to a 55% reduction for 3D and video inputs, improving cross-modal efficiency, and enabling training at 7B–32B parameter scales in approximately 4,000–40,000 GPU hours. Across 30 public in-domain and out-of-domain medical benchmarks—covering text reasoning, visual question answering, report generation, multilingual dialogue, video understanding, and rare disease diagnosis—**Hulu-Med** surpasses existing open-source models on 27 of 30 benchmarks and outperforms proprietary systems such as GPT-4o on 16 benchmarks. Despite being a VLM, Hulu-Med outperforms GPT-4o and matches GPT-o1 on the text-only HealthBench. For the first time in the community, we provide a fully transparent, reproducible and cost-effective pipeline for holistic medical vision-language understanding by releasing our end-to-end data curation, training procedures, and model parameters. Code and models are available at <https://github.com/ZJUI-AI4H/Hulu-Med>.

Introduction

Clinical decision-making is inherently multimodal, requiring the integration of diverse data sources such as free-text notes, structured records, and visual inputs—including 2D images, 3D scans, and videos—spanning a patient’s care journey^{1,2}. While clinicians must synthesize these signals over time, current healthcare AI systems remain fragmented and task-specific, leading to inefficiencies and missed cross-modal insights^{3,4}. A generalist medical vision–language model (VLM) capable of processing both visual and textual data natively could streamline workflows, reduce diagnostic errors, and extend the reach of multimodal analysis^{1,5–9}.

Despite the rapid advances in general-purpose VLMs, their deployment in the medical sector is impeded by substantial limitations in technical unification and transparency^{10–16}. Current models, which rely heavily on instruction tuning to bridge the pretrained vision and language encoders with image–text pairs, excel in specific tasks but fail to comprehensively cover the full spectrum of clinical needs, for example, language-based tasks such as diagnosis and medical reporting, 2D/3D image analysis in radiology and pathology, complex video analysis in endoscopy and surgery^{17–24}. Moreover, the development of these specialized medical AI tools is often opaque, dominated by proprietary datasets and non-transparent curation processes, which hinder community scrutiny, reproducibility, and, critically, clinical adoption^{25–29}. To overcome these limitations, a new approach is necessary: a unified, multimodal architecture that integrates text, 2D/3D images, and video data with full transparency in its development and training processes^{14,19,30,31}.

In this paper, we present **Hulu-Med**, a generalist medical VLM that achieves holistic multimodal coverage by unifying text, 2D images, 3D volumes, and video understanding within a single architecture ([Fig. 1a](#), [Extended Tab. 1-2](#)). Hulu-Med is built upon three core design principles: **holistic coverage, efficiency at scale**, and **end-to-end transparency**. Hulu-Med is trained on a comprehensive corpus of 16.7 million samples which are sourced from publicly available data and synthesized by us, spanning 12 anatomical systems and 14 medical imaging modalities, including CT, MRI, X-ray, endoscopy, and histopathology, as shown in [Fig. 1b](#), [Extended Tab. 3](#). The corpus integrates 9M medical multimodal samples, 4.9 M medical text samples, 1.3M general multimodal samples, and 1.5M general text samples, balancing domain specialization with broad linguistic and visual competence ([Extended Tab. 4-6](#)). We provide access to our complete pipeline—including a 3-stage training regime (medical alignment, continuous medical pretraining, and mixed modality finetuning), detailed data curation documentation, training code, evaluation scripts, and model weights—to ensure full reproducibility and auditability. This transparent approach facilitates understanding from 2D to complex 3D and video data, enhancing textual reasoning capabilities ([Extended Fig. 1-2](#), [Extended Tab. 7-9](#), [Methods](#))²⁵.

Technically, the model introduces a novel stack that integrates a SigLIP-based vision encoder with two-dimensional rotary position embeddings (2D RoPE)—seamlessly extended to 3D and video data—and a large language model (LLM) decoder through a unified patch-based encoding strategy. This strategy treats visual patches as universal input units across all modalities, eliminating the need for separate encoders. Our architecture supports arbitrary medical image resolutions and spatio-temporal understanding, enabling the flexible combination of LLMs and ViTs for continuous pretraining and eliminating the need for pretrained VLMs. Moreover, we develop a progressive three-stage training curriculum, which scales understanding from 2D images to complex 3D volumes and videos, demonstrates emergent cross-modal generalization. Crucially, to manage the high computational demands typical of medical data processing, we introduce a medical-aware token reduction mechanism that reduces visual tokens by approximately 55%. This significant reduction enhances computational efficiency and supports extended context processing across 3D volumes and videos without compromising data fidelity. Ultimately, Hulu-Med scales efficiently from 7 billion to 32 billion parameters, maintaining exceptional performance with low compute requirements—ranging from 4,000 to 40,000 GPU hours for the largest model variant. This scalability makes advanced medical VLM capabilities more accessible to the broader research community.

We thoroughly evaluate Hulu-Med across 30 public medical benchmarks covering diverse tasks, including language-based reasoning, 2D/3D/video question answering (VQA), medical report generation (MRG), etc. Hulu-Med consistently delivers **leading performance** among open medical and general VLMs, and is highly competitive with proprietary systems across diverse tasks. It demonstrates robust generalization across modalities, anatomies, and task formats, particularly those requiring intensive knowledge and textual reasoning, showing robust generalization on challenging benchmarks for multilingual understanding, rare disease diagnosis, and clinical dialogue. This high performance, achieved with calibrated compute and full transparency, validates the feasibility of a unified, accessible, and high-performing medical generalist model.

Our work makes three key contributions:

1. **Architectural Unification:** We introduce the first medical VLM capable of natively processing text, 2D images, 3D volumes, and video within a single, unified architecture, solving the long-standing challenge of modality-specific encoders.
2. **Efficiency and Transparency:** We provide a fully transparent and highly efficient training pipeline, demonstrating the feasibility of scaling generalist medical VLMs (7B–32B parameters) within realistic, accessible compute budgets. Additionally, the privacy and copyright concerns inherent in proprietary systems can be mitigated, empowering the development of customized trustworthy models.
3. **Strong Performance:** We demonstrate strong performance in 30 public medical benchmarks, encompassing language-based reasoning, 2D/3D/video question answering, report generation, etc. To our knowledge, this represents the first systematic benchmarking of a medical VLM at this scale and diversity. This work marks a significant step toward a holistic understanding of medical data and fostering greater accessibility for the broader community.

Results

Overview of Hulu-Med

Hulu-Med refers to a versatile multimodal model adept at navigating an extensive range of medical tasks, encompassing from answering complex language-only queries, to performing sophisticated analyses involving 2D and 3D medical images, to interpreting long-duration medical videos.

Problem Formulation. Hulu-Med is designed to be a generalist medical VLM capable of processing heterogeneous inputs and generating textual responses for diverse clinical tasks (Fig. 1a). Formally, given a textual instruction \mathbf{t} and optional visual input $\mathbf{v} \in \{\mathbf{v}_{2D}, \mathbf{v}_{3D}, \mathbf{v}_{video}, \emptyset\}$ (where \mathbf{v} can be a 2D image, 3D volume, video sequence, or absent), the model generates a textual response \mathbf{y} as:

$$\mathbf{y} = \Phi([g(f_v(\mathbf{v})); f_t(\mathbf{t})]),$$

where $f_v(\cdot)$ and $f_t(\cdot)$ denote the visual encoder and text tokenizer, respectively, which transform inputs into variable-length sequences of visual tokens $f_v(\mathbf{v}) \in \mathbb{R}^{N_v \times d_v}$ and text tokens $f_t(\mathbf{t}) \in \mathbb{R}^{N_t \times d_t}$, where N_v and N_t represent the number of visual and text tokens, d_v and d_t denote the visual and text feature dimensions, respectively. A projection layer $g(\cdot)$ aligns visual features to the LLM’s embedding space: $g(f_v(\mathbf{v})) \in \mathbb{R}^{N_v \times d}$, where d is the hidden dimension of the language model. The notation $[\cdot; \cdot]$ indicates concatenation along the sequence dimension. The language model decoder $\Phi(\cdot)$ then autoregressively generates responses conditioned on the concatenated token sequence. Critically, when visual input is absent ($\mathbf{v} = \emptyset$), the model seamlessly operates in text-only mode, where text tokens are directly fed into the LLM backbone for autoregressive generation: $\mathbf{y} = \Phi(f_t(\mathbf{t}))$ (Fig. 1b).

This unified formulation enables Hulu-Med to flexibly handle various input configurations: (i) text-only queries for medical knowledge reasoning and clinical dialogue; (ii) vision-language tasks, for example,

medical images/videos with textual instructions for visual question answering, report generation, and diagnostic reasoning; and (iii) interleaved multimodal inputs, where diverse visual modalities (2D images, 3D volumes, videos) and text can be arbitrarily interspersed within a single context. The model’s architecture, as detailed in [Extended Fig. 2](#), encapsulates the ability to integrate and transition between various data modalities and analytical demands within a single, unified system, supporting diverse clinical applications from radiological interpretation to surgical video analysis.

Training Dataset. To support broad generalist capabilities and promote transparency, we curated an unprecedented multimodal dataset of 16.7 million samples—the largest publicly available to our knowledge—compiled from open sources and augmented with synthetic data (see [Extended Fig.1](#); [Extended Tab. 4-6](#)). The corpus comprises 9 million multimodal medical samples, 4.9 million medical text QA pairs, 1.3 million multimodal general samples, and 1.5 million general text QA pairs. The medical subset spans 12 major anatomical systems ([Fig. 1c](#)) and 14 distinct imaging modalities ([Fig. 1d](#)), covering more than 60 specific types and a broad range of clinical tasks ([Extended Tab. 3](#)).

Raw public datasets typically suffer from limited modality coverage, suboptimal alignment between text and visual data, and pronounced long-tail distributions, all of which can hinder both model performance and generalizability. To address these challenges, we developed **five dedicated synthesis pipelines** to generate high-quality, instruction-aligned visual–text pairs. These pipelines encompass: (i) rewriting brief captions into detailed descriptions; (ii) generating novel, long-form medical image captions; (iii) constructing medical VQA pairs; (iv) producing multilingual Chain-of-Thought (CoT) reasoning data; and (v) annotating surgical videos ([Methods](#), [Extended Fig. 1](#)). The resulting synthetic data proved instrumental in the multi-stage training of Hulu-Med.

Model Architecture and Training. Hulu-Med consists of four core components: a rotary position-adaptive visual transformer (ViT) encoder, a multimodal projector, a language tokenizer, and an LLM decoder ([Fig. 1b](#), [Extended Fig. 2](#); for details, see [Methods](#)).

For visual encoding, we adopt image patch as a universal processing unit, that allows 2D images, 3D volumes, and videos to be handled as variable-length patch sequences by a single encoder, obviating the need for modality-specific architectures. In particular, we adapt a pre-trained SigLIP model, enhancing it with 2D RoPE to extend compatibility with 3D and video data^{32,33}. To demonstrate scalability and address varying computational constraints, we developed three model variants: **Hulu-Med-7B**, **Hulu-Med-14B**, and **Hulu-Med-32B**. Their respective LLM decoders were continuously pretrained from Qwen2.5-7B, Qwen3-14B, and Qwen2.5-32B³⁴. To efficiently manage the substantial computational demands imposed by long sequences of 3D and video patches, we devised a medical-aware token reduction strategy that enables holistic and efficient training.

Hulu-Med is trained using a progressive, three-stage curriculum ([Fig. 1e](#)). At Stage-1, the model establishes the medical vision–language alignment, with only the visual encoder and multimodal projector being trained on concise 2D medical image–caption pairs ([Extended Tab. 4](#)). At Stage-2, Hulu-Med undergoes continuous training on large-scale, long-form medical image–caption pairs (2D images), supplemented by mixed general data ([Extended Tab. 5](#)). Stage-3 comprises comprehensive finetuning on an extensive multimodal dataset encompassing both medical and general domains, spanning diverse downstream tasks across text, 2D, 3D, and video modalities ([Extended Tab. 6](#)). Throughout Stage-2 and Stage-3, all model parameters—including the LLM decoder, visual encoder, and multimodal projector—remain fully trainable to maximize performance and generalization. This training curriculum leverages the abundance of 2D data to cultivate robust visual representations, enabling the model to excel on complex 3D and video tasks with comparatively less specialized data.

Evaluation Protocols. We conducted a comprehensive evaluation of Hulu-Med across 30 diverse benchmarks spanning language, 2D and 3D images, and video modalities ([Fig. 1f](#)), rigorously assessing both in-distribution (ID) and out-of-distribution (OOD) tasks to evaluate generalization. Our comparisons en-

compass 46 state-of-the-art models, including leading proprietary systems (e.g., GPT-4.1, Claude Sonnet 4, Gemini-2.5-Flash), large-scale general-purpose vision–language models (e.g., Qwen2.5VL-7B/72B, InternVL3-8B/38B)^{35,36}, medical generalist VLMs (e.g., Lingshu-7B/32B, MedGemma-4B, HuatuoGPT-V-7B/34B), and specialized medical foundation models (e.g., M3D series, RadFM, Surgical-LLaVA)^{22,37,37–40}.

To further probe real-world utility, we also include more comprehensive evaluation for language-only tasks, including multilingual medical understanding (MMedBench), rare disease diagnosis (RareBench), and multi-turn clinical dialogue (HealthBench)^{41–43}. Standard evaluation metrics were employed for each benchmark and task, with detailed protocols provided in the [Methods](#).

Evaluation on 2D Medical Vision–Language Understanding

We systematically evaluated Hulu-Med’s 2D medical image understanding across 11 established benchmarks, comprising seven medical VQA datasets, three MRG benchmarks, and the MedMNIST classification task. Across these benchmarks, Hulu-Med surpassed all open-source models (medical or general) in 10 of 11 benchmarks. It also outperforms the leading proprietary models in 8 benchmarks ([Tab. 1](#), [Fig. 2](#)).

In particular, the VQA suite encompasses multi-modal understanding (OmniMedVQA, PMC-VQA)^{44,45}, modality-specific reasoning (VQA-RAD, SLAKE, PathVQA), advanced clinical reasoning (MedXQA), and knowledge-intensive tasks (MMMU-Med)^{46–49}, as shown in [Tab. 1](#). Hulu-Med-7B/32B set new state-of-the-art performance on the multi-modal understanding and modality-specific reasoning benchmarks, spanning ID and OOD tasks. On MedXQA, Hulu-Med-7B/32B outperformed all open-source VLMs of comparable scale (both below and above 10B parameters), though they remained behind proprietary models (e.g., 34% of Hulu-Med-32B versus 45.2% of GPT-4.1). We attribute this performance gap primarily to the text-based reasoning requirements of MedXQA, which favor models with more powerful LLMs. Similarly, on the knowledge-intensive benchmark (MMMU-Med), Hulu-Med surpassed other medical VLMs and most generalist models, although trailed the strongest open model InternVL-38B, as this benchmark requires extra capabilities like optical character recognition (OCR), which is not a central focus of our architecture. To validate the robustness of these findings, we performed statistical significance tests across three independent runs of Hulu-Med-7B, which demonstrated consistently superior performance ($p < 0.001$ for PMC-VQA, VQA-RAD, and MedXQA; $p < 0.05$ for OmniMedVQA, SLAKE, and PathVQA; [Extended Fig. 3](#)).

On MRG, we assessed Hulu-Med on three standard benchmarks—MIMIC-CXR, CheXpert, and IU X-ray—using both conventional natural language metrics (BLEU, ROUGE, METEOR) and the clinically oriented RaTEScore^{50–53} ([Fig. 2a–b](#)). All Hulu-Med variants established new state-of-the-art results. Notably, as shown in [Fig. 2b](#), Hulu-Med-7B achieved a RaTEScore of 57.0 on MIMIC-CXR, substantially outperforming MedGemma-4B/27B (RaTEScore 51.3). This improvement is clinically meaningful, as MedGemma’s score corresponded to 81% of reports leading to the same or superior clinical decisions as original reports, as assessed by board-certified radiologists⁴⁰. Our results further reveal that larger model size does not guarantee superior MRG performance: Hulu-Med-7B occasionally surpassed its 32B counterpart, mirroring trends observed with MedGemma. This underscores that domain-specific pretraining is paramount for specialized tasks such as MRG, reaffirming the necessity of dedicated medical VLMs.

Hulu-Med’s 2D medical image understanding was further validated on the MedMNIST-2D benchmark, which spans seven distinct domains⁵⁴. Hulu-Med achieved a leading average accuracy exceeding 85%, dramatically outperforming all baselines—including proprietary models such as GPT-4o, which attained less than 40% ([Fig. 2c](#)). Hulu-Med’s robust performance across diverse data modalities and task types—including binary, multi-class, and multi-label classification—further highlights the critical importance of domain-specific medical training.

Evaluation on 3D Medical Vision–Language Understanding

We systematically evaluated Hulu-Med’s 3D medical image understanding on VQA and MRG benchmarks, including M3D, 3D-RAD, and AMOS-MM^{37,55,56}. For comprehensive comparison, we benchmarked our model against both medical foundation models specialized for 3D data (e.g., RadFM, M3D-Llama2/Phi/Mistral) and adapted generalist models (e.g., Lingshu, Qwen2.5-VL). As these generalist models do not natively support 3D volumetric data, we enabled 3D evaluation by slicing each volume into a sequence of images, thus treating it as a multi-image task (Methods).

On 3D VQA tasks, Hulu-Med achieved state-of-the-art performance for both open- and closed-ended question answering (Fig. 3a-b). On the M3D benchmark, which assesses anatomical understanding, Hulu-Med outperformed all specialized 3D models and general-purpose VLMs (Fig. 3a). Hulu-Med further excelled at complex 3D reasoning tasks on the 3D-RAD benchmark (Fig. 3b). The performance advantage was particularly pronounced on challenging tasks requiring multi-step inference, such as problems involving biomarker characteristics (e.g., size, thickness, and shape) and static/longitudinal temporal diagnosis. Hulu-Med-7B exceeded the best baseline by 22.8% on longitudinal temporal diagnosis, a task demanding comprehensive understanding of disease progression across multiple time points. The consistent, superior performance of Hulu-Med across diverse 3D tasks underscores the effectiveness of a unified architecture for the nuanced interpretation of volumetric medical data.

For 3D MRG tasks on the AMOS-MM benchmark, all Hulu-Med variants demonstrated leading performance on conventional natural language generation metrics (BLEU, ROUGE-L) and exhibited clear superiority on the clinically oriented RaTEScore, underscoring the model’s ability to generate comprehensive and clinically accurate radiology reports from volumetric scans (Fig. 3c, Extended Fig. 14, Extended Fig. 19). Their performance on METEOR was also competitive to models trained for MRG on this dataset, validating the effectiveness of our unified training approach.

Evaluation on Medical Video Benchmarks

We evaluated Hulu-Med variants on multi-frame temporal reasoning and surgical video analysis (Methods). As shown in Fig. 3d, for multi-frame temporal reasoning, we assess zero-shot performance on MedFrameQA⁵⁷—i.e., without any task-specific training or fine-tuning. In this OOD setting, Hulu-Med markedly outperforms the leading proprietary models reported in the original study, achieving higher accuracy and lower variance as the number of frames increases (Extended Tab. 8). This stability under growing temporal complexity underscores robust temporal reasoning. The radar plot further illustrates the unified understanding of Hulu-Med across modalities.

In specialized surgical video benchmarks: Cholec80-VQA⁵⁸, EndoVis18-VQA⁵⁹, and PSI-AVA-VQA⁶⁰, Hulu-Med was compared with proprietary systems, general and medical VLMs, and surgical video foundation models (Fig. 3e). It achieves superior accuracy and recall to the video foundation models on Cholec80-VQA and EndoVis18-VQA, and delivers competitive results on PSI-AVA-VQA, given that several baselines are tailored for video data. For VLM baselines lacking reported quantitative metrics, we used ChatGPT-4o-latest as an automated judge, Hulu-Med consistently surpasses all baselines across the three benchmarks (Fig. 3f).

Additionally, the SurgeryVideoQA⁶¹ presents a distinct OOD challenge, drawing on educational video content that integrates medical images, diagrams, and narrative explanations—unlike conventional surgical footage. Here, Hulu-Med-32B led all open-source models, achieving a score of 30.1% and outperforming other specialized medical VLMs such as Lingshu-32B (29.9%), while proprietary models like GPT-4o attained the highest score at 44.8% (Fig. 3g). Overall, Hulu-Med demonstrated competitive performance in this complex, educationally-focused benchmark while maintaining strong advantages on specialized surgical video analysis.

Evaluation on Medical Text-Only Benchmarks

We evaluated Hulu-Med on eight medical text understanding benchmarks, assessing capabilities in complex reasoning, textual comprehension, and medical examination^{49,62-67} (Tab. 2). Additionally, we assessed the model’s generalization capability on challenging real-world tasks including multilingual reasoning (MMedBench), rare disease diagnosis (RareBench), and realistic clinical dialogues (HealthBench)⁴¹⁻⁴³.

State-of-the-art performance among open-source models. Hulu-Med delivered substantial gains over prior open-source systems. Against Lingshu-7B—the strongest medical VLM baseline under 10B parameters—Hulu-Med-7B improves by 10.2 points on MMLU-Pro-Med, 3.1 on MedXQA, 5.3 on Medbullets, 4.8 on SGPQA, 11.7 on MedMCQA, 10.2 on MedQA, and 5.0 on MMLU-Med. For larger models, Hulu-Med-32B similarly surpasses Lingshu-32B with gains of 2.7 points on MMLU-Pro-Med, 3.4 on Medbullets, 6.7 on MedMCQA, and 5.7 on MedQA. Notably, Hulu-Med is competitive even against larger open-source models: Hulu-Med-7B attains an average accuracy of 58.9%, exceeding InternVL3-8B (52.9%) by 6.0 points, while Hulu-Med-32B reaches 65.9%, outperforming InternVL3-38B (60.1%) by 5.8 points. Statistical testing on three independent runs confirms these improvements; Hulu-Med demonstrated superior performance ($p < 0.001$) on seven benchmarks (Extended Fig. 4).

Competitive with proprietary models. Hulu-Med-32B attains state-of-the-art performance on PubMedQA, surpassing proprietary systems including Claude Sonnet 4, DeepSeek-V3, GPT-4.1, and Gemini 2.5 Flash. This strength in biomedical literature comprehension likely reflects the extensive PubMed content used in continuous pretraining (Extended Tab. 1). On complex reasoning benchmarks such as MMLU-Pro-Med, Hulu-Med-32B outperforms Gemini 2.5 Flash and substantially narrows the gap to top-tier models, including Claude Sonnet 4 and GPT-4.1. More broadly, with an average accuracy of 65.9% across eight benchmarks, Hulu-Med-32B exceeds DeepSeek-V3 (59.8%) by 6.1 points and approaches o3-mini (67.9%) within 2.0 points, demonstrating competitive performance overall against proprietary systems.

Performance gap on complex reasoning tasks. On challenging reasoning-intensive benchmarks requiring multi-step clinical reasoning, Hulu-Med substantially narrowed but did not fully close the gap with top-tier proprietary models. On MedXpertQA, Hulu-Med-32B outperformed DeepSeek-V3 but trailed Claude Sonnet 4 by 9.4 points. Similarly, on Medbullets, while exceeding DeepSeek-V3, Hulu-Med-32B remained 11.4 points behind Claude Sonnet 4. The performance gap was most pronounced on MedQA, with an 11.7 point difference from Claude Sonnet 4. These gaps primarily reflect the advantages of larger model capacity and more sophisticated reasoning capabilities in proprietary systems.

Scaling effects with model size. We observed substantial performance improvements with increasing model scale from 7B to 32B parameters across all benchmarks (Tab. 2). The gains were particularly pronounced on reasoning-intensive tasks, with improvements of 4.6 percentage points on MedXQA, 7.3 points on Medbullets, 10.7 points on SGPQA, and 6.9 points on MedQA. This scaling effect indicates that textual reasoning capabilities strongly depend on the capacity of the underlying language model, explaining the remaining performance disparity with even larger-scale proprietary models and suggesting that further scaling combined with enhanced reasoning-focused training represents a promising direction for closing this gap.

Strong generalization to real-world scenarios. Beyond standard benchmarks, we evaluate Hulu-Med on three challenging, real-world tasks. On MMedBench, a multilingual benchmark spanning six languages (English, Chinese, Japanese, French, Russian, Spanish), Hulu-Med-32B attains 75.13% average accuracy, surpassing GPT-4 (74.27%), while Hulu-Med-7B (67.81%) exceeds the prior state-of-the-art, MMed-Llama 3-8B (67.75%) (Fig. 4a). With CoT prompting, Hulu-Med-32B-Thinking reaches 78.41%, outperforming all tested proprietary models, including Gemini 2.5 Flash (77.63%) and Claude Sonnet 4 (76.04%), underscoring strong multilingual reasoning and practical utility.

On HealthBench—which assesses clinical conversation quality and safety using physician-defined

rubrics—Hulu-Med-32B achieves an overall score of 41.6, outperforming general-purpose models such as GPT-4o (32.0) and matching GPT-o1 (Fig. 4b, Extended Tab. 2). Hulu-Med consistently surpasses specialized medical VLMs across all seven conversational themes; notably, Hulu-Med-7B (38.3) more than doubles the scores of HuatuoGPT-Vision-34B (17.2) and Lingshu-7B (15.9).

Finally, on RareBench Task 4, containing 1,114 rare-disease cases (Fig. 4c)—standard Hulu-Med-7B/32B performs modestly on this OOD, long-tail task. However, with explicit CoT prompting (“Please reason step by step”) (Extended Fig. 7), Hulu-Med surpasses all proprietary models in 7 of 8 testing scenarios, indicating strong latent reasoning for complex, low-prevalence conditions.

Analysis of Model Design and Data Curation

To elucidate the principles underlying Hulu-Med’s performance, we conducted a series of analytical studies on model architecture, data composition, data enhancements and training efficiency.

Expert vs. generalist model. To assess the value of a unified multimodal architecture versus specialized systems, we trained five modality-specific models (ultrasound, Optical Coherence Tomography (OCT), fundus, microscopy, dermoscopy). Hulu-Med, trained on a mixed dataset spanning these and additional modalities, consistently outperforms all specialized counterparts (Fig. 5a). These results indicate that a single unified model not only achieves broad competency but also delivers superior cross-modal transfer and understanding.

Data scale and mixture strategy. We next investigated the impact of data scale and mixture composition. Performance on both text and multimodal tasks improved monotonically with training volume, consistent with established scaling laws in LLMs and VLMs^{68,69} (Fig. 5b). Ablations further show that two axes of diversity: domain (medical vs. general) and modality (text-only vs. multimodal), are critical: removing any single component degrades performance (Fig. 5c). Further analysis of the mixing ratios showed optimal performance at a 3:1 medical-to-general and a 1:1 text-to-multimodal balance (Fig. 5d-e). These findings indicate that performance depends not only on scale but also on domain specificity and modality composition, providing practical guidance for future data mixture design.

Effectiveness of synthetic data. Adding synthetically generated long captions increases accuracy on OmniMedVQA (Fig. 5f). Likewise, incorporating generated CoT data boosts both textual and multimodal reasoning (MedXpert-Text, MedXpert-Multimodal), with especially pronounced gains in multimodal settings (Fig. 5g-h). These results indicate that synthetic data provides valuable supervision for complex tasks beyond what public datasets afford.

Token reduction for efficiency. We further validated the medical-aware token reduction strategy for 3D and video inputs. With approximately 55% fewer visual tokens, performance on surgical video benchmarks was effectively unchanged, and degradation on 3D benchmarks (M3D, 3D-RAD) was minimal (Fig. 5i, Extended Fig. 7a-b). This efficiency was critical for practical training: Hulu-Med-7B/32B required roughly 4,100/38,000 GPU-hours on 80G memory GPUs (Extended Fig. 7c), improving accessibility for both academic and industrial use.

Discussion

We present Hulu-Med, the first transparent generalist medical VLM for holistic understanding of medical text, 2D/3D images, and videos. Hulu-Med is trained in a three-stage pipeline with the ever-largest open corpus of 16.7M samples, showing a cost-effective strategy with affordable computing. Hulu-Med’s leading performance across 30 benchmarks, combined with its openness and unified understanding, establishes it as a foundational resource for medical AI.

Superior performance through guaranteed transparency and reproducibility. Hulu-Med was developed exclusively from open-access datasets using a fully transparent workflow, from data curation to model release. Its training corpus is unprecedented in scale and diversity, integrating clinical and

literature data across broader modalities than existing medical VLMs, such as RadFM and Lingshu^{21–23,39} ([Extended Tab. 1](#)). Hulu-Med’s superior performance demonstrates that the systematic consolidation of public data is a viable pathway to state-of-the-art medical VLMs. To ensure full reproducibility and establish a trustworthy foundation for clinical application, we publicly release all data pipelines, training code, and model parameters ([Extended Tab. 5–8, Methods](#)). This open approach mitigates the privacy and copyright risks inherent in proprietary models and private data^{70,71}.

Technical novelty for holistic medical understanding. Hulu-Med introduces the first unified architecture that concurrently achieves state-of-the-art performance across medical text, 2D/3D images and video understanding tasks, as demonstrated by leading results on 30 diverse benchmarks^{14,72,73} ([Extended Tab. 1](#)). This is enabled by three technical designs. First, a unified visual encoding strategy treats all visual patches as universal input units, employing 2D RoPE to natively represent multiple modalities and resolutions as dynamic, variable-length sequences within a single encoder ([Methods](#)). Second, an adaptive token-reduction scheme—combining bilinear interpolation for shorter sequences with medical-aware pruning for longer ones—reduces 3D and video tokens by approximately 55% with minimal accuracy loss, ensuring computational efficiency ([Fig. 5i, Extended Fig. 7](#)). Third, a progressive training curriculum that establishes robust 2D understanding before introducing 3D and video modalities outperforms mixed-modality training, providing a more effective learning pathway ([Extended Fig. 8a](#)). Together, these designs offer a cost-efficient solution for holistic medical understanding, overcoming critical bottlenecks of limited data and high computational cost^{28,74}.

Scalable training recipe. Hulu-Med offers a practical recipe for multimodal medical generalist models, grounded in extensive analysis. Our decoupled architecture—integrating a separate visual encoder with an LLM decoder—provides critical flexibility over methods that merely fine-tune general-purpose VLMs. This modular design facilitates tailored model configurations, allowing state-of-the-art components like Qwen LLMs and specialized ViTs to be matched to specific clinical needs ([Extended Fig. 10](#))^{34,73}. The progressive strategy yields emergent generalization: Hulu-Med-Image-7B, trained solely on 2D data, extrapolates strongly to 3D and video ([Extended Fig. 8b–c](#)), while adding 3D/video in the final stage further improves 2D performance ([Extended Fig. 8d](#)). Detailed benchmarks further validate consistent gains from scaling both data and model size within the same family ([Extended Figs. 6, 9](#)). Together, our approach ensures scalable training and strengthens domain-specific reasoning.

Real-world clinical utility. Hulu-Med demonstrates substantial real-world clinical utility through superior performance on widely used clinical benchmarks ([Tab. 1–2, Fig. 5](#)) and scenario-specific evaluations including HealthBench, MMedBench, and RareBench^{41–43} ([Fig. 4](#)). Extensive case studies across text, 2D/3D images, and video modalities confirm robust understanding and reasoning capabilities ([Extended Fig. 11–12](#)). In 2D/3D medical report generation, Hulu-Med produces more accurate findings with fewer hallucinations than Med-Gemma ([Extended Fig. 13–14](#)), exhibits step-by-step diagnostic reasoning ([Extended Fig. 15–16](#)), and generates detailed surgical video captions ([Extended Fig. 17](#)). Notably, it efficiently processes hour-long videos while pruning 55% of tokens and reducing GPU memory by 43% ([Extended Fig. 18](#)), demonstrating suitability for resource-constrained environments. The model shows strong multilingual capability, rare disease diagnostics ([Extended Fig. 19–20](#)), and robust multi-turn dialogue performance ([Extended Fig. 21–23](#)). Without reinforcement learning, it performs reflective reasoning with self-correction when prompted ([Extended Fig. 24–27](#)), particularly valuable for complex, low-prevalence conditions. With its transparent pipeline and cost-effective training, Hulu-Med provides a credible foundation for real-world clinical deployment.

Limitations and future directions. Hulu-Med has limitations that chart a course for future work. First, the model’s input is presently restricted to medical text and visual data. A critical next frontier involves integrating genomic and molecular data to enable a truly multi-scale understanding of disease, moving towards predictive and personalized medicine. Furthermore, the landscape of public data remains underutilized; a more exhaustive aggregation of global datasets represents a straightforward path to

further scale model performance and generalizability. Second, the reasoning capabilities of medical VLMs are not fully realized. Future work could leverage advanced training paradigms, such as large-scale reinforcement learning on diverse long CoT and long-horizon data to better capture the nuanced logic of clinical reasoning. This would enhance both the interpretability and reliability. Concurrently, establishing efficient continual pretraining mechanisms will be crucial for the model to remain current with the rapid evolution of medical knowledge. Finally, although Hulu-Med has been comprehensively evaluated on established benchmarks, further integration into specialist models and multi-agent systems for clinical validation is of high necessity to ensure safe and effective workflows.

References

1. Moor, M. *et al.* Foundation models for generalist medical artificial intelligence. *Nature* **616**, 259–265 (2023).
2. Topol, E. J. High-performance medicine: the convergence of human and artificial intelligence. *Nature Medicine* **25**, 44–56 (2019).
3. Rajkomar, A., Dean, J. & Kohane, I. Machine learning in medicine. *New England Journal of Medicine* **380**, 1347–1358 (2019).
4. Lambin, P. *et al.* Radiomics: the bridge between medical imaging and personalized medicine. *Nature Reviews Clinical Oncology* **14**, 749–762 (2017).
5. Tu, T. *et al.* Towards conversational diagnostic artificial intelligence. *Nature* **642**, 1–9 (2025).
6. Tiu, E. *et al.* Expert-level detection of pathologies from unannotated chest x-ray images via self-supervised learning. *Nature Biomedical Engineering* **6**, 1399–1406 (2022).
7. Maier-Hein, L. *et al.* Surgical data science for next-generation interventions. *Nature Biomedical Engineering* **1**, 691–696 (2017).
8. McKinney, S. M. *et al.* International evaluation of an ai system for breast cancer screening. *Nature* **577**, 89–94 (2020).
9. Vasey, B. *et al.* Reporting guideline for the early stage clinical evaluation of decision support systems driven by artificial intelligence: Decide-ai. *British Medical Journal* **377** (2022).
10. Brown, T. *et al.* Language models are few-shot learners. *Advances in Neural Information Processing Systems* **33**, 1877–1901 (2020).
11. Radford, A. *et al.* Language models are unsupervised multitask learners. *OpenAI blog* **1**, 9 (2019).
12. Wang, P. *et al.* Qwen2-VL: Enhancing vision-language model’s perception of the world at any resolution. *ArXiv preprint arXiv:2409.12191* (2024).
13. Comanici, G. *et al.* Gemini 2.5: Pushing the frontier with advanced reasoning, multimodality, long context, and next generation agentic capabilities. *ArXiv preprint arXiv:2507.06261* (2025).
14. Li, F. *et al.* LLaVA-Interleave: Tackling multi-image, video, and 3d in large multimodal models. In *The Thirteenth International Conference on Learning Representations* (2025).
15. Lu, J., Clark, C., Zellers, R., Mottaghi, R. & Kembhavi, A. Unified-io: A unified model for vision, language, and multi-modal tasks. In *The Eleventh International Conference on Learning Representations* (2023).
16. Jin, P., Takanobu, R., Zhang, W., Cao, X. & Yuan, L. Chat-univi: Unified visual representation empowers large language models with image and video understanding. In *Proceedings of the IEEE/CVF Conference on Computer Vision and Pattern Recognition*, 13700–13710 (2024).
17. Lu, M. Y. *et al.* A multimodal generative ai copilot for human pathology. *Nature* **634**, 466–473 (2024).
18. Yan, S. *et al.* A multimodal vision foundation model for clinical dermatology. *Nature Medicine* **31**, 1–12 (2025).
19. Zhang, K. *et al.* A generalist vision–language foundation model for diverse biomedical tasks. *Nature Medicine* **30**, 1–13 (2024).
20. Qiu, J. *et al.* Development and validation of a multimodal multitask vision foundation model for generalist ophthalmic artificial intelligence. *NEJM AI* **1**, Aloa2300221 (2024).
21. Li, C. *et al.* LLaVA-Med: Training a large language-and-vision assistant for biomedicine in one day. *Advances in Neural Information Processing Systems* **36**, 28541–28564 (2023).

22. Wu, C. *et al.* Towards generalist foundation model for radiology by leveraging web-scale 2d&3d medical data. *Nature Communications* **16**, 7866 (2025).

23. Chen, J. *et al.* Towards injecting medical visual knowledge into multimodal llms at scale. In *Proceedings of the 2024 conference on Empirical Methods in Natural Language Processing*, 7346–7370 (2024).

24. Li, J. *et al.* LLaVA-Surg: towards multimodal surgical assistant via structured surgical video learning. *ArXiv preprint arXiv:2408.07981* (2024).

25. Kim, C., Gadgil, S. U. & Lee, S.-I. Transparency of medical artificial intelligence systems. *Nature Reviews Bioengineering* 1–19 (2025).

26. Mahmood, F. A benchmarking crisis in biomedical machine learning. *Nature Medicine* **31**, 1060–1060 (2025).

27. Shick, A. A. *et al.* Transparency of artificial intelligence/machine learning-enabled medical devices. *NPJ Digital Medicine* **7**, 21 (2024).

28. Saenz, A., Chen, E., Marklund, H. & Rajpurkar, P. The MAIDA initiative: establishing a framework for global medical-imaging data sharing. *The Lancet Digital Health* **6**, e6–e8 (2024).

29. Guo, D. *et al.* Deepseek-r1 incentivizes reasoning in llms through reinforcement learning. *Nature* **645**, 633–638 (2025).

30. Ma, W. *et al.* Evolution of future medical ai models—from task-specific, disease-centric to universal health. *NEJM AI* **1**, Alp2400289 (2024).

31. Huang, Y. *et al.* Position: Trustllm: Trustworthiness in large language models. In *International Conference on Machine Learning*, 20166–20270 (PMLR, 2024).

32. Zhai, X., Mustafa, B., Kolesnikov, A. & Beyer, L. Sigmoid loss for language image pre-training. In *Proceedings of the IEEE/CVF International Conference on Computer Vision*, 11975–11986 (2023).

33. Su, J. *et al.* Roformer: Enhanced transformer with rotary position embedding. *Neurocomputing* **568**, 127063 (2024).

34. Yang, A. *et al.* Qwen3 technical report. *ArXiv preprint arXiv:2505.09388* (2025).

35. Bai, S. *et al.* Qwen2. 5-VL technical report. *ArXiv preprint arXiv:2502.13923* (2025).

36. Zhu, J. *et al.* Internvl3: Exploring advanced training and test-time recipes for open-source multimodal models. *ArXiv preprint arXiv:2504.10479* (2025).

37. Bai, F., Du, Y., Huang, T., Meng, M. Q.-H. & Zhao, B. M3D: Advancing 3d medical image analysis with multi-modal large language models. *ArXiv preprint arXiv:2404.00578* (2024).

38. Jin, J. & Jeong, C. W. Surgical-LLaVA: Toward surgical scenario understanding via large language and vision models. *ArXiv preprint arXiv:2410.09750* (2024).

39. Xu, W. *et al.* LingShu: A generalist foundation model for unified multimodal medical understanding and reasoning. *ArXiv preprint arXiv:2506.07044* (2025).

40. Sellergren, A. *et al.* MedGemma technical report. *ArXiv preprint arXiv:2507.05201* (2025).

41. Qiu, P. *et al.* Towards building multilingual language model for medicine. *Nature Communications* **15**, 8384 (2024).

42. Chen, X. *et al.* RareBench: can llms serve as rare diseases specialists? In *Proceedings of the 30th ACM SIGKDD conference on knowledge discovery and data mining*, 4850–4861 (2024).

43. Arora, R. K. *et al.* HealthBench: Evaluating large language models towards improved human health. *ArXiv preprint arXiv:2505.08775* (2025).

44. Hu, Y. *et al.* OmniMedVQA: A new large-scale comprehensive evaluation benchmark for medical lvIm. In *Proceedings of the IEEE/CVF Conference on Computer Vision and Pattern Recognition*, 22170–22183 (2024).

45. Zhang, X. *et al.* PMC-VQA: Visual instruction tuning for medical visual question answering. *ArXiv preprint arXiv:2305.10415* (2023).

46. Lau, J. J., Gayen, S., Ben Abacha, A. & Demner-Fushman, D. A dataset of clinically generated visual questions and answers about radiology images. *Scientific data* **5**, 1–10 (2018).

47. Liu, B. *et al.* SLAKE: A semantically-labeled knowledge-enhanced dataset for medical visual question answering. In *2021 IEEE 18th International Symposium on Biomedical Imaging (ISBI)*, 1650–1654 (IEEE, 2021).

48. He, X., Zhang, Y., Mou, L., Xing, E. & Xie, P. PathVQA: 30000+ questions for medical visual question answering. *ArXiv preprint arXiv:2003.10286* (2020).

49. Zuo, Y. *et al.* MedXpertQA: Benchmarking expert-level medical reasoning and understanding. In *Forty-second International Conference on Machine Learning* (2025).

50. Demner-Fushman, D. *et al.* Preparing a collection of radiology examinations for distribution and retrieval. *Journal of the American Medical Informatics Association* **23**, 304–310 (2015).

51. Zhao, W. *et al.* RaTEScore: A metric for radiology report generation. In *Proceedings of the 2024 Conference on Empirical Methods in Natural Language Processing*, 15004–15019 (2024).

52. Irvin, J. *et al.* CheXpert: A large chest radiograph dataset with uncertainty labels and expert comparison. In *Proceedings of the AAAI conference on artificial intelligence*, vol. 33, 590–597 (2019).

53. Johnson, A. E. *et al.* MIMIC-CXR, a de-identified publicly available database of chest radiographs with free-text reports. *Scientific data* **6**, 317 (2019).

54. Yang, J., Shi, R. & Ni, B. Medmnist classification decathlon: A lightweight automl benchmark for medical image analysis. In *2021 IEEE 18th International Symposium on Biomedical Imaging (ISBI)*, 191–195 (IEEE, 2021).

55. Ji, Y. *et al.* AMOS: A large-scale abdominal multi-organ benchmark for versatile medical image segmentation. *Advances in Neural Information Processing Systems* **35**, 36722–36732 (2022).

56. Gai, X. *et al.* 3D-RAD: A comprehensive 3d radiology med-vqa dataset with multi-temporal analysis and diverse diagnostic tasks. *ArXiv preprint arXiv:2506.11147* (2025).

57. Yu, S., Wang, H., Wu, J., Xie, C. & Zhou, Y. MedFrameQA: A multi-image medical vqa benchmark for clinical reasoning. *ArXiv preprint arXiv:2505.16964* (2025).

58. Nwoye, C. I. *et al.* CholecTriplet2021: A benchmark challenge for surgical action triplet recognition. *Medical Image Analysis* **86**, 102803 (2023).

59. Allan, M. *et al.* 2018 robotic scene segmentation challenge. *ArXiv preprint arXiv:2001.11190* (2020).

60. Valderrama, N. *et al.* Towards holistic surgical scene understanding. In *International conference on medical image computing and computer-assisted intervention*, 442–452 (Springer, 2022).

61. Thapa, R. *et al.* How well can general vision-language models learn medicine by watching public educational videos? *ArXiv preprint arXiv:2504.14391* (2025).

62. Wang, Y. *et al.* MMLU-Pro: A more robust and challenging multi-task language understanding benchmark. *Advances in Neural Information Processing Systems* **37**, 95266–95290 (2024).

63. Chen, H., Fang, Z., Singla, Y. & Dredze, M. Benchmarking large language models on answering and explaining challenging medical questions. In *Proceedings of the 2025 Conference of the Nations of the Americas Chapter of the Association for Computational Linguistics: Human Language Technologies (Volume 1: Long Papers)*, 3563–3599 (2025).

64. Du, X. *et al.* SuperGPQA: Scaling IIm evaluation across 285 graduate disciplines. *ArXiv preprint arXiv:2502.14739* (2025).

65. Jin, Q., Dhingra, B., Liu, Z., Cohen, W. & Lu, X. PubMedQA: A dataset for biomedical research question answering. In *Proceedings of the 2019 Conference on Empirical Methods in Natural Language Processing and the 9th International Joint Conference on Natural Language Processing (EMNLP-IJCNLP)*, 2567–2577 (2019).

66. Pal, A., Umapathi, L. K. & Sankarasubbu, M. MedMCQA: A large-scale multi-subject multi-choice dataset for medical domain question answering. In *Conference on health, inference, and learning*, 248–260 (PMLR, 2022).

67. Hendrycks, D. *et al.* Measuring massive multitask language understanding. In *International Conference on Learning Representations* (2021).

68. Hoffmann, J. *et al.* Training compute-optimal large language models. In *Proceedings of the 36th International Conference on Neural Information Processing Systems*, 30016–30030 (2022).

69. Henighan, T. *et al.* Scaling laws for autoregressive generative modeling. *ArXiv preprint arXiv:2010.14701* (2020).

70. Lu, M. Y. *et al.* A multimodal generative ai copilot for human pathology. *Nature* **634**, 466–473 (2024).

71. Price, W. N. & Cohen, I. G. Privacy in the age of medical big data. *Nature Medicine* **25**, 37–43 (2019).

72. Xu, J. *et al.* Qwen3-Omni technical report. *ArXiv preprint arXiv:2509.17765* (2025).

73. Guo, D. *et al.* Seed1. 5-VL technical report. *ArXiv preprint arXiv:2505.07062* (2025).

74. Acosta, J. N., Falcone, G. J., Rajpurkar, P. & Topol, E. J. Multimodal biomedical ai. *Nature Medicine* **28**, 1773–1784 (2022).

75. Sennrich, R., Haddow, B. & Birch, A. Neural machine translation of rare words with subword units. In *Proceedings of the 54th Annual Meeting of the Association for Computational Linguistics (Volume 1: Long Papers)*, 1715–1725 (2016).

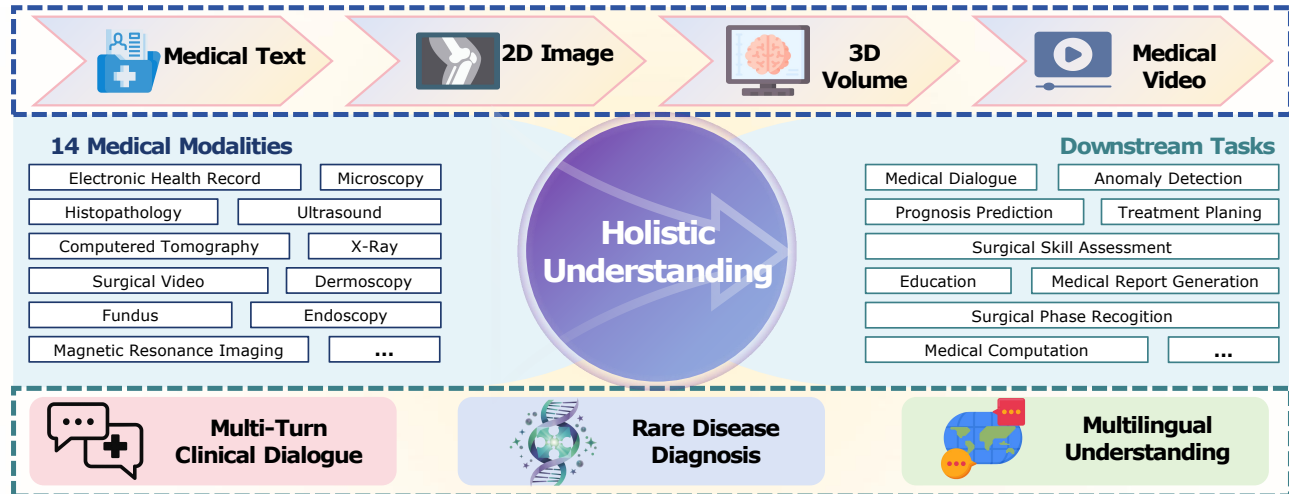
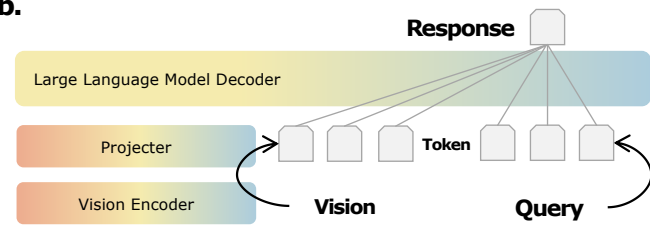
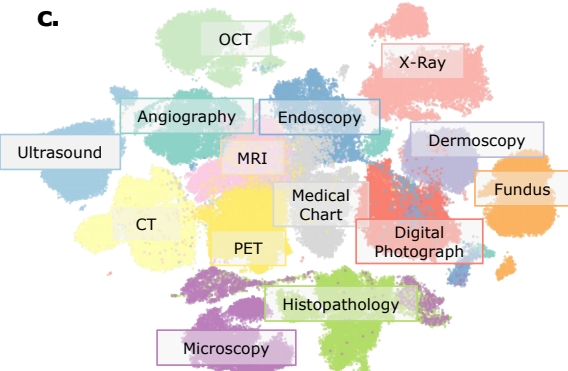
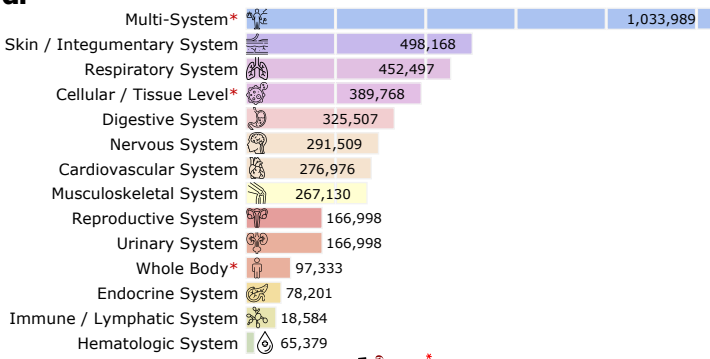
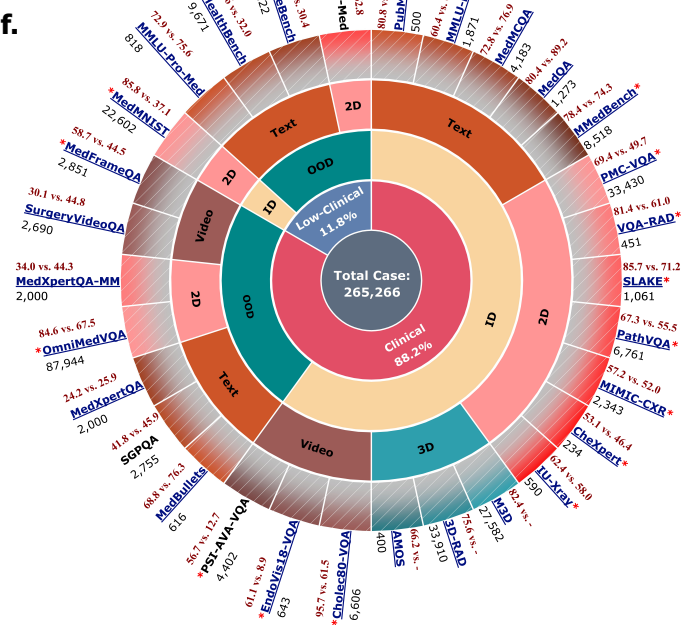
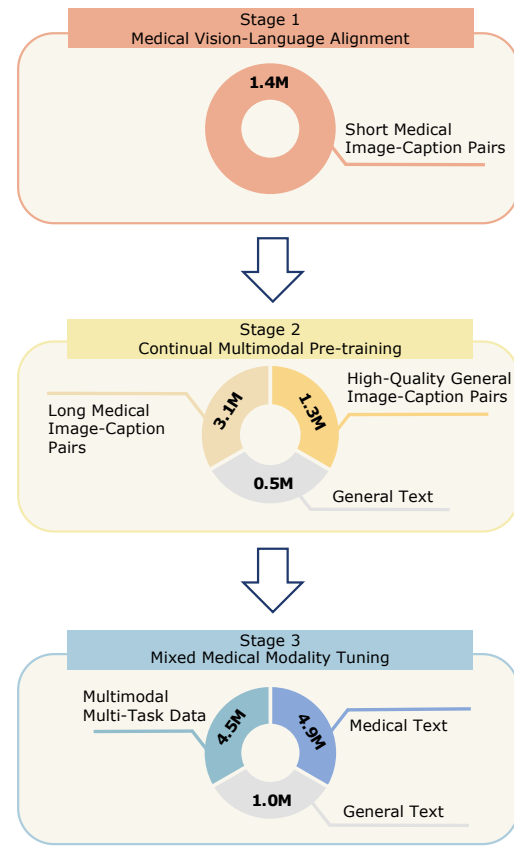
a.**b.****c.****d.****f.****e.**

Figure 1. Overview of the Hulu-Med architecture, data composition, training strategy and Evaluation. **a**, The model's unified architecture is designed to holistically process a diverse spectrum of medical inputs—spanning text, 2D images, 3D volumes, and video—to support a wide array of downstream clinical tasks. **b**, A schematic of the core model components, including the vision encoder, projector, and LLM decoder, is presented. **c,d**, The training corpus spans 12 major anatomical systems and 14 imaging modalities, forming a comprehensive basis for the model's generalist reasoning and understanding capabilities. **e**, The progressive three-stage training curriculum is detailed, beginning with foundational vision-language alignment, advancing to continual pre-training with enriched data, and culminating in mixed-modality instruction tuning. **f**, Comprehensive benchmark evaluation overview. This visualization encompasses 30 medical benchmarks, hierarchically organized by clinical domain and task complexity, totaling 265,266 test cases. The scores in the outermost ring denote performance of Hulu-Med (left score) vs. GPT-4o (right score). The **red asterisks (*)** indicates 17 benchmarks where Hulu-Med-32B outperforms GPT-4o; **blue underlined text** indicates 27 benchmarks where Hulu-Med attains the best open-source performance; and **black bolded text** indicates 3 benchmarks where Hulu-Med is the second-best. GPT-4o's performance is marked as "—" for 3D benchmarks due to its inability to process 3D inputs and limitations on the number of image inputs.

Table 1. Performance comparison among three categories of VLMs (Proprietary, General-purpose, and Medical) on 2D medical VQA benchmarks, with benchmarks categorized by task type. **bold** and underline scores indicate the best and second-best medical VLMs in two subgroups with different model sizes, respectively.

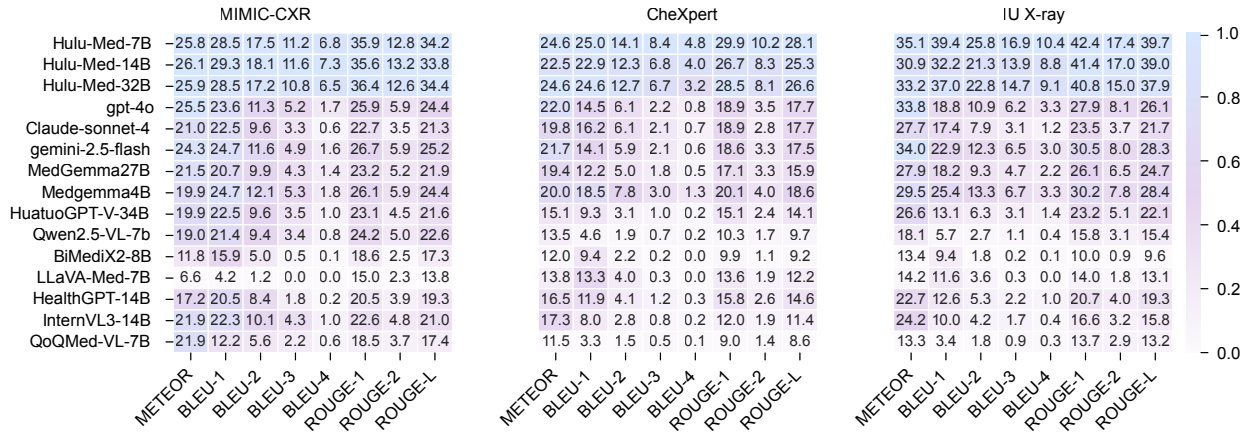
Models	Multi-modality Benchmarks		Specific-modality Benchmarks			Reasoning Benchmark	Knowledge-intensive Benchmark
	OM.VQA	PMCVQA	VQA-RAD	SLAKE	PathVQA		
<i>Proprietary Models</i>							
GPT-4.1	75.5	55.2	65.0	72.2	55.5	45.2	75.2
GPT-4o	67.5	49.7	61.0	71.2	55.5	44.3	62.8
Claude Sonnet 4	65.5	54.4	67.6	70.6	54.2	43.3	74.6
Gemini-2.5-Flash	71.0	55.4	68.5	75.8	55.4	52.8	76.9
<i>General-purpose Multimodal VLMs</i>							
— Models < 10B —							
Qwen2.5VL-7B	63.6	51.9	63.2	66.8	44.1	20.1	50.6
Janus-Pro-7B	59.6	50.1	49.7	55.2	35.4	18.4	36.1
InternVL2.5-8B	81.3	51.3	59.4	69.0	42.1	21.7	53.5
InternVL3-8B	79.1	53.8	65.4	72.8	48.6	22.4	59.2
— Models > 10B —							
Llama3.2-11B	43.8	48.1	58.8	65.8	32.9	20.1	51.0
InternVL3-14B	78.9	54.1	66.3	72.8	48.0	23.1	63.1
Qwen2.5V-32B	68.2	54.5	71.8	71.2	41.9	25.2	59.6
InternVL2.5-38B	79.9	57.2	61.4	70.3	46.9	24.4	61.6
InternVL3-38B	79.8	56.6	65.4	72.7	51.0	25.2	65.2
<i>Medical Multimodal VLMs</i>							
— Models < 10B —							
BiomedGPT [♡]	27.9	27.6	16.6	13.6	11.3	-	24.9
Med-R1-2B [◊]	-	47.4	39.0	54.5	15.3	21.1	34.8
MedVLM-R1-2B	77.6	48.8	49.2	56.3	36.0	21.4	35.2
HealthGPT-M3	71.5	55.4	56.8	70.8	55.4	22.4	42.8
BioMediX2-8B	66.0	41.8	55.7	54.1	34.6	21.9	39.8
LLaVA-Med-7B	34.8	22.7	46.6	51.9	35.2	20.8	28.1
MedGemma-4B-IT	70.7	49.2	<u>72.3</u>	78.2	48.1	25.4	43.2
HuatuoGPT-V-7B	74.3	53.1	67.6	68.1	44.8	23.2	<u>49.8</u>
Lingshu-7B [†]	<u>82.9</u>	<u>56.3</u>	67.9	<u>83.1</u>	<u>61.9</u>	<u>26.7</u>	-
Hulu-Med-7B	84.2	66.8	78.0	86.8	65.6	29.0	51.4
— Models > 10B —							
HealthGPT-14B	75.2	56.4	65.0	66.1	56.7	24.7	49.6
HuatuoGPT-V-34B	74.0	56.6	61.4	69.5	44.4	22.1	51.8
Lingshu-32B [†]	83.4	57.9	<u>76.7</u>	86.7	<u>65.5</u>	<u>30.9</u>	-
MedDr-40B [♡]	64.3	13.9	65.2	66.4	53.5	-	49.3
Hulu-Med-14B	<u>85.1</u>	<u>68.9</u>	76.1	<u>86.5</u>	64.4	30.0	<u>54.8</u>
Hulu-Med-32B	84.6	69.4	81.4	85.7	67.3	34.0	60.4

[◊]Med-R1 trained on OmniMedVQA test set. [♡]No multi-image support. [†]Lingshu trained on MMMU-Med val set.

Table 2. Performance comparison among three categories of VLMs (Proprietary, General-purpose, and Medical) on medical text benchmarks. Within each open-source medical VLM subgroup, **bold** and underline scores indicate the best and second-best methods, respectively. Note that MedQA, MedXQA, and SGPQA denote MedQA-USMLE, MedXpertQA-Text, and SuperGPQA-Medical benchmarks, respectively.

Models	Complex Reasoning Benchmarks				Text Understanding Benchmark PubMedQA	Medical Exam Benchmarks		
	MMLU-Pro-Med	MedXQA	Medbullets	SGPQA		MedMCQA	MedQA	MMLU-Med
<i>Proprietary Models</i>								
GPT-4.1	78.0	30.9	77.0	49.9	75.6	77.7	89.1	89.6
<u>o3-mini</u>	78.1	35.4	83.7	50.1	73.6	60.6	74.5	87.0
GPT-4o	75.6	25.9	76.3	45.9	71.8	76.9	89.2	88.2
Claude Sonnet 4	79.5	33.6	80.2	56.3	78.6	79.3	92.1	91.3
Gemini-2.5-Flash	70.0	35.6	77.6	53.3	73.8	73.6	91.2	84.2
Deepseek-V3	74.6	20.0	48.4	32.1	77.7	88.0	51.0	86.5
<i>General-purpose Multimodal VLMs</i>								
<i>— Models < 10B —</i>								
Qwen2.5VL-7B	50.5	12.8	42.1	26.3	76.4	52.6	57.3	73.4
Janus-Pro-7B	20.2	10.0	30.2	14.8	72.0	37.5	37.4	46.4
InternVL2.5-8B	50.6	11.6	42.4	26.1	76.4	52.4	53.7	74.2
InternVL3-8B	57.9	13.1	48.5	31.2	75.4	57.7	62.1	77.5
<i>— Models > 10B —</i>								
Qwen2.5VL-32B	66.5	15.6	54.2	37.6	68.4	63.0	71.6	83.2
InternVL3-14B	65.4	14.1	49.5	37.9	77.2	62.0	70.1	81.7
InternVL2.5-38B	71.5	14.7	55.0	39.9	74.2	65.9	74.4	84.6
InternVL3-38B	72.1	16.0	54.6	42.5	73.2	64.9	73.5	83.8
<i>Medical Multimodal VLMs</i>								
<i>— Models < 10B —</i>								
MedVLM-R1-2B	24.9	11.8	33.8	19.1	66.4	39.7	42.3	51.8
BioMediX2-8B	40.8	13.4	45.9	25.2	75.2	52.9	58.9	68.6
MedGemma-4B-IT	38.6	12.8	45.6	21.6	72.2	52.2	56.2	66.7
HealthGPT-M3	38.3	11.5	41.4	18.9	57.8	54.2	55.0	72.5
LLaVA-Med-7B	16.6	9.9	34.4	16.1	26.4	39.4	42.0	50.6
HuatuoGPT-V-7B	44.6	10.1	40.9	21.9	72.8	51.2	52.9	69.3
Lingshu-7B	<u>50.4</u>	<u>16.5</u>	<u>56.2</u>	<u>26.3</u>	<u>76.6</u>	<u>55.9</u>	<u>63.3</u>	<u>74.5</u>
Hulu-Med-7B	60.6	19.6	61.5	31.1	77.4	67.6	73.5	79.5
<i>— Models > 10B —</i>								
HealthGPT-14B	63.4	11.3	39.8	25.7	68.0	63.4	66.2	80.2
Lingshu-32B	<u>70.2</u>	22.7	65.4	<u>41.1</u>	77.8	66.1	74.7	<u>84.7</u>
HuatuoGPT-V-34B	51.8	11.4	42.7	26.5	72.2	54.7	58.8	74.7
MedDr-40B	55.6	12.0	44.3	24.0	77.4	38.4	59.2	65.2
Hulu-Med-14B	68.0	<u>23.2</u>	<u>68.5</u>	37.7	<u>79.8</u>	<u>70.4</u>	<u>78.1</u>	83.3
Hulu-Med-32B	72.9	24.2	68.8	41.8	80.8	72.8	80.4	85.6

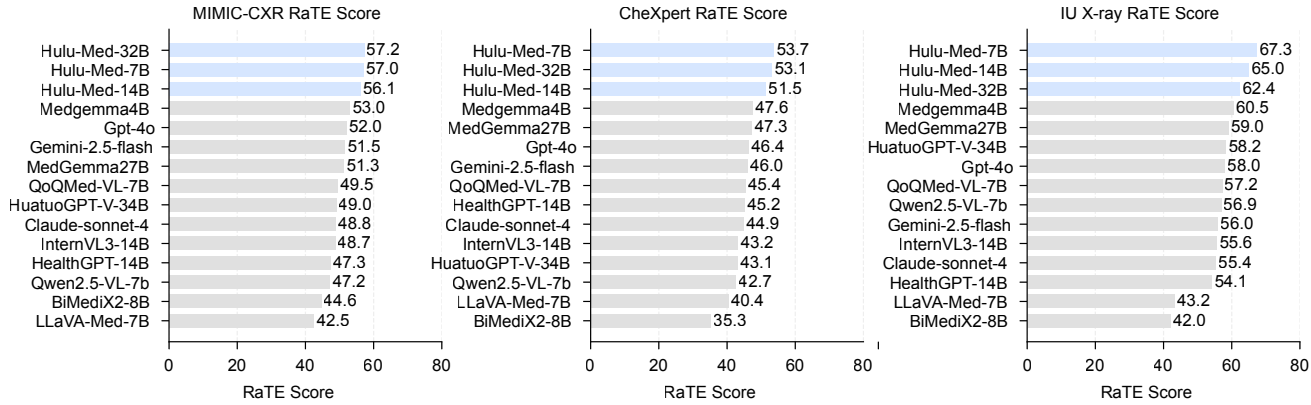
a Natural Language Generation Metrics



b Clinical Entity Evaluation Metric

Hulu-Med Series

Baseline Models



c

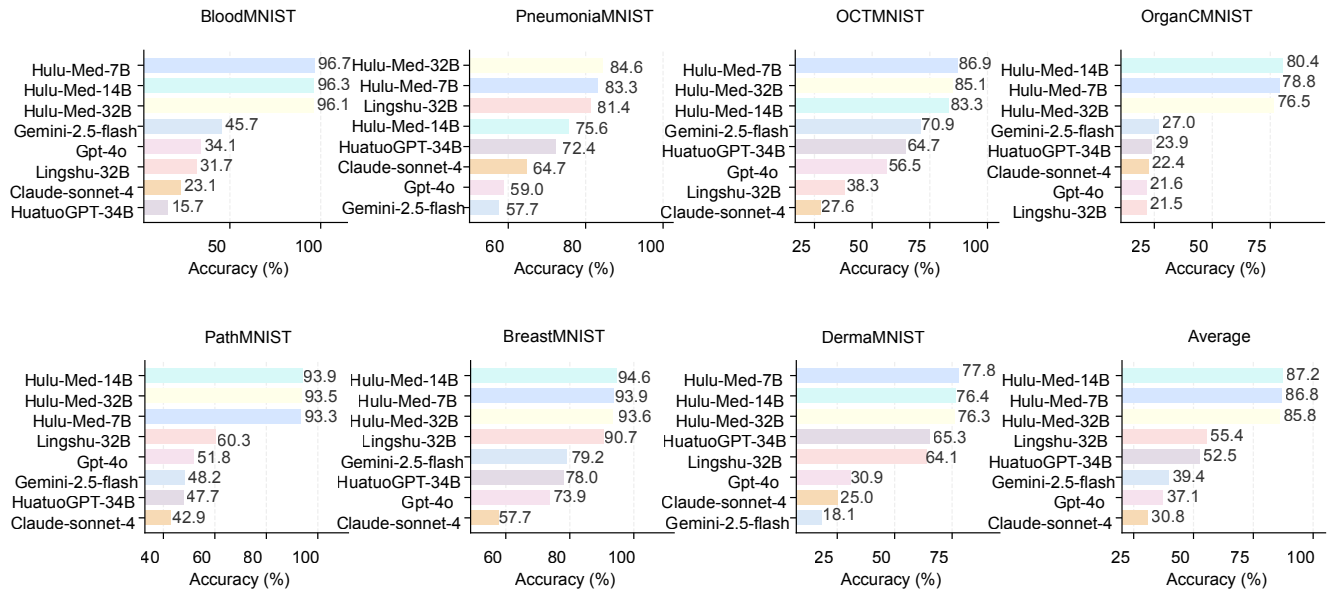


Figure 2. Performance evaluation of Hulu-Med on 2D medical image understanding tasks. a,

Quantitative results for MRG on the MIMIC-CXR, CheXpert, and IU X-ray datasets are presented using standard NLG metrics. **b**, A head-to-head comparison of clinical fidelity in generated reports is shown using RaTEScore, a metric that more accurately reflects the semantic correctness of clinical entities than traditional language metrics. **c**, Comparative analysis of classification accuracy on seven sub-tasks of the MedMNIST benchmark demonstrates Hulu-Med's proficiency across a diverse range of 2D medical images.

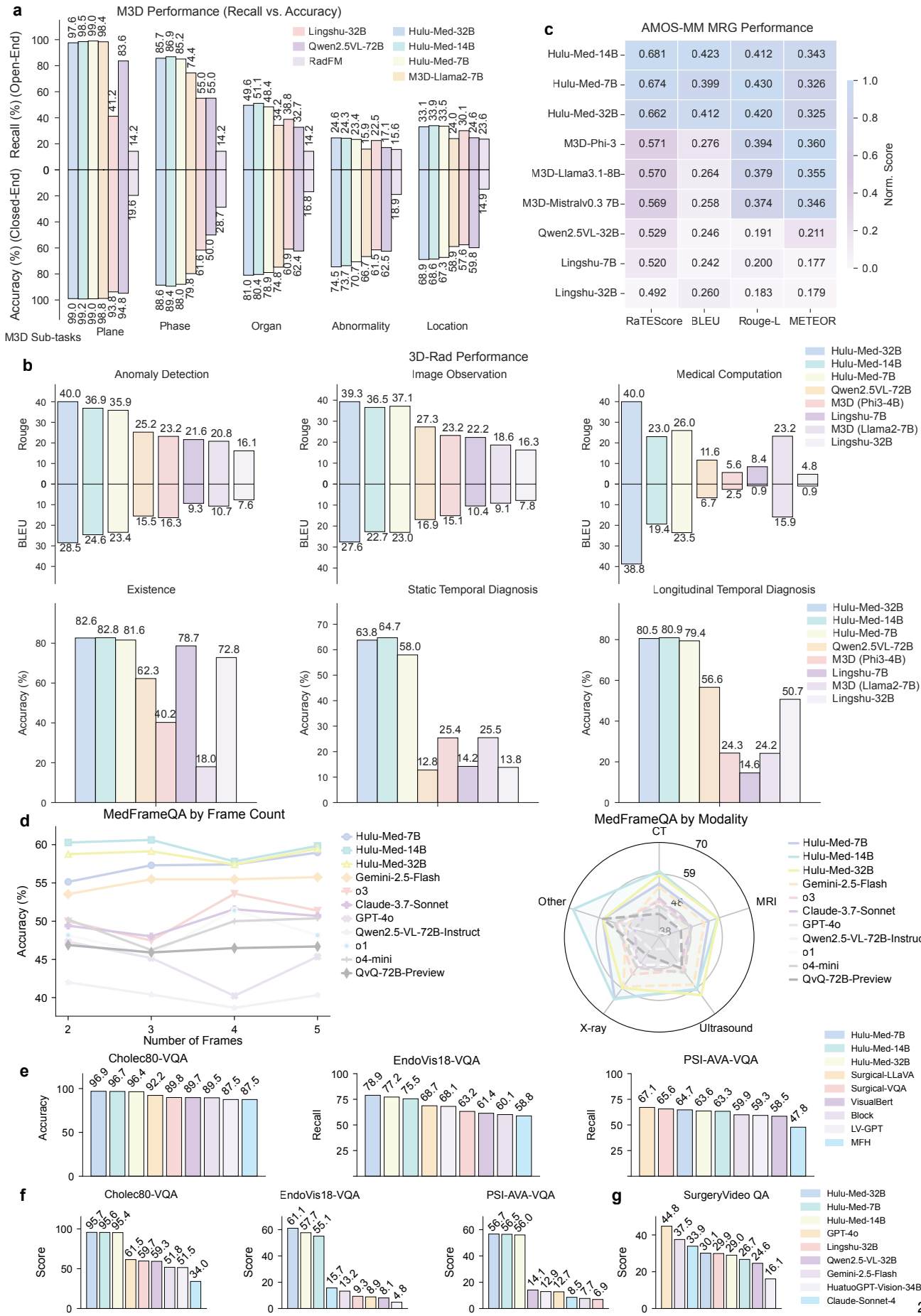


Figure 3. Performance evaluation of Hulu-Med on 3D and video understanding tasks. a,

Performance on M3D benchmark demonstrates high accuracy in discriminative (primarily closed yes/no questions) tasks and strong recall for descriptive (predominantly open-ended questions) tasks across anatomical categories. **b**, Results on 3D-RAD benchmark show proficiency in temporal reasoning for 3D volumetric data, including static and longitudinal diagnosis tasks critical for tracking disease dynamics. **c**, 3D MRG quality evaluated on AMOS-MM benchmark, where Hulu-Med achieves superior RaTEScore indicating high clinical fidelity, alongside strong performance on standard NLG metrics. **d**, Multi-frame temporal reasoning on MedFrameQA benchmark shows leading performance than general VLMs and proprietary models. **e**, Surgical video comprehension evaluation comparing against surgery-specific models trained on Cholec80, EndoVis18, and PSI-AVA. Accuracy is reported for Cholec80 (closed-ended), while recall is used for EndoVis18 and PSI-AVA (open-ended). **f**, Comparison with general and medical VLMs using ChatGPT-4o-latest as judge to mitigate potential misjudgments from NLG metrics when answers are semantically similar but syntactically divergent. **g**, Results on the newly introduced SurgeryVideoQA benchmark containing both surgery-related and other medical educational videos for OOD evaluation. ChatGPT-4o-latest judges answer correctness to ensure fair comparison across different VLM output formats.

a

Performance on MMedBench

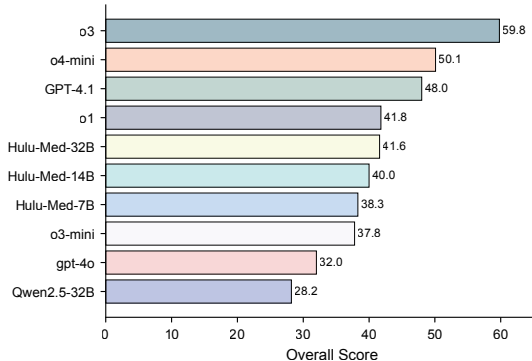
Method	Size	English	Chinese	Japanese	French	Russian	Spanish	Avg.
GPT-3.5	-	56.88	52.29	34.63	32.48	66.36	66.06	51.47
GPT-4	-	78.00	75.07	72.91	56.59	83.62	85.67	74.27
Gemini-2.5-flash	-	72.51	86.92	83.42	59.16	82.81	80.96	77.63
Claude-Sonnet-4	-	71.96	86.02	72.36	51.77	83.98	90.15	76.04
Gemini-1.0 pro	-	53.73	60.19	44.22	29.90	73.44	69.69	55.20
BLOOMZ	7B	43.28	58.06	32.66	26.37	62.89	47.34	45.10
InternLM	7B	44.07	64.62	37.19	24.92	58.20	44.97	45.67
Llama 2	7B	43.36	50.29	25.13	20.90	66.80	47.10	42.26
MedAlpaca	7B	46.74	44.80	29.64	21.06	59.38	45.00	41.11
ChatDoctor	7B	43.52	43.26	25.63	18.81	62.50	43.44	39.53
PMC-LLAMA	7B	47.53	42.44	24.12	20.74	62.11	43.29	40.04
Mistral	7B	61.74	71.10	44.72	48.71	74.22	63.86	60.73
MEDITRON	7B	55.46	61.88	40.20	35.05	67.58	53.28	52.24
InternLM 2	7B	57.27	77.55	47.74	41.00	68.36	59.59	58.59
BioMistral	7B	57.82	71.54	37.19	47.27	69.92	60.98	57.45
Llama 3	8B	63.86	78.23	48.24	50.80	71.48	64.15	62.79
MMedLM	7B	49.88	70.49	46.23	36.66	72.27	54.52	55.01
MMedLM 2	7B	61.70	80.01	61.81	52.09	80.47	67.65	67.30
MMed-Llama 3	8B	66.06	79.25	61.81	55.63	75.39	68.38	67.75
Lingshu-7B	7B	58.92	67.22	46.23	32.15	73.44	65.35	57.22
Hulu-Med-7B	7B	71.56	78.37	60.30	50.64	79.30	66.70	67.81
Hulu-Med-14B	14B	74.71	86.05	64.82	59.65	80.86	78.01	74.02
Hulu-Med-32B	32B	75.81	87.19	71.36	59.65	78.12	78.67	75.13
Hulu-Med-7B-Thinking	7B	80.75	81.61	61.31	60.29	75.39	75.20	72.42
Hulu-Med-14B-Thinking	14B	80.75	86.34	67.84	69.61	74.61	81.47	76.77
Hulu-Med-32B-Thinking	32B	83.90	88.03	71.86	71.38	72.66	82.60	78.41

b

Performance on HealthBench with Proprietary Model

Performance on HealthBench with Open-Source Model

a. Healthbench Overall Score



Metric	HuatuoGPT-V-34B	Lingshu-7B	Lingshu-32B	Hulu-Med-7B	Hulu-Med-14B	Hulu-Med-32B
Overall Score	0.1717	0.1590	0.1904	0.3831	0.3987	0.4158
Global Health	0.1115	0.1084	0.1678	0.3151	0.3474	0.3793
Communication	0.1661	0.1547	0.1506	0.4062	0.4156	0.4329
Context Seeking	0.0611	0.0209	0.0575	0.3180	0.3494	0.3428
Emergency Referrals	0.2611	0.2576	0.2493	0.5298	0.5541	0.5558
Hedging	0.2533	0.2569	0.2927	0.4721	0.4731	0.4918
Health Data Tasks	0.2288	0.1858	0.2425	0.3677	0.3729	0.3798
Complex Responses	0.1157	0.1023	0.1427	0.2103	0.2104	0.2551

c

Performance on RareBench

Legend: Hulu-Med-7B (light blue), Hulu-Med-14B (medium blue), Hulu-Med-7B-Thinking (dark blue), Hulu-Med-32B (yellow), Hulu-Med-32B-Thinking (orange), Gemini-2.5-Flash (purple), gpt-40 (pink), Claude-3.7-Sonnet (light green), o3-mini (dark green)

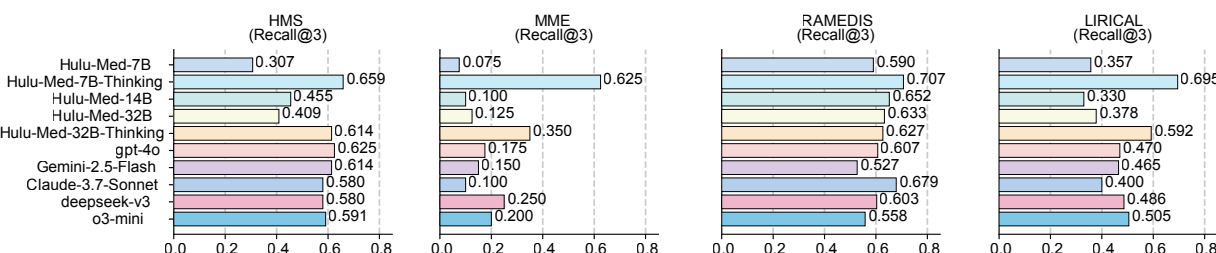
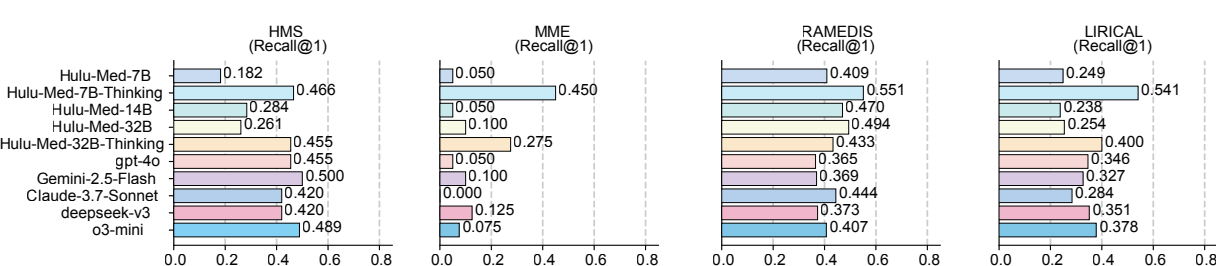


Figure 4. Evaluation of Hulu-Med's generalization capabilities in clinically critical, real-world scenarios. **a**, Multilingual medical reasoning proficiency is demonstrated on the MMedBench benchmark across six languages. **Bold text** indicates the best performance, while Hulu-Med establishes a new state-of-the-art average performance for open-source models and the proprietary GPT-4. **b**, Evaluation of conversational safety and clinical dialogue on HealthBench indicates that Hulu-Med outperforms general-purpose leaders such as GPT-4o and o3-mini, closes the gap with top-performing models including o3, o4-mini, and GPT-4.1, and significantly exceeds other specialized open-source models in multi-turn interactions, as assessed by physician-authored rubrics. **c**, Diagnostic reasoning on the long-tail rare diseases is evaluated on the RareBench benchmark, highlighting Hulu-Med's strong performance in data-constrained scenarios and its utility as a diagnostic aid.

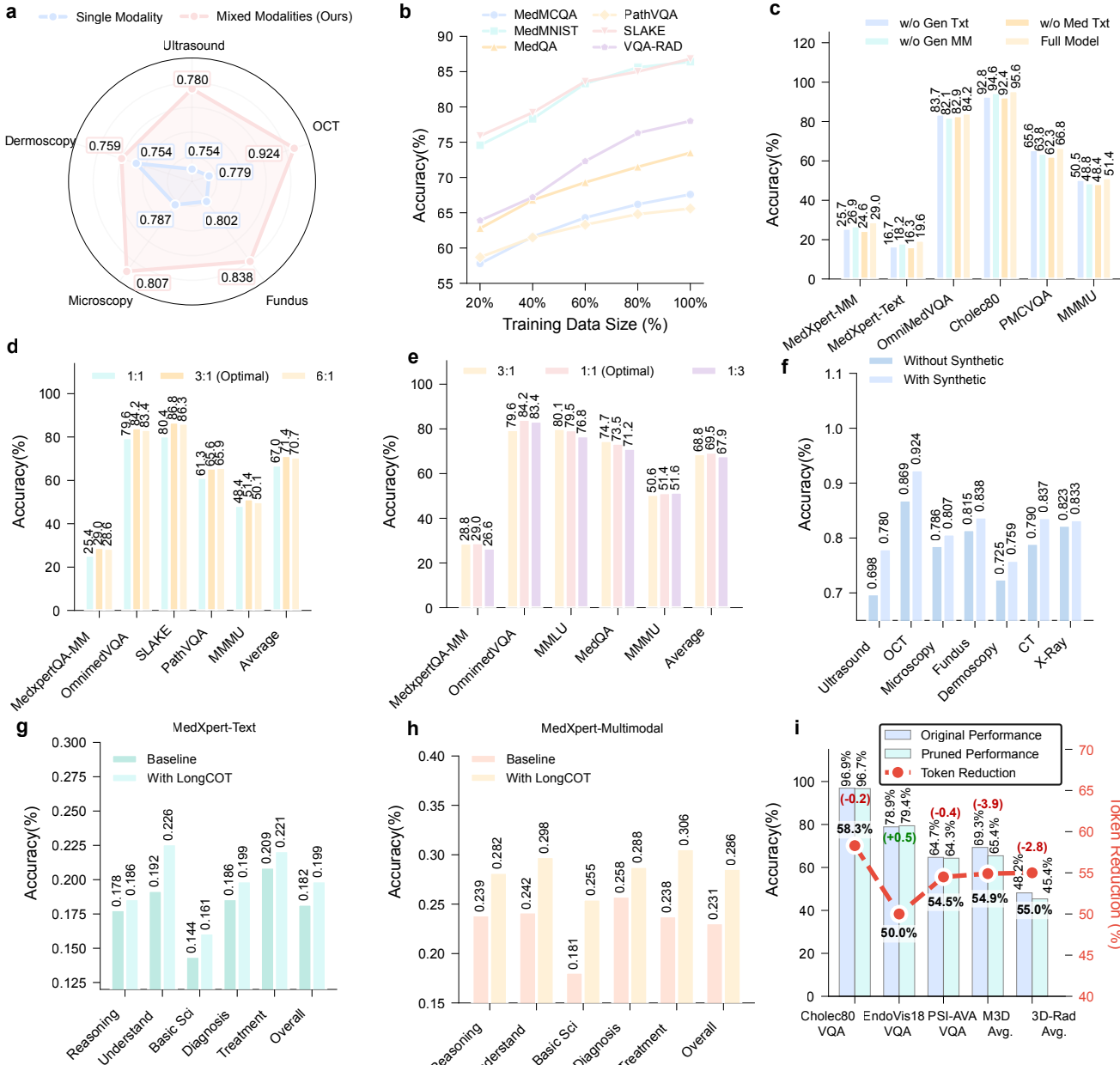


Figure 5. Data curation and architectural analysis of Hulu-Med. **a**, The unified generalist architecture outperforms five individually trained specialist models on their respective underrepresented modalities. **b**, Performance exhibits a positive scaling law, monotonically increasing across text and multimodal benchmarks as training data grows from 20% to 100%. **c**, Ablation on data composition shows that removing any component—general text, general multimodal data, or medical text—degrades performance, confirming each is critical for robust reasoning. **d,e**, Analysis of data mixing ratios reveals optimal balances: 3:1 medical-to-general data mix and 1:1 text-to-multimodal mix yield best performance. **f**, Data enrichment through synthetic long captions improves accuracy across multiple imaging modalities on OmniMedVQA benchmark. **g,h**, Synthetically generated long CoTs provide valuable supervision, significantly improving performance on both text-only (MedXpert-Text) and multimodal (MedXpert-Multimodal) reasoning tasks. **i**, Medical-Aware Token Reduction achieves 55% average token pruning during inference while maintaining performance comparable to the non-pruned model.

Methods

Model Architecture

Hulu-Med is a unified VLM that enables processing a wide spectrum of medical input, including text, 2D images, 3D volumes, and videos, and generates coherent textual responses with a single, end-to-end framework. The model consists of four core components: (1) a rotary position-adaptive visual encoder, (2) a text tokenizer, (3) a multimodal projector, and (4) an LLM decoder.

Rotary Position-Adaptive Visual Encoder The visual processing pipeline begins with the rotary position-adaptive visual encoder, designed to handle heterogeneous medical data by treating all visual inputs as a unified sequence of 2D image planes and adopting image patches as a universal processing unit. The encoder is a 27-layer Vision Transformer (ViT) with a hidden size of 1152, an intermediate MLP size of 4304, and 16 attention heads. Specifically, 3D medical volumes (e.g., CT, MRI) are decomposed into their constituent slices, and videos are sampled into frames. Each plane is then partitioned into a grid of non-overlapping 16×16 pixel patches, which are linearly embedded.

A key innovation is the replacement of standard, fixed-size absolute positional embeddings with 2D RoPE. To encode the relative position of a patch at grid coordinates (m, n) , we apply 1D RoPE along the height and width dimensions independently. Let $\mathbf{q} \in \mathbb{R}^d$ denote a query (or key) vector (d is even). We partition these d features into $d/2$ pairs, where dimensions $2i-1$ and $2i$ form the i -th pair for $i \in \{1, \dots, d/2\}$. For each spatial dimension $p \in \{m, n\}$, we apply a rotation transformation to each pair:

$$\begin{pmatrix} q'_{2i-1} \\ q'_{2i} \end{pmatrix} = \begin{pmatrix} \cos(p\theta_i) & -\sin(p\theta_i) \\ \sin(p\theta_i) & \cos(p\theta_i) \end{pmatrix} \begin{pmatrix} q_{2i-1} \\ q_{2i} \end{pmatrix} \quad (1)$$

where the frequencies are $\theta_i = 10000^{-2i/d}$. The first $d/2$ dimensions encode the height position m , while the remaining $d/2$ dimensions encode the width position n . This design embeds relative spatial information directly into the self-attention mechanism without requiring learned positional embeddings, enabling the encoder to process images of arbitrary resolutions and aspect ratios within a single unified framework.

To manage the heavy computational load from 3D and video modalities, we employ a two-stage token reduction strategy. First, at the **intra-plane level**, we apply local spatial pooling to 3D and video inputs by setting a merge factor of 2. This step combines each 2×2 block of adjacent patch tokens into a single token via bilinear interpolation, reducing the number of visual tokens for each plane by a factor of 4. This pooling is omitted for single 2D images, which pose less computational burden. Second, at the **inter-plane level**, we implement a medical-aware token reduction strategy. This mechanism prunes redundant visual tokens by comparing corresponding patches across adjacent slices or frames. Specifically, for video inputs, we compute the L_1 distance between the embeddings of spatially corresponding patches from consecutive frames: $\text{diff}_t^{(i)} = \|f_v(\mathbf{v}_t)^{(i)} - f_v(\mathbf{v}_{t-1})^{(i)}\|_1$ where $f_v(\mathbf{v}_t) \in \mathbb{R}^{N_v \times d_v}$ represents the visual token embeddings at frame t output by the vision encoder, $f_v(\mathbf{v}_t)^{(i)} \in \mathbb{R}^{d_v}$ denotes the embedding vector of the i -th patch at frame t , and $f_v(\mathbf{v}_{t-1})^{(i)} \in \mathbb{R}^{d_v}$ denotes the embedding of the spatially corresponding patch at frame $t-1$. Patches with $\text{diff}_t^{(i)} < \tau$ (where $\tau = 0.1$) are considered temporally redundant and pruned from frame t . This patch-level pruning strategy is applied during the forward pass after visual encoding and is performed dynamically based on the current visual encoder parameters. The strategy reduces the final visual token count by up to 60% for 3D and video inputs while maintaining comparable performance.

Text Tokenizer For textual input, we employ the tokenizer native to the LLM backbone, which is a Byte-Pair Encoding (BPE) tokenizer with a vocabulary size of 152,064 tokens⁷⁵.

Multimodal Projector To bridge the visual and text domains, a multimodal projector ($g(\cdot)$) aligns the output of the vision encoder with the LLM’s embedding space with a two-layer Multilayer Perceptrons (MLPs). It takes the final sequence of visual patch embeddings from the vision encoder, $f_v(\mathbf{v}) \in \mathbb{R}^{N_v \times d_v}$ ($d_v = 1152$),

and transforms it into a sequence of language-compatible embeddings, $g(f_v(\mathbf{v})) \in \mathbb{R}^{N_v \times d}$:

$$g(f_v(\mathbf{v})) = W_2 \cdot \text{GELU}(W_1 \cdot f_v(\mathbf{v}) + b_1) + b_2, \quad (2)$$

where W_1, W_2, b_1, b_2 refer to the learnable parameters in projector, which is crucial for enabling the LLM $\Phi(\cdot)$ to interpret the visual information as if it were part of its native language space.

LLM Decoder For our primary configuration, Hulu-Med-7B adopts Qwen2.5-7B-Instruct as language model backbone. The processed text embeddings and the projected visual embeddings are concatenated into a single, unified input sequence. The model then processes this sequence auto-regressively, predicting the next token based on all preceding visual and textual tokens. This architecture allows Hulu-Med to perform a diverse array of generative tasks without requiring any task-specific modifications. To demonstrate framework scalability, we also developed Hulu-Med-14B and Hulu-Med-32B, which are built upon Qwen3-14B and Qwen2.5-32B backbone respectively, providing a range of model sizes to balance performance and computational efficiency.

Training Strategy

Hulu-Med is trained with a progressive three-stage curriculum: (1) vision–language alignment, (2) continual medical multimodal pretraining, and (3) mixed-modality instruction tuning. Specifically, stages 1 and 2 consolidate 2D single-image competence, stage 3 introduces interleaved multi-image contexts and spatiotemporal reasoning over 3D volumes and videos. Each stage uses a distinct large-scale data mixture that combines public datasets with targeted synthetic pipelines, addressing two common bottlenecks in medical VLMs: the limited volume and diversity of visual instruction data, and the insufficient integration of general and medical knowledge.

Stage 1: Vision-Language Alignment The initial stage focuses on establishing a foundational alignment between the vision encoder and the LLM backbone. The primary task is short caption generation, where the model learns to produce text for a given image, and the training loss is calculated against the ground-truth caption. To this end, we utilized a corpus of 1.4 million image-text pairs sourced entirely from a collection of public medical datasets ([Extended Tab. 4](#)) including Quilt, MedICaT, and ROCO. This data spans a wide range of modalities and resolutions, enabling the rotary position-adaptive visual encoder to learn to handle diverse visual inputs. During this stage, the LLM backbone remains frozen; we only fine-tune the multimodal projector and the vision encoder with learning rates of 1×10^{-3} and 1×10^{-5} , respectively.

Stage 2: Medical Multimodal Pre-training The second stage aims to inject extensive medical knowledge while enhancing the model’s visual understanding capability, training on a corpus of 4.9 million samples. The training objective is elevated to more complex generative tasks, primarily long-form caption generation and open-ended question answering. For this, we first compiled a 2.6 million sample corpus from public datasets ([Extended Tab. 5](#)). This included long-form medical captions (e.g., PubMedVision) and a variety of general-domain data such as documents and charts, along with approximately 10% general-domain text to preserve core language capabilities.

However, public datasets exhibit a significant long-tail distribution, where modalities like ultrasound and dermatology with detailed text annotations are underrepresented. To mitigate this, we synthesized an additional 2.3 million high-quality long captions. For images with only short captions, a multi-agent pipeline employed a large VLM (Gemini-2.5-Pro) to rewrite them into rich, detailed descriptions, yielding 1.4 million enhanced captions. For images that lacked any text annotations, we implemented a distinct multi-agent generation process where a core VLM generated candidate captions that were then evaluated and ranked by specialized ‘judge’ models. At this pre-training stage, all model components are trainable, with learning rates of 2×10^{-6} (vision encoder), 1×10^{-5} (projector), and 2.5×10^{-5} (LLM), managed by a cosine scheduler.

Stage 3: Mix-Modality Instruction Tuning The final stage trains on a wide spectrum of downstream tasks to encourage the instruction-following ability. We train on a dataset with 10.5 million instances, including discriminative tasks like, VQA and classification, as well as complex generative tasks such as MRG and CoT reasoning. The dataset was gathered from public instruction-tuning data (Extended Tab. 6), including 5.9 million text-based and 4.5 million multimodal instructions, which include diverse formats such as multi-image, interleaved, 3D, and video data.

To address critical data limitation in public resources, we developed three novel synthesis pipelines. First, to enhance multilingual reasoning, we synthesized a 45K sample CoT dataset. Our methodology employed a role-play prompting strategy combined with rejection sampling, where we retained only the reasoning paths that ends up with correct final answers. Second, we generated 600K high-quality VQA pairs by prompting Gemini-2.5-Pro to create questions directly answerable from our generated long captions. Finally, to overcome the scarcity of annotated medical videos, we developed a “divide-and-conquer” captioning method, yielding 20K video captions. During this stage, all model parameters remained trainable, with the LLM learning rate increased to 5×10^{-5} .

Evaluation Framework and Metrics

To comprehensively assess the capabilities of **Hulu-Med**, we established a comprehensive and rigorous evaluation framework, examining the model’s performance on various data modalities and clinical tasks, ensuring a holistic understanding of its strengths and limitations. The benchmarks are organized by modality—text, 2D images, 3D volumes, and video—with appropriate metrics tailored to each task type.

Text-Based Medical Reasoning and Generalization To ensure that multimodal training maintains core textual knowledge and reasoning ability, we evaluated the model on both standard medical benchmarks and specialized generalization tasks. For text-only question-answering, we assess medical knowledge without visual input across eight challenging benchmarks simulating professional medical board examinations (MedQA-USMLE, MedMCQA, MMLU-Med, MedBullets), evaluating factual recall from biomedical literature (PubMedQA), and probing advanced expert-level reasoning skills (MMLU-Pro-Med, MedXpertQA-Text, SuperGPQA-Medical). For these multiple-choice benchmarks, we report accuracy as the primary performance measure, quantifying the percentage of correct predictions against ground-truth labels.

In addition, we also assess the model for real-world deployment on three benchmarks. MMedBench evaluates multilingual medical understanding across six languages (English, Chinese, Spanish, French, Russian, and Japanese), with performance measured using accuracy on multiple-choice questions. HealthBench assesses conversational safety and clinical performance in realistic multi-turn dialogues against fine-grained physician-authored rubrics, covering seven core clinical competency themes: Global Health, Communication, Context Seeking, Emergency Referrals, Hedging, Health Data Tasks, and Complex Responses. RareBench measures diagnostic reasoning on rare diseases, testing performance in data-scarce scenarios where the model must handle uncommon clinical presentations with limited training examples.

For complex open-ended response tasks requiring nuanced evaluation, we employ advanced LLMs as judges. In HealthBench, given the complexity of physician-designed rubrics and the need to assess long-form conversational responses, we use Gemini-2.5-Pro as judge. For diagnostic reasoning tasks in RareBench, evaluation is conducted using ChatGPT-4o-latest, which assesses the correctness and clinical appropriateness of differential diagnoses.

2D Medical Image Understanding We assess performance on two primary tasks: VQA and MRG. For VQA, we adopt seven benchmarks to test visual-language alignment across multiple dimensions: broad multi-modal understanding across various imaging types (OmniMedVQA, PMC-VQA), domain-specific knowledge in radiology (VQA-RAD, SLAKE) and pathology (PathVQA), and higher-order cognitive skills integrating external knowledge with visual reasoning (MedXQA, MMMU-Med). For classification tasks

on MedMNIST and the majority of closed-ended VQA benchmarks, we report accuracy as the primary metric.

For MRG, we evaluate the model’s ability to produce clinically accurate reports from chest radiographs on the MIMIC-CXR, CheXpert, and IU X-ray datasets. We employ a multi-faceted approach for these generative tasks: linguistic fluency is assessed using standard NLG metrics, including BLEU (1-4), ROUGE-L, and METEOR; to measure the inclusion of key clinical concepts, we compute recall; and to assess clinical utility beyond lexical similarity, we incorporate RaTEScore, a domain-specific metric that evaluates the semantic correctness of medical entities, their attributes, and negations.

3D Volumetric and Spatiotemporal Analysis To evaluate Hulu-Med’s ability to process 3D volumetric data, we select benchmarks that test both anatomical understanding and temporal reasoning within image series. Specifically, for 3D spatial reasoning, including tasks like plane detection and organ identification, we primarily evaluate on the M3D benchmark. To assess a broader spectrum of clinical reasoning skills, we employ the comprehensive 3D-RAD benchmark, which is composed of multiple distinct sub-tasks, from descriptive generation (e.g., anomaly detection and image observation) and closed-ended classification (e.g., existence) to both static and longitudinal temporal diagnosis.

Our evaluation strategy for 3D tasks mirrors that of the 2D domain. For reasoning tasks within the M3D and 3D-RAD benchmarks, performance on closed-ended questions is measured by accuracy, while descriptive, open-ended sub-tasks are evaluated using recall to assess the coverage of key clinical information. To test its generative capabilities, we use the AMOS-MM benchmark to assess the quality and clinical fidelity of 3D medical report generation, employing the same combination of NLG metrics (BLEU, ROUGE-L, METEOR) and the clinically-aligned RaTEScore.

Surgical and Medical Video Comprehension The model’s ability to interpret dynamic visual data is tested on a set of video-based benchmarks. Surgical video datasets, including Cholec80-VQA, EndoVis18-VQA, PSI-AVA-VQA, and the general SurgeryVideoQA, are used to evaluate the understanding of surgical phases, instruments, and actions. Additionally, the MedFrameQA benchmark is used to specifically assess multi-frame temporal reasoning across various medical imaging sequences, testing the model’s ability to comprehend dynamic processes.

Our evaluation strategy is tailored to the specific characteristics of each dataset. For Cholec80-VQA, where most questions are closed-ended, we primarily use accuracy as the evaluation metric. For EndoVis18-VQA and PSI-AVA-VQA, where answers consist of short descriptive phrases, we employ recall to evaluate whether the model captures the essential clinical concepts. For MedFrameQA, we similarly adopt accuracy as the metric since it comprises multiple-choice questions. For SurgeryVideoQA, which features open-ended questions requiring free-form responses, traditional metrics are insufficient; therefore, we utilize ChatGPT-4o-latest as an automated judge to assess answer quality through semantic evaluation. Furthermore, to ensure a more comprehensive evaluation, we extend the use of ChatGPT-4o-latest beyond SurgeryVideoQA to Cholec80-VQA, EndoVis18-VQA, and PSI-AVA-VQA, where answers range from single words to short phrases, as a supplementary metric. This provides a semantic assessment that captures clinical correctness beyond simple lexical matching.

Code and Data Availability

The detailed implementation, including fine-tuned models and code, as well as all datasets used in this work, are publicly available at <https://github.com/ZJUI-AI4H/Hulu-Med>. Detailed licensing information and data download links can be found in [Extended Table 9](#).

Author Contributions Statement

W.X., J.S., J.W., and Z.L. conceived the project. S.J. designed the algorithm and performed model training. Y.W., C.Z., Y.Z., B.P., and S.S. carried out data collection. S.J., Y.W., and T.H. designed the experiments.

Data analysis was conducted by S.J., J.T.Z., J.H., Z.C., R.W., J.L., H.X., T.T., K.L., J.X., B.F., and F.Z. The figures were generated and revised by C.Z., S.J., T.H., Z.Y., and Y.F. The results were interpreted by S.J., W.X., J.S., J.W., and Z.L. The manuscript was written by S.J., T.H., Z.L., J.S., and W.X. All authors contributed to the final revision of the manuscript.

Competing Interests Statement

S.S. and Z.Y. are employees of Alibaba Inc. Y.F. is an employee of Angelalign Technology Inc. T.T. is an employee of China Mobile Group Zhejiang Company Limited. The remaining authors declare no competing interests.

Extended Table 1. Comparison of medical vision-language models

Model	Model Sizes	Open Model	Open Data	Data Size	General	Data Source			Modalities	Downstream Tasks			
						From Papers	Medical	Real-world		Text	2D	3D	Video
Lingshu	7B, 32B	✓	✗	12.2M	7.15M	2.6M	2.45M	12	✓	✓	✗	✗	✗
HuatuogPT-Vision	7B, 34B	✓	✓	1.3M	-	1.3M	-	9	✗	✓	✗	✗	✗
LLaVA-Med	7B	✓	✓	560K	-	560K	-	4	✗	✓	✗	✗	✗
RadFM	16M	✓	✓ [*]	-	-	14.16M	1.84M	6	✗	✓	✓	✗	✗
HealthGPT	4B, 14B	✓	✓	1.82M	558K	1.21M	56K	7	✗	✓	✗	✗	✗
Hulu-Med (Ours)	4B, 7B, 14B, 32B	✓	✓	16.6M	4.5M	1.8M	10.3M	14	✓	✓	✓	✓	✓

^{*}Partially open-sourced, requires application for some datasets. "From Papers" refers to data from PubMed/PMC.

Extended Table 2. Overview of medical benchmarks

Benchmark	Type	Mod.	w/ Clin.	Num.	Dist.	Data Source Description
MMLU-Med	QA	text	No	633	in-domain	USMLE practice exams, textbooks, prep materials
PubMedQA	QA	text	Yes	1000	in-domain	PubMed biomedical abstracts and conclusions
MedMCQA	QA	text	No	6150	in-domain	AIIMS PG & NEET-PG official exam banks (1991–present)
MedQA	QA	text	No	1273	in-domain	USMLE, Chinese & Taiwanese medical license exam questions
MedBullets	QA	text	No	124	ood	USMLE Step 2 & 3 style questions from MedBullets platform
SGPQA	QA	text	No	2755	ood	Graduate-level multiple-choice expert-authored questions
MMLU-Pro-Med	QA	text	No	818	ood	Academic exams & textbooks (medical portion)
MedXpertQA-Text	QA	text	Yes	2000	ood	Expert-level exam questions + clinical images & patient records
MedXpertQA-MM	QA	2D	Yes	2000	ood	Expert-level exam questions + clinical images & patient records
OmniMedVQA	Mixed	Mixed	Yes	87944	ood	Images and QAs from 73 medical datasets (12 modalities)
PMC-VQA	VQA	2D	Yes	33430	in-domain	Figures and captions from PubMed Central OA articles
MMMU-Med	VQA	2D	No	1751	ood	College-level exams, quizzes, and textbooks (Health & Medicine)
VQA-RAD	VQA	2D	Yes	451	in-domain	Radiology images with clinician-authored QAs
SLAKE	VQA	2D	Yes	1061	in-domain	Radiology images + knowledge graph generated QAs
PathVQA	VQA	2D	Yes	6761	in-domain	Pathology images from textbooks & digital libraries
MedMNIST	Class.	2D	No	22602	in-domain	Biomedical images (public datasets, downsampled, CC licensed)

Continued on next page

Benchmark	Type	Mod.	w/ Clin.	Num.	Dist.	Data Source Description
MIMIC-CXR	MRG	2D	Yes	2343	in-domain	377,110 chest X-rays + reports from BIDMC hospital (2011–2016)
CheXpert	MRG	2D	Yes	234	in-domain	224,316 chest radiographs with uncertainty labels
IU-Xray	MRG	2D	Yes	590	in-domain	3,996 reports, 8,121 X-rays from Indiana Network for Patient Care
M3D	Mixed	3D	Yes	27582	in-domain	120K 3D CT image-report pairs, plus 25 public segmentation datasets
3D-Rad	Mixed	3D	Yes	33910	in-domain	25,692 chest CT scans + reports, 21,304 patients
AMOS	MRG	3D	Yes	400	ood	500 abdominal CT + 100 MRI with 15 organ annotations
MedFrameQA	VQA	Video	Yes	2850	ood	Multi-image QA from clinical/educational surgical videos (YouTube etc.)
Cholec80-VQA	VQA	Video	Yes	6606	in-domain	QA based on Cholec80 dataset (80 laparoscopic cholecystectomy videos)
EndoVis18-VQA	VQA	Video	Yes	643	in-domain	QA derived from EndoVis 2018 surgical scene segmentation dataset
PSI-AVA-VQA	VQA	Video	Yes	4402	in-domain	Holistic surgical scene dataset with ~4402 QA pairs
SurgeryVideoQAVQA	VQA	Video	Yes	2690	in-domain	QA derived from Cholec80 surgical workflow dataset
HealthBench	Case	text	No	5000	ood	5,000+ simulated medical conversations with evaluation rubrics designed by 262 physicians
RareBench	Case	text	Yes	1122	ood	1,197 rare disease patient cases (Electronic Health Records)
MMedBench	VQA	text	Yes	8518	in-domain	21 medical fields, including Internal Medicine, Biochemistry, Pharmacology, and Psychiatry

Extended Table 3. Comprehensive modality coverage in the Hulu-Med dataset, detailing its 14 main modalities and 65 listed sub-modality examples.

Main Modality	Sub-modalities and Examples
CT	CTA, CECT, DECT, HRCT, CBCT, Cardiac CT, etc.
MRI	fMRI, DTI, DWI, SWI, MRA, MRCP, MRV, Cardiac MRI/CMR, etc.
Radiography (X-ray)	Chest X-ray (CXR), Mammography/DBT, DXA/DEXA, etc.
Ultrasound	Echocardiography, Doppler, CEUS, IVUS, etc.
Nuclear Medicine	PET, FDG-PET, PET/CT, PET/MRI, SPECT, Scintigraphy, Gamma Camera, etc.
Fluoroscopy	C-arm Fluoroscopy, Cinefluoroscopy, Voiding Cystourethrography (VCUG), etc.
Angiography	Catheter Angiography, Coronary Angiography, Venography, DSA, etc.
Endoscopy	Gastroscopy, Colonoscopy, Bronchoscopy, Arthroscopy, Laparoscopy, etc.
OCT	SD-OCT, SS-OCT, OCTA, OFDI, LC-OCT, HF-OCT, etc.
Ophthalmic Imaging	Fundus Photography, Fluorescein Angiography (FA), ICG Angiography (ICGA), SLO/SLO-AF, RetCam, Ophthalmoscopy, etc.
Dermatology Imaging	Dermoscopy, Trichoscopy, Reflectance Confocal Microscopy (RCM), etc.
Pathology/Microscopy	Histopathology, Cytology/Cytopathology, Immunohistochemistry (IHC), Electron Microscopy (SEM/TEM), Gross Pathology, etc.
Clinical Photography	Digital Photography, Clinical Photograph/Image/View, etc.
Physiological Signals	Medical Graph/Chart/Diagram, ECG/EKG/EEG, etc.

Extended Table 4. Stage 1 training data composition (1.42M entries)

Category	Modality	Dataset Name	Entry Count
Short Caption	<i>Histopathology</i>	Quilt-LLaVA-Pretrain	723,328
	<i>Clinical</i>	biomedica-clinical	395,616
	<i>Multimodal</i>	Medcat	217,060
	<i>Radiology</i>	ROCOv2-radiology	79,793
		Medpix2.0	2050
		GRAND TOTAL	1,417,847

Extended Table 5. Stage 2 training data composition (4.85M entries)

Source	Modality / Domain	Dataset Name	Entry Count
Synthetic Data	<i>Medical Clinical Caption</i>	biomedica_clinical_synthetic	350,768
	<i>Medical Dermatology Caption</i>	biomedica_dermatology_synthetic	111,901
		dermoscopy_synthetic	196,537
	<i>Medical Histopathology</i>	biomedica_histopathology_synthetic	194,075
	<i>Medical Microscopy Caption</i>	biomedica_microscopy_synthetic	104,830
		Microscopy_synthetic	22,417
	<i>Medical Surgery Caption</i>	biomedica_surgery_synthetic	99,024
	<i>Medical Radiology Caption</i>	ROCOv2_radiology_synthetic	79,788
		mimic_synthetic	242,009
		iu_xray_synthetic	2365
Public Released	<i>Medical Multimodal Caption</i>	medicat_synthetic	217,052
		medmnist_synthetic	149,704
		train_all_reformat2_synthetic	3363
	<i>Medical Fundus Caption</i>	Fundus_OCT_synthetic	86,139
	<i>Medical Ultrasound Caption</i>	Ultrasound_synthetic	28,559
		Radimagenet_synthetic	379,030
	Synthetic Data Subtotal		2,267,561
	<i>Medical Multimodal Caption</i>	PubMedVision_Alignment_VQA2	646,759
	<i>Medical Grounded Caption</i>	MedTrinity161K	161,630
	<i>General Multimodal Caption</i>	LLaVA-ReCap-558K	558,128
		pixmo-cap	706,830
	<i>General Chart Caption</i>	processed_charts_data	4000
	<i>General Document Caption</i>	textOCR_train	25,117
	<i>General Text</i>	Infinity-Instruct	479,997
	Public Data Subtotal		2,582,461
	GRAND TOTAL		4850022

Extended Table 6. Stage 3 training data composition (~10.4M entries)

Text Data (5.9M)			Multimodal Data (4.5M)			
	Task	Dataset	Count	Task	Dataset	Count
Medical	Factoid QA	Apollo-Pre	1,859,880	2D VQA	PubMedVision	646,750
		MedQuAD	16,407		Generated QA	594,237
	LongCoT Data	II-Medical SFT	700,000		PMC-VQA	152,602
		ReasonMed	369,983		MIMIC-CXR-VQA	77,035
	Reasoning Data	medical-o1	65,531		PathVQA	39,510
		MedReason	32,682		SLAKE	9837
		medical-r1	22,000		RADVQA	6128
		MedThought	7716		GMAI-Reasoning	7004
	Clinical Dialogue	Miriad (Sampled)	1,255,356	Classification	MedMNIST	74,689
		HealthCareMagic	112,165		MIMIC-CXR-MRG	242,310
		iCliniq	7321		CheXpert-MRG	223,228
	Medical Instruct	AlpaCare	52,002		IU-Xray-MRG	2365
		Apollo-SFT	417,241	3D Caption	M3D-Cap	31,928
	Multilingual QA	MMedC	45,048		CT-Rate-Cap	47,149
			Subtotal 4963332		RadFM-Cap	26,891
	General	Openhermes	496,743		AMOS-Cap	1286
		Glaive-code-assist	182,240	3D VQA	M3D-VQA	84,144
		CamelAI	78,390		RadFM-VQA	83,049
		Metamath	56,448		CT-Rate-VQA	46,033
		Evollnstruct_70k	51,948		AMOS-VQA	13,735
		Cot_alpaca_gpt4	42,026	Video Caption	Cholec80-Cap	17,010
		Airoboros2.2	35,380		PSI-AVA-Cap	1195
		Platypus	22,280		EndoVis-Cap	165
		GPT-4 Comparison	14,928	Video QA	Cholec80-VQA	24,829
		UnnaturalInstruct	8610		PSI-AVA-VQA	5244
		CogStackMed	4443		EndoVis-VQA	4358
	LMsys Chatbot Arena	LMSys Chatbot Arena	3136	Ground QA	CoPESD	74,561
		Caseus_custom	2688		Quilt-Instruct	105,745
		Lmsys1m	1631		Llava-Med-Instruct	56,408
		Econ_domain_expert	660	Subtotal 1001551		Subtotal 2699370
				Instruction	LLaVA_NeXT	779,287
					VQA	268,309
	General			Interleaved	Llava-Interleaved	36,541
					Mantis	696,781
				Video QA	NextQA	3870
					STAR	3032
	3D Imaging			3D Imaging	Embodied 3D	4989
					Subtotal 1792809	

GRAND TOTAL

10,457,117

Extended Table 7. Prompt templates for different task types during inference

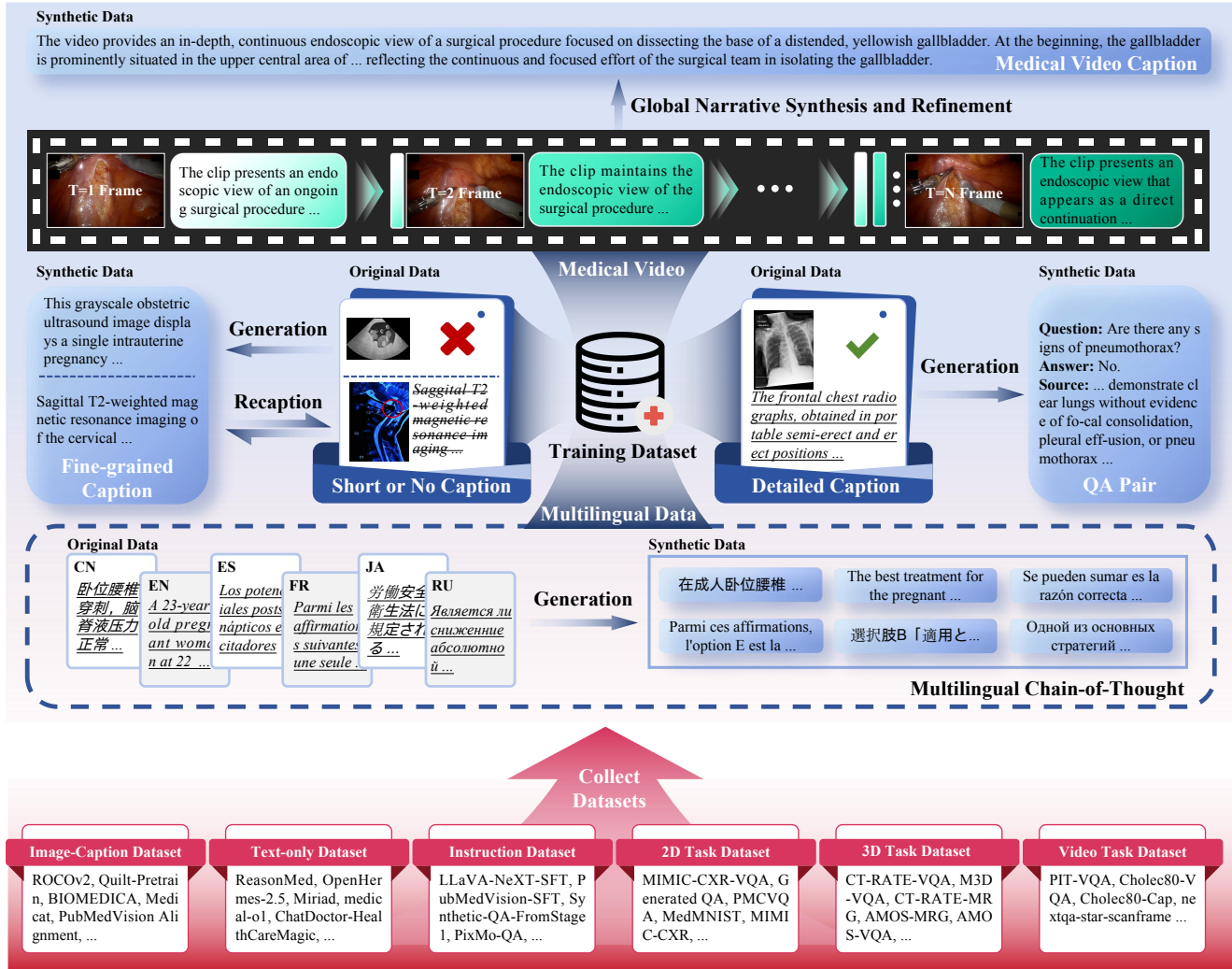
Task Type	Prompt for Direct Answering	Prompt for CoT Reasoning
Multiple-Choice	Question: {Question} Options: {Options} Answer with the option's letter from the given choices directly.	Question: {Question} Options: {Options} Please reason step by step, and put your final answer within \boxed{ }.
Judgement	{Question} Please output 'yes' or 'no' (no extra output).	{Question} Please reason step by step, and put your final answer within \boxed{ }.
Close-Ended	{Question} Answer the question using a single word or phrase.	{Question} Please reason step by step, and put your final answer within \boxed{ }.
Open-Ended	{Question} Please answer the question concisely.	{Question} Please reason step by step, and put your final answer within \boxed{ }.
Report Generation	You are a helpful assistant. Please generate a report for the given images, including both findings and impressions. Return the report in the following format: Findings: {} Impression: {}.	

Extended Table 8. Performance comparison on MedFrameQA. For each metric (column), the best and second-best results are highlighted in **bold** and with an underline, respectively. *SD* indicates the standard deviation of accuracy across frame counts (2–5), reflecting prediction stability.

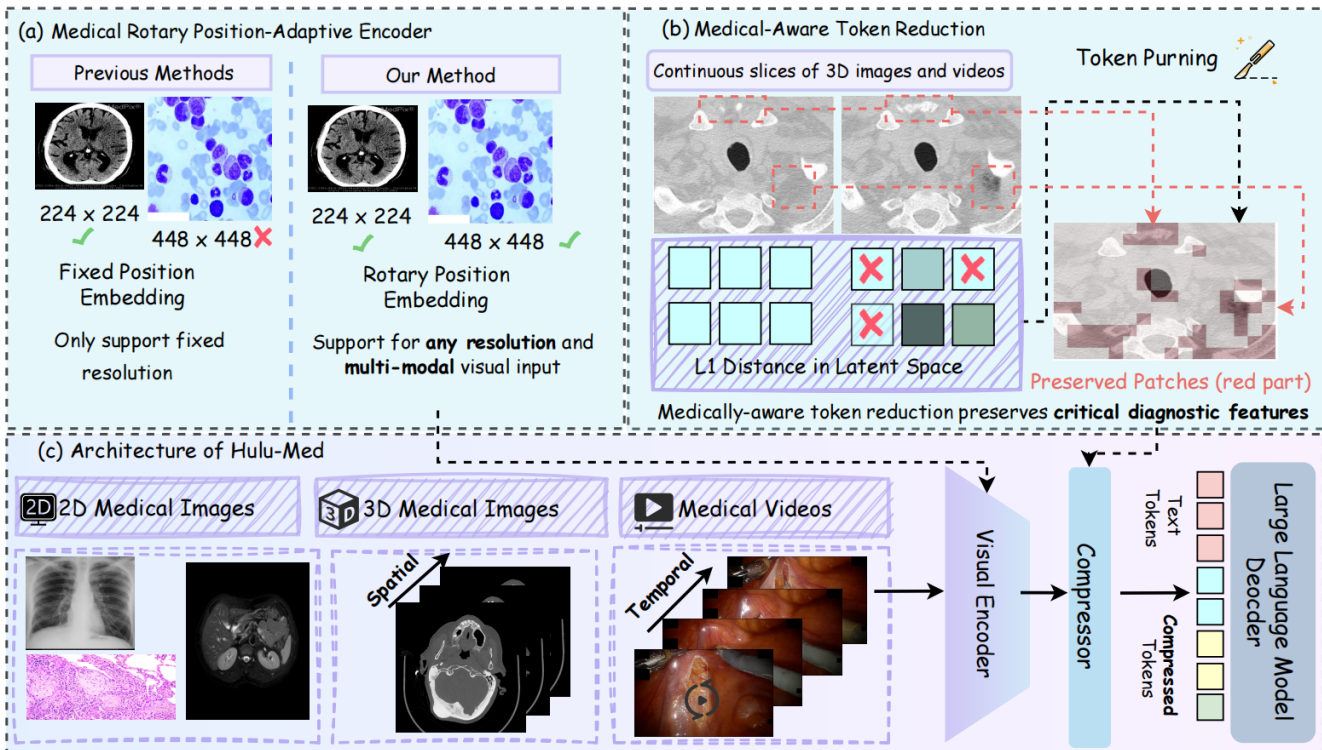
Model	Accuracy (%) by Frame Count					Accuracy (%) by Modality				
	2	3	4	5	SD	CT	MRI	Ultrasound	X-ray	Other
o1	48.16	45.64	51.43	48.15	2.37	48.98	45.40	49.05	49.16	51.64
o3	50.00	47.46	53.60	51.38	2.57	50.09	48.57	51.45	53.06	52.38
o4-mini	50.21	46.23	50.00	50.37	1.99	48.08	48.85	52.34	50.33	53.49
Gemini-2.5-Flash	53.54	55.48	55.47	55.76	1.02	54.57	53.60	57.36	58.14	49.24
QvQ-72B-Preview	46.88	45.91	46.48	46.69	0.42	45.45	45.24	50.65	44.85	57.58
GPT-4-Turbo-V	47.47	45.51	46.88	46.34	0.83	46.83	43.48	50.65	49.17	51.52
GPT-4o	47.30	45.18	40.23	45.35	3.01	45.52	43.27	48.58	47.51	51.52
GPT-4o-mini	35.16	36.21	32.42	33.09	1.77	35.26	34.31	34.88	34.55	29.55
Claude-3.7-Sonnet	49.41	48.01	51.56	50.68	1.55	50.75	49.11	49.10	49.83	46.21
Qwen2.5-VL-72B-Instruct	41.99	40.40	38.67	40.32	1.36	38.99	40.73	42.38	42.52	49.24
Hulu-Med-7B	55.14	57.31	57.42	58.98	1.47	55.69	55.16	<u>59.43</u>	63.12	57.58
Hulu-Med-14B	60.29	60.63	57.81	59.85	1.26	59.89	<u>58.29</u>	59.17	63.46	68.18
Hulu-Med-32B	58.77	59.14	57.42	<u>59.48</u>	0.80	58.58	58.39	61.76	58.80	57.58

Extended Table 9. Data availability and licenses for datasets used in our study. “Access” directly lists the dataset license. Synthetically generated datasets and those requiring specific permissions are marked as *Credentialed Access*.

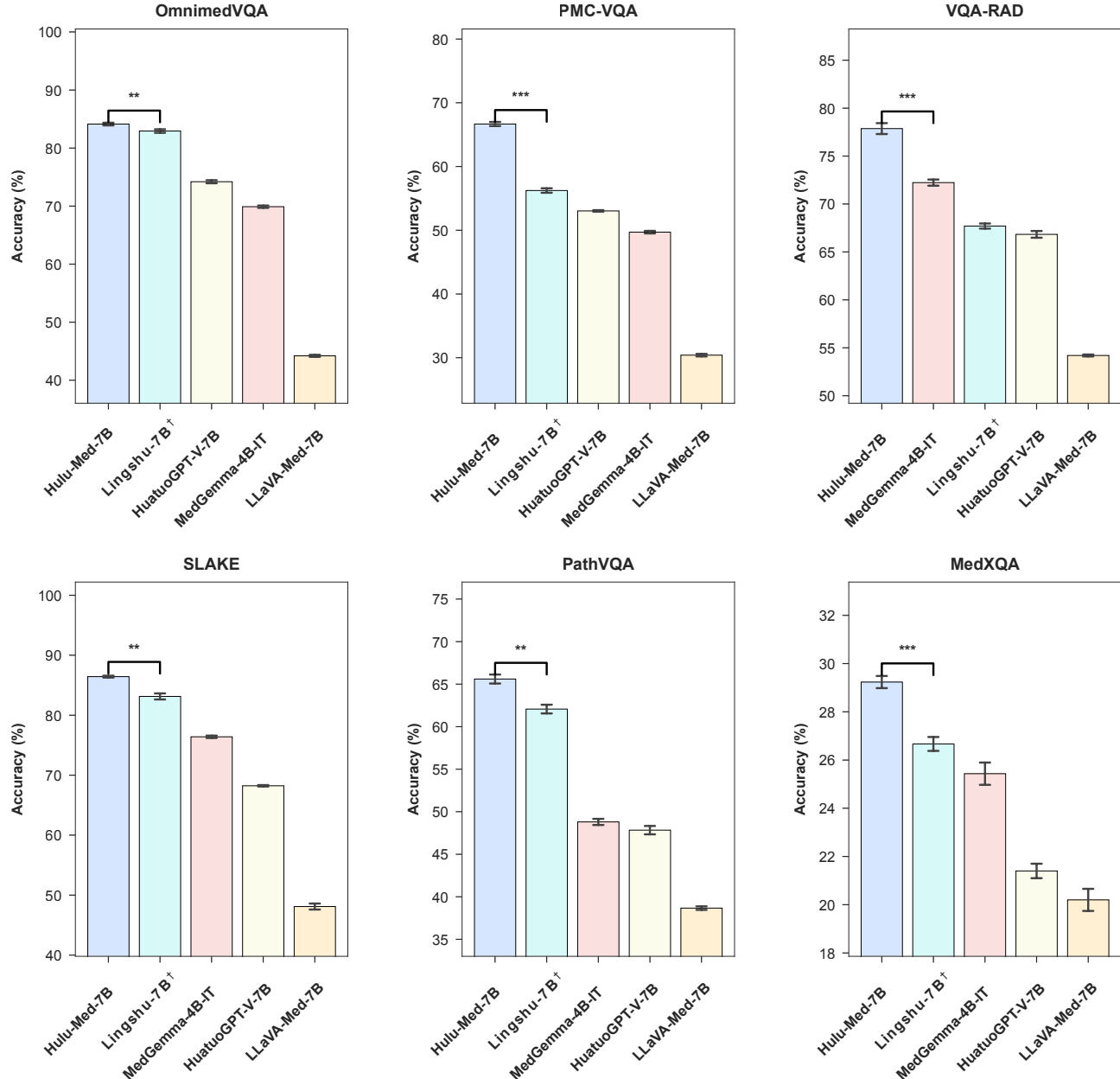
Dataset Name	Link	Access
Stage 1		
BIOMEDICA Clinical Subset (medical multimodal)	https://minwoosun.github.io/biomedica-website/	Under CC
Medicat (medical multimodal)	https://github.com/allenai/medicat	PhysioNet License
MedPix 2.0 (medical multimodal)	https://huggingface.co/datasets/CHILab1/MedPix-2.0	CC BY-NC-SA 4.0
Quilt-Pretrain (medical multimodal)	https://huggingface.co/datasets/wisdomik/Quilt-LLaVA-Pretrain	CC BY 4.0
ROCOv2 (medical multimodal)	https://huggingface.co/datasets/eltorio/ROCOv2-radiology	CC BY 4.0
Stage 2		
biomedica_clinical_recaption (medical multimodal)	Synthetic Data	Credentialed Access
biomedica_dermatology_recaption (medical multimodal)	Synthetic Data	Credentialed Access
biomedica_histopathology_recaption (medical multimodal)	Synthetic Data	Credentialed Access
biomedica_microscopy_recaption (medical multimodal)	Synthetic Data	Credentialed Access
biomedica_surgery_recaption (medical multimodal)	Synthetic Data	Credentialed Access
Dermoscopy_SyntheticCap (medical multimodal)	Synthetic Data	Credentialed Access
Fundus_OCT_SyntheticCap (medical multimodal)	Synthetic Data	Credentialed Access
LLaVA-ReCap-558K (general multimodal)	https://huggingface.co/datasets/lmms-lab/LLaVA-ReCap-558K	CC BY 4.0
medicat_recaption (medical multimodal)	Synthetic Data	Credentialed Access
medmnist_generated_captions (medical multimodal)	Synthetic Data	Credentialed Access
MedTrinity161K (medical multimodal)	https://proceedings.iclr.cc/paper_files/paper/2025/hash/11c483499c285f30daf832c17dc752bd-Abstract-Conference.html	Unknown
Microscopy_SyntheticCap (medical multimodal)	Synthetic Data	Credentialed Access
mimic-pretrain-recaption (medical multimodal)	Synthetic Data	Credentialed Access
pixmo-cap (general multimodal)	https://huggingface.co/datasets/allenai/pixmo-cap	odc-by
processed_charts_data (general multimodal-Chart)	https://huggingface.co/datasets/LeroyDyer/chart_text_to_Base64	MIT
PubMedVision_Alignment (medical multimodal)	https://huggingface.co/datasets/FreedomIntelligence/PubMedVision	CC BY 4.0
Rad-Slake-Pvqa-SyntheticCap (medical multimodal)	Synthetic Data	Credentialed Access
RadImagenet_SyntheticCap-Ultrasound (medical multimodal)	Synthetic Data	Credentialed Access
ROCOv2-radiology-recap (medical multimodal)	https://huggingface.co/datasets/eltorio/ROCOv2-radiology	CC BY 4.0
TextOCR (general multimodal-Scene Text Image)	https://www.kaggle.com/datasets/robikscube/textocr-text-extraction-from-images-dataset	MIT
Ultrasound_SyntheticCap (medical multimodal)	Synthetic Data	Credentialed Access
Mimic-recaption (medical multimodal)	Synthetic Data	Credentialed Access
IUXray-recaption (medical multimodal)	Synthetic Data	Credentialed Access
Infinstruct (general text)	https://huggingface.co/datasets/BAII/Infinity-Instruct	CC BY SA 4.0
Stage 3		
AlpaCare-MedInstruct-52k (medical text)	https://huggingface.co/datasets/lavita/AlpaCare-MedInstruct-52k	CC BY 4.0
ChatDoctor-HealthCareMagic-100k (medical text)	https://huggingface.co/datasets/lavita/ChatDoctor-HealthCareMagic-100k	CC BY 4.0
GMAI-Reasoning10K (medical multimodal)	https://huggingface.co/datasets/General-Medical-AI/GMAI-Reasoning10K	CC BY 4.0
iCliniq-10K (medical text)	https://huggingface.co/datasets/zhengComing/iCliniq-10K	CC BY 4.0
LLaVA-Med (interleaved) (medical multimodal)	https://github.com/microsoft/LLaVA-Med	CC BY 4.0
LLaVA-NeXT-SFT (general multimodal)	https://huggingface.co/datasets/lmms-lab/LLaVA-NeXT-Data	Apache 2.0
Manitis-Instruct (interleaved) (general multimodal)	https://huggingface.co/datasets/TIGER-Lab/Manitis-Instruct	Apache 2.0
Medical-01 (medical text)	https://huggingface.co/datasets/FreedomIntelligence/medical-01-verifiable-problem	CC BY 4.0
Medical-R1-Distill (medical text)	https://huggingface.co/datasets/FreedomIntelligence/Medical-R1-Distill-Data	CC BY 4.0
MedQuAD (medical text)	https://huggingface.co/datasets/lavita/MedQuAD	CC BY 4.0
MedReason (medical text)	https://huggingface.co/datasets/UCSC-VLAA/MedReason	CC BY 4.0
MedThoughts-8K (medical text)	https://huggingface.co/datasets/hw-hwei/MedThoughts-8K	MIT
Miriad (20% sample) (medical text)	https://huggingface.co/miriad	Apache 2.0
OpenHermes-2.5 (general text)	https://huggingface.co/datasets/tekrium/OpenHermes-2.5	Apache 2.0
Pixmo-QA (general multimodal)	https://huggingface.co/datasets/allenai/pixmo-cap	ODC-BY v1.0
PubMedVision-SFT (medical multimodal)	https://huggingface.co/datasets/FreedomIntelligence/PubMedVision	CC BY 4.0
QUILT-Instruct (medical multimodal)	https://huggingface.co/datasets/wisdomik/QUILT-LLaVA-Instruct-107K	CC BY 4.0
ReasonMed (medical text)	https://huggingface.co/datasets/lingshu-medical-mllm/ReasonMed	Apache 2.0
Synthetic-QA (medical multimodal)	Synthetic Data	Credentialed Access
Apollo (medical text)	https://huggingface.co/datasets/FreedomIntelligence/ApolloCorpus	Apache 2.0
II-Medical-Reasoning-SFT (medical text)	https://huggingface.co/datasets/Intelligent-Internet/II-Medical-Reasoning-SFT	Open Access
Multilingual_COT (medical text)	Synthetic Data	Credentialed Access
LLaVA-Next-Interleaved (general multimodal)	https://huggingface.co/datasets/lmms-lab/LLaVA-NeXT-Interleave-Bench	CC BY 4.0
AMOS-MRG (medical multimodal)	https://huggingface.co/datasets/mrrmx/CADS-dataset/blob/0d144b4c8c487d1337e80cae1762a501451349a2/0038_amos/README_0038_amos.md	CC BY-NC-SA
AMOS-VQA (medical multimodal)	https://huggingface.co/datasets/mrrmx/CADS-dataset/blob/0d144b4c8c487d1337e80cae1762a501451349a2/0038_amos/README_0038_amos.md	CC BY-NC-SA
CheXpert (medical multimodal)	https://imai.stanford.edu/datasets/chexpert-plus	PhysioNet License
Cholec80-Cap (medical multimodal)	https://camma.unistra.fr/datasets	CC BY 4.0
Cholec80-VQA (medical multimodal)	https://camma.unistra.fr/datasets	CC BY 4.0
CT-RATE-MRG (medical multimodal)	https://huggingface.co/datasets/brahimhamamci/CT-RATE	CC BY-NC-SA 4.0
CT-RATE-VQA (medical multimodal)	https://huggingface.co/datasets/brahimhamamci/CT-RATE	CC BY-NC-SA 4.0
Endovis-18-Cap (medical multimodal)	https://github.com/lalithjets/Surgical_VQA	CC BY-NC-SA
Endovis-18-VQA (medical multimodal)	https://github.com/lalithjets/Surgical_VQA	CC BY-NC-SA
IU-Xray (medical multimodal)	https://openi.nlm.nih.gov	Open Access
M3D-MRG (medical multimodal)	https://github.com/BAFI-DCAI/M3D	Apache 2.0
M3D-VQA (medical multimodal)	https://huggingface.co/datasets/GoodBaiBai88/M3D-VQA	Apache 2.0
MedMNIST (medical multimodal)	https://huggingface.co/datasets/albertvillanova/medmnist-v2	CC BY 4.0
MIMIC-CXR (medical multimodal)	https://physionet.org/content/mimic-cxr	PhysioNet License
MIMIC-CXR-VQA (medical multimodal)	https://github.com/baeseongsu/mimic-cxr-vqa	MIT license
nextqa-star-scanframe	https://huggingface.co/datasets/ShareGPTVideo/train_video_and_instruction	MIT license
PMC-VQA (medical multimodal)	https://huggingface.co/datasets/RadGenome/PMC-VQA	CC BY-NC-SA 4.0
PSI-AVA-Cap (medical multimodal)	https://github.com/BCV-Uniondes/TAPIR	CC BY-NC-SA 4.0
PSI-AVA-VQA (medical multimodal)	https://github.com/BCV-Uniondes/TAPIR	MIT
RadVQA Rewriting (medical multimodal)	Synthetic Data	Credentialed Access
SLAKE Rewriting (medical multimodal)	Synthetic Data	Credentialed Access
PathVQA Rewriting (medical multimodal)	Synthetic Data	Credentialed Access
RP3D-VQA (medical multimodal)	https://github.com/chaoyi-wu/RadFM	Credentialed Access
RP3D-MRG (medical multimodal)	https://github.com/chaoyi-wu/RadFM	Credentialed Access
CoPESD (medical multimodal)	https://github.com/gkw0010/CoPESD	Apache 2.0



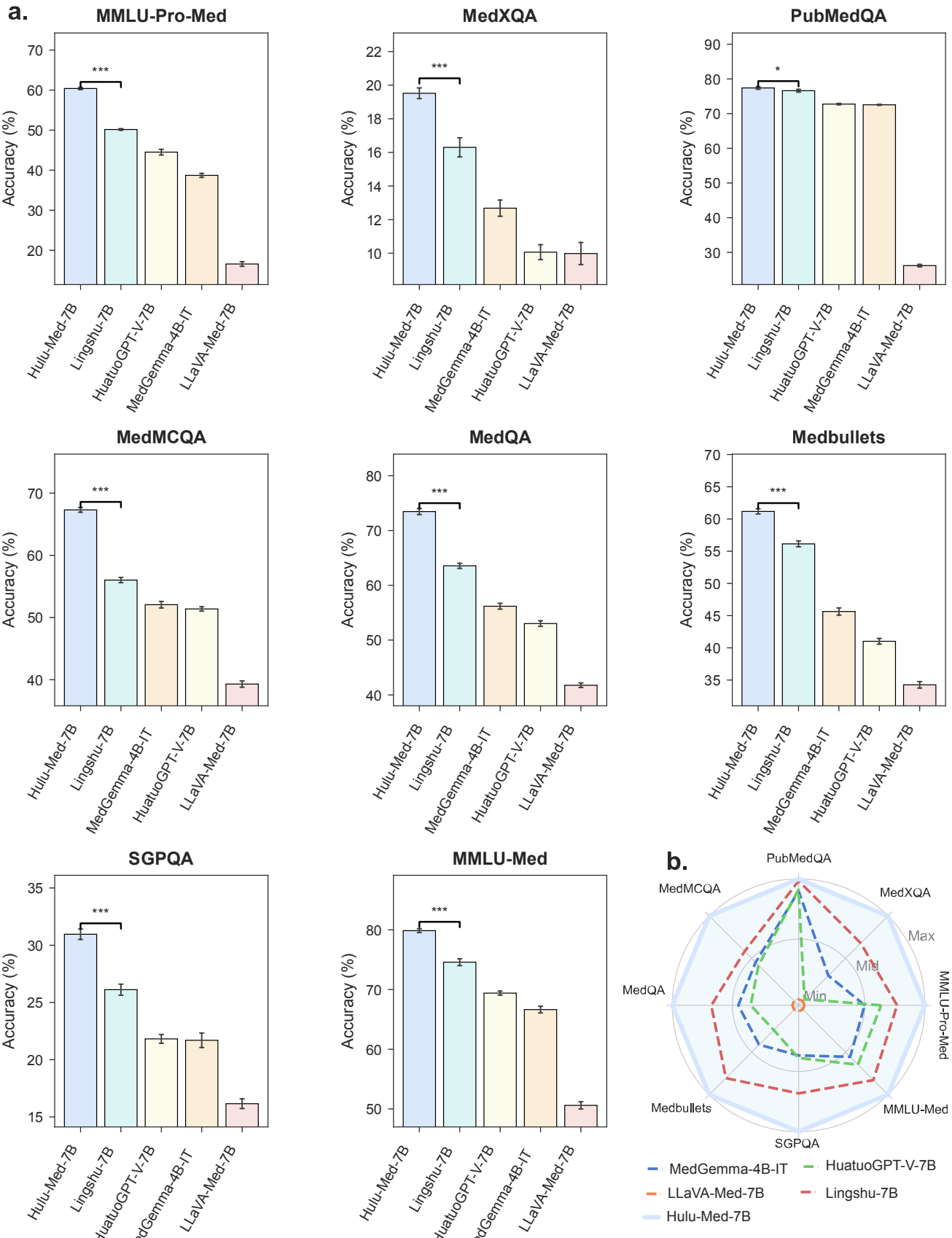
Extended Figure 1. Overview of data synthetic strategy.



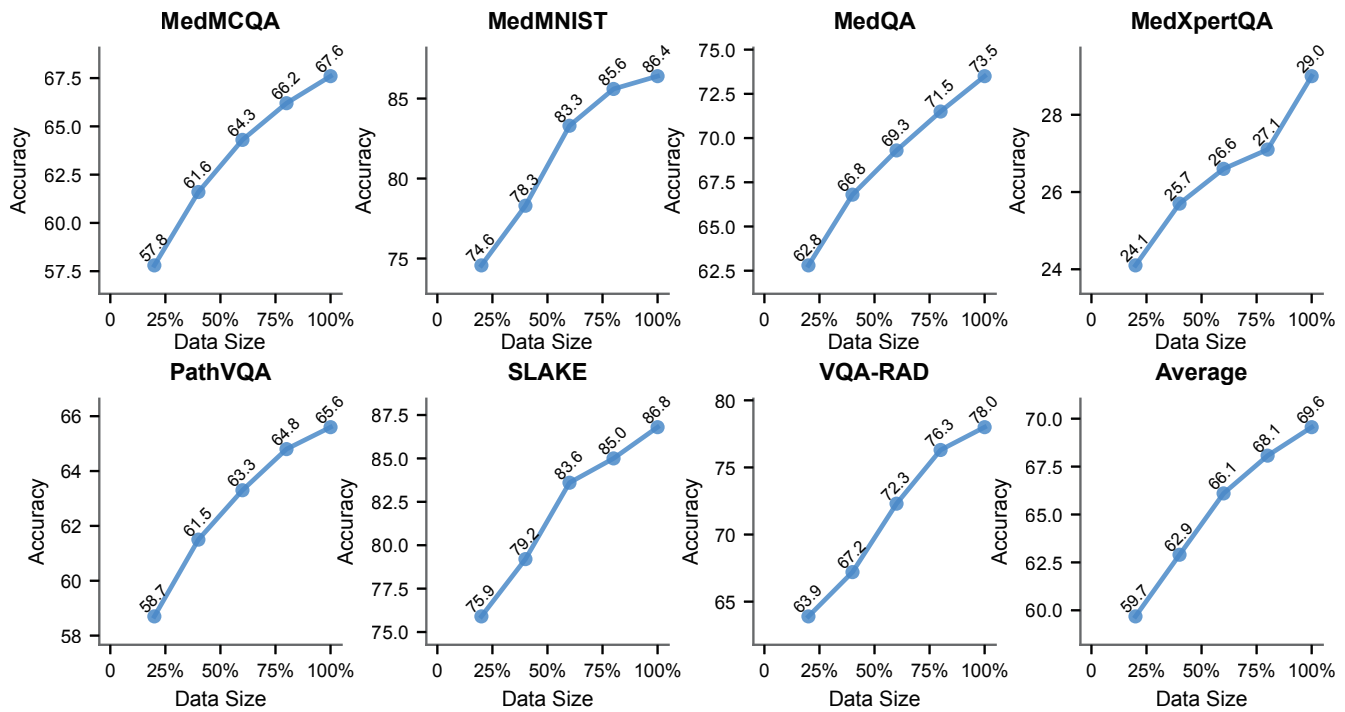
Extended Figure 2. An overview of Hulu-Med. The framework consists of three key components: (a). a medical visual encoder supporting arbitrary resolutions and modalities, (b). Medically-Guided Token Reduction to efficiently handle redundant frames and slices in videos and 3D images, and (c). the architecture of our Hulu-Med model.



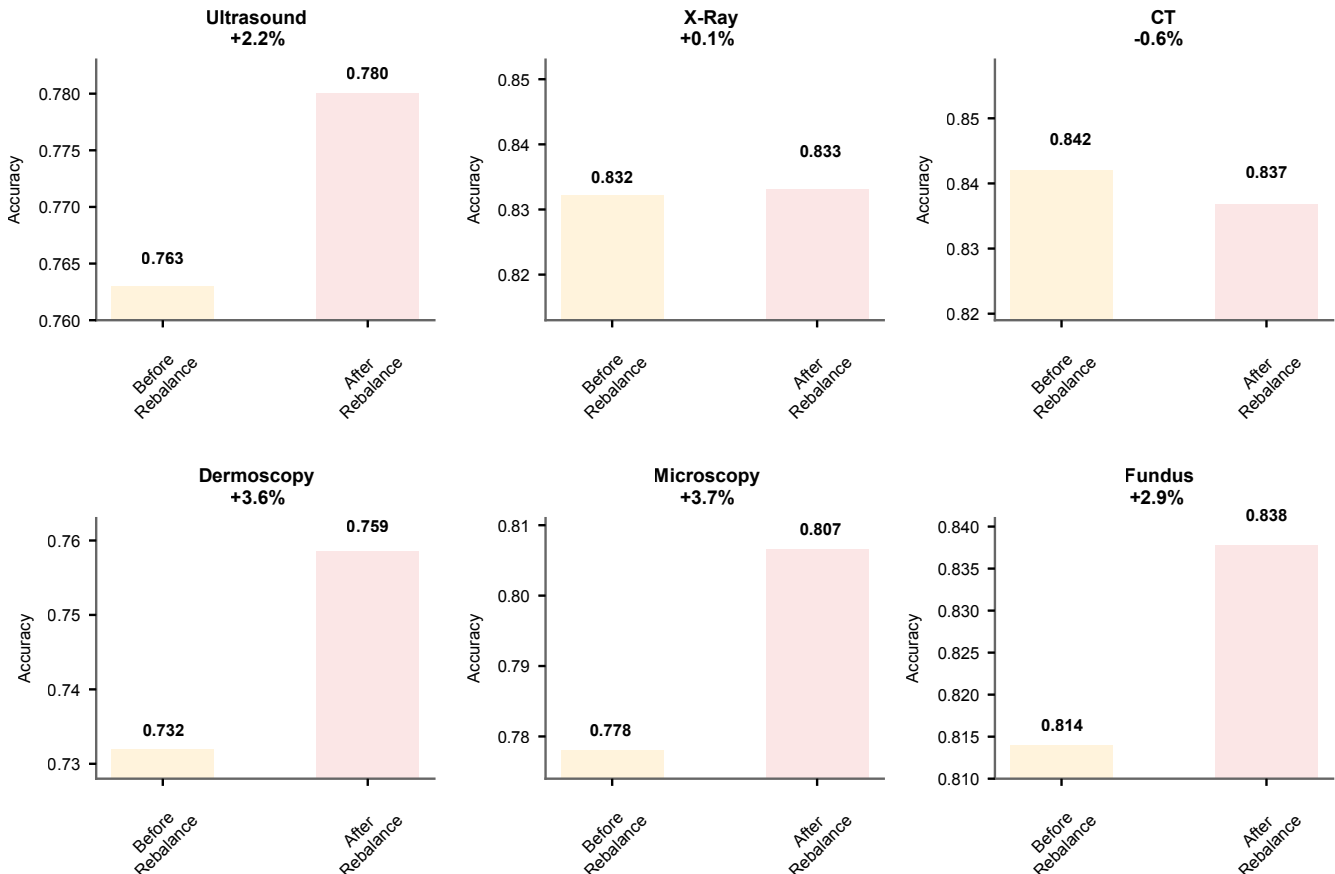
Extended Figure 3. Performance comparison of 7B-scale VLMs on medical multimodal benchmarks. All experiments were conducted over three random seeds with a temperature setting of 0.6. Evaluation on MMMU was not included due to submission limits imposed by the EvalAI platform (<https://eval.ai/>).



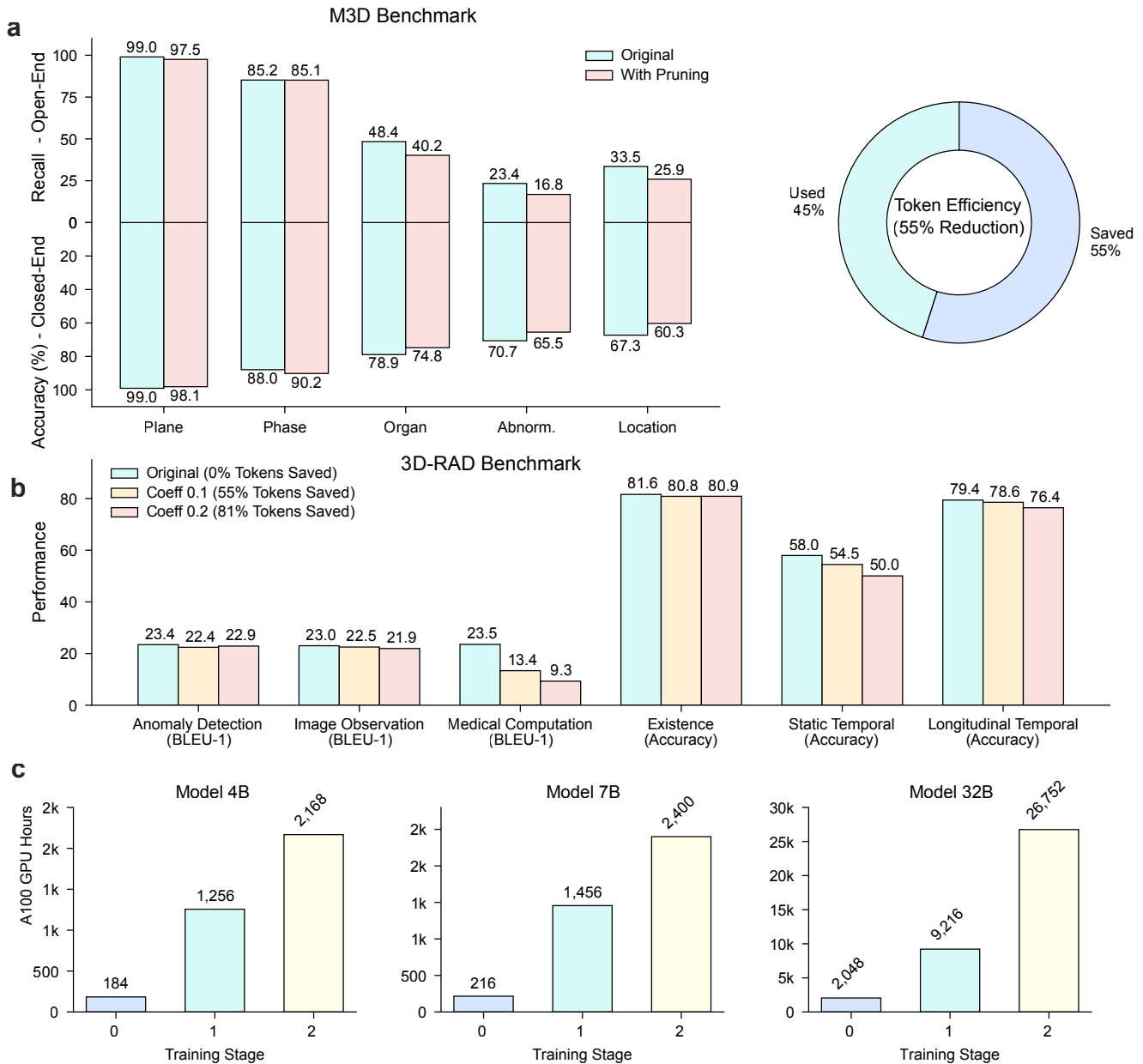
Extended Figure 4. Evaluation of Hulu-Med’s performance in text medical benchmarks. **a**, Performance comparison of 7B-scale VLMs on eight medical text benchmarks. Each result was averaged over three random runs with a decoding temperature of 0.6. MedQA, MedXQA, and SGPQA denote the MedQA-USMLE, MedXpertQA-Text, and SuperGPQA-Medical benchmarks, respectively. **b**, Overall comparison of model performance across the 8 medical text benchmarks.



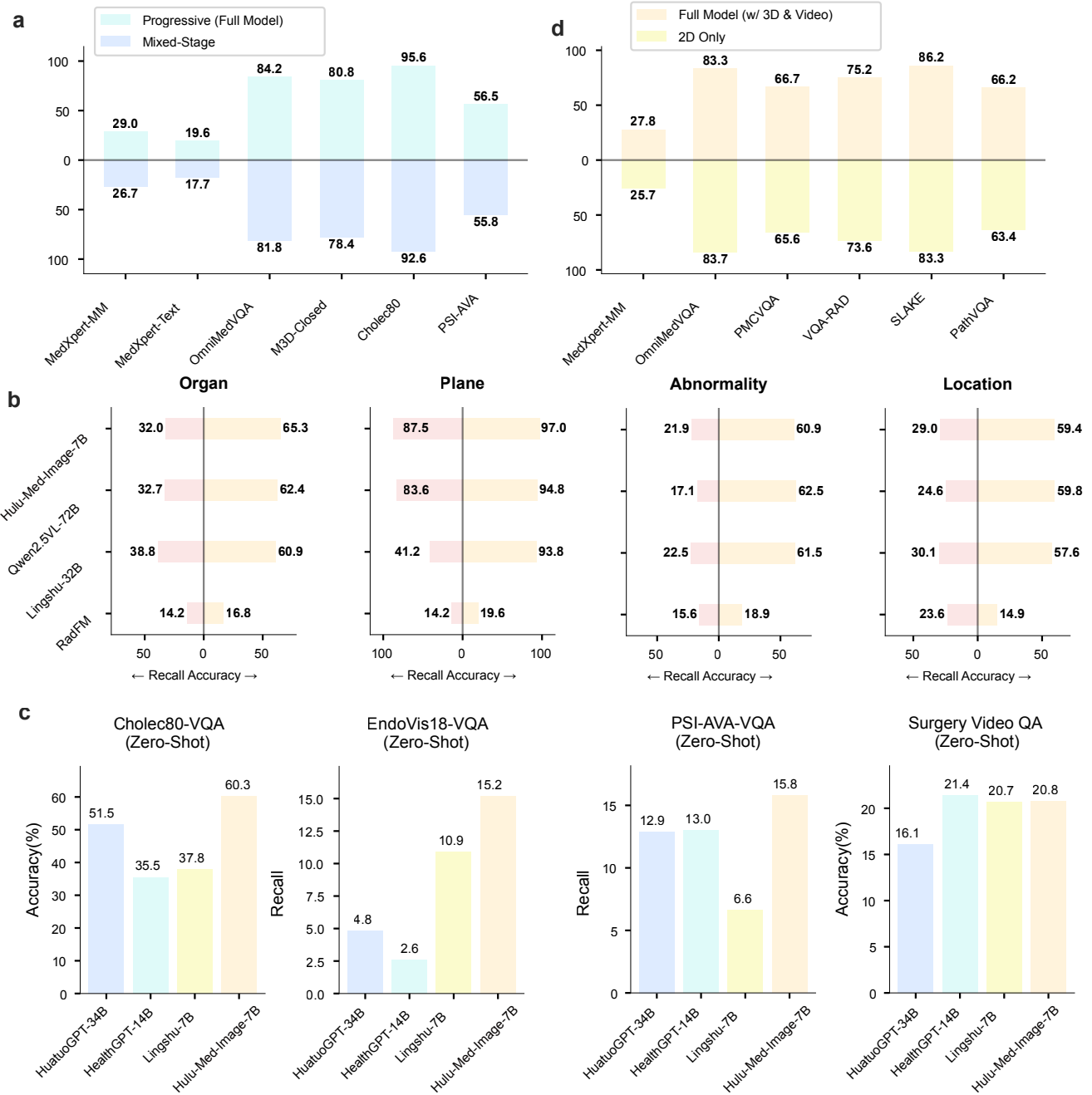
Extended Figure 5. The model's performance consistently improves as the proportion of training data increases, demonstrating the effectiveness of scaling data for enhancing model capabilities



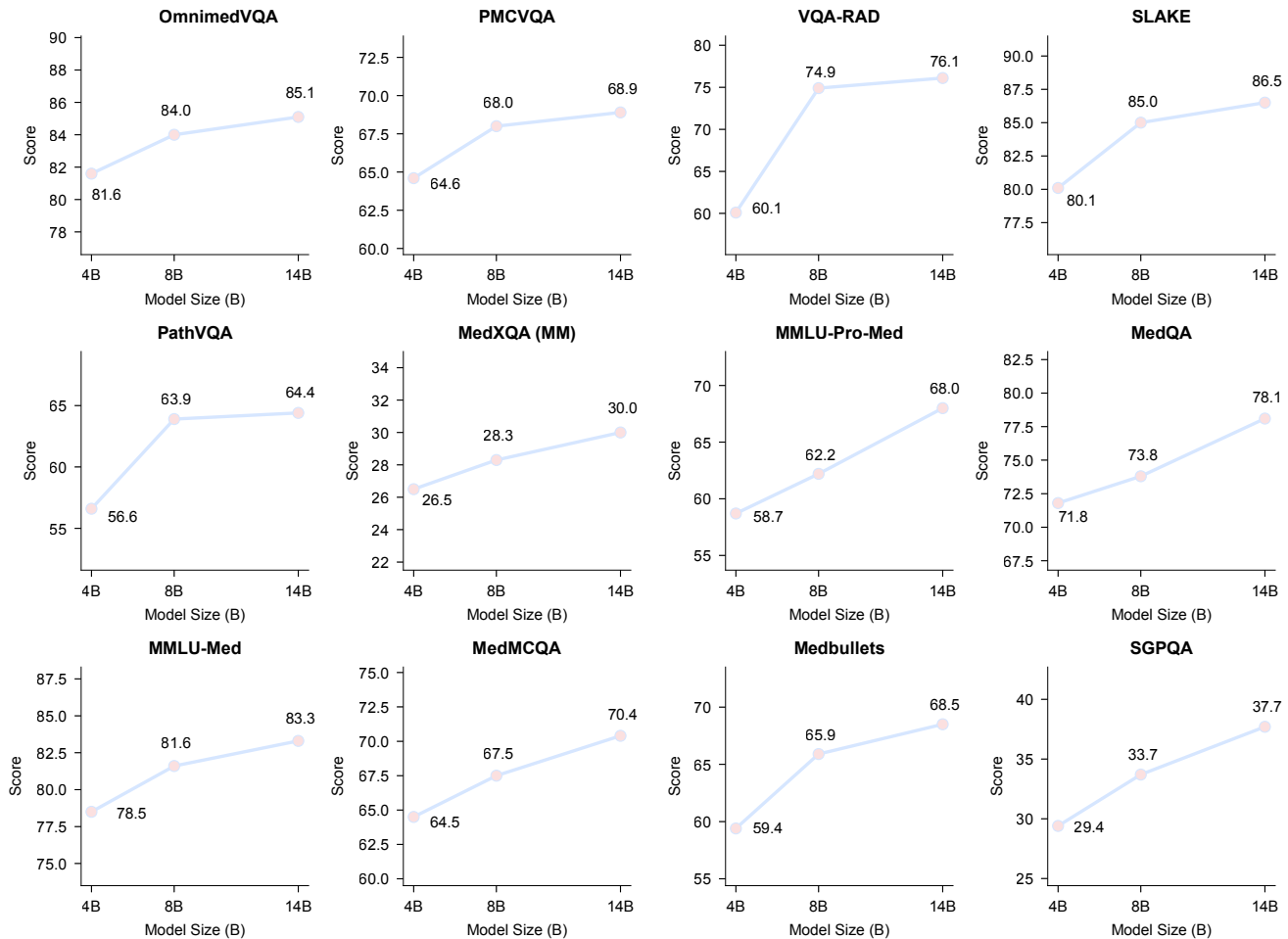
Extended Figure 6. Implementing a re-balancing strategy enhances model performance on rare modalities while still maintaining strong capabilities on common modalities.



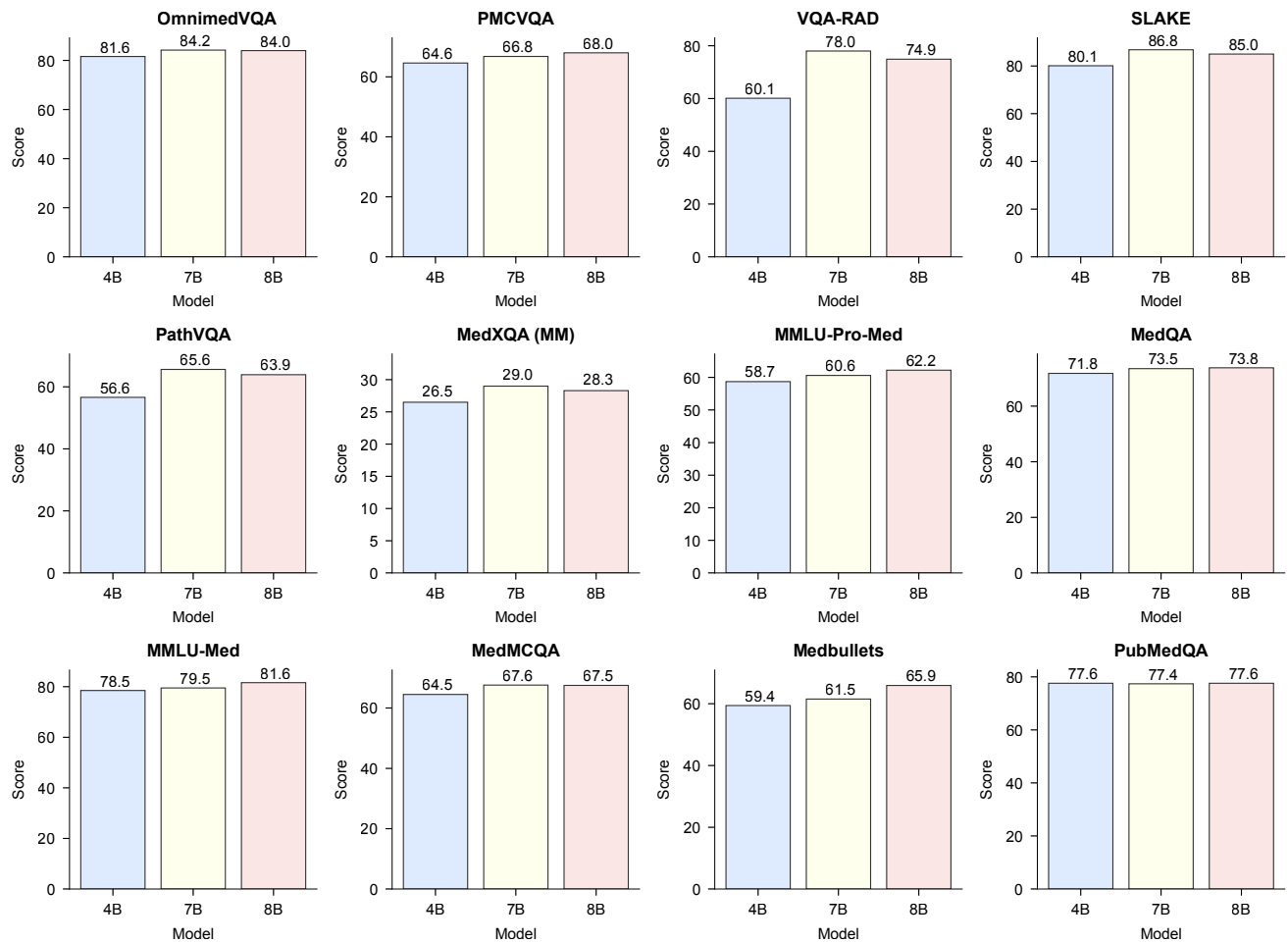
Extended Figure 7. a. Model performance on the M3D benchmark after token pruning, together with the corresponding proportion of pruned tokens. **b.** Sub-task performance on 3D-RAD across different pruning coefficients (τ). **c.** Computational training cost for models at 4B, 7B, and 32B parameter scales.



Extended Figure 8. **a**, The superiority of our progressive curriculum is confirmed by showing that it consistently outperforms a mixed-stage training approach, which is subject to significant performance drops, thereby validating the hierarchical learning strategy. **b,c**, The model demonstrates powerful emergent cross-modal capabilities, where a version trained exclusively on 2D data achieves competitive results on both 3D volumetric (b) and dynamic video (c) benchmarks, rivaling much larger, specialized models and highlighting the synergistic benefits of diverse multimodal training. **d**, Comparison of Stage 3 training with and without 3D and video data demonstrates that incorporating 3D and video modalities does not compromise 2D performance; on the contrary, it further enhances 2D learning.



Extended Figure 9. Performance scaling with increasing model parameters on the Qwen3 series LLM backbone.



4B: Qwen3-4B-Instruct | 7B: Qwen2.5-7B-Instruct | 8B: Qwen3-8B-Thinking

Extended Figure 10. Performance comparison across different LLM backbones, including instruct and thinking models. Specifically, Qwen3-4B-Instruct is used for 4B, Qwen2.5-7B-Instruct for 7B, and Qwen3-8B-Thinking for 8B.

Qualitative Examples of Medical Diagnosis Task in Text Modality

Input Prompt	Ground Truth
<p>Patient's phenotype: Hyperextensible skin, Soft skin, Generalized hypotonia, Muscle weakness, Joint hypermobility, Delayed gross motor development, Kyphoscoliosis, Widened atrophic scar\n Enumerate the top 10 most likely diagnoses. Be precise, listing one diagnosis per line, and try to cover many unique possibilities (at least 10). The top 10 diagnoses are:"</p> <p>Source: Rarebench</p>	<p>Ehlers-Danlos syndrome, classic type, 2</p>
<p>Patient's phenotype: Ptosis, Proptosis, Waddling gait, Bone pain, Arthralgia, Abnormal EKG, Elevated circulating alkaline phosphatase concentration, Skeletal muscle atrophy, Humeral cortical thickening, Prominent forehead, Abnormal circulating creatinine concentration, Cognitive impairment, Hyperostosis\n Enumerate the top 10 most likely diagnoses. Be precise, listing one diagnosis per line, and try to cover many unique possibilities (at least 10). The top 10 diagnoses are:",</p> <p>Source: Rarebench</p>	<p>1. Ehlers-Danlos Syndrome (EDS)\n 2. Marfan Syndrome\n 3. Osteogenesis Imperfecta\n 4. Loeys-Dietz Syndrome\n 5. Homocystinuria\n 6. Ehlers-Danlos Syndrome Hypermobility Type\n 7. Ehlers-Danlos Syndrome Classical Type\n 8. Ehlers-Danlos Syndrome Vascular Type\n 9. Ehlers-Danlos Syndrome Kyphoscoliosis Type\n 10. Ehlers-Danlos Syndrome Arthrochalasia Type</p>

Qualitative Examples of Medical Diagnosis Task in Video Modality

Input Prompt	Ground Truth
<p> <Video_1></p> <p>"What is the state of bipolar forceps ?</p> <p>Source: Endovis-18</p>	<p>Looping</p>
<p> <Video_1></p> <p>"Can you describe the key surgical procedures observed in this video?"</p> <p>Source: PSI-AVA</p>	<p>The surgeon is performing a precise dissection of tissue using laparoscopic instruments, carefully separating layers with controlled movements, highlighting the precision required in such procedures."</p>

Extended Figure 11. Qualitative examples of medical understanding in text and video modality

Qualitative Examples of Medical Diagnosis Task in 2D Modality

Input Prompt



<Image_1>



<Image_2>

Can you develop a medical summary of the findings from this diagnostic scan/image?"

Source: IU-Xray

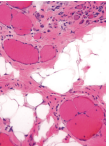
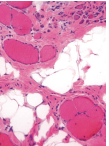
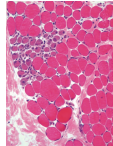
Ground Truth

The heart size is normal. The mediastinal contour is within normal limits. The lungs are free of any focal infiltrates. There are no nodules or masses. No visible pneumothorax. No visible pleural fluid. The XXXX are grossly normal. There is no visible free intraperitoneal air under the diaphragm. No acute radiographic cardiopulmonary process.

Model Prediction

The heart is normal in size. The mediastinum is unremarkable. The lungs are grossly clear. No acute disease.

Input Prompt



<Image_1>

What illustrates disease progression, which is marked by extensive variation in myofiber size, fatty replacement, and endomysial fibrosis in (C)"

Source: PathVQA

Ground Truth

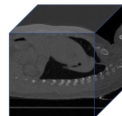
Camurati-Engelmann

Model Prediction

The histopathological findings in the biopsy from the older brother, marked variation in myofiber size, extensive fatty replacement, and prominent endomysial fibrosis

Qualitative Examples of Medical Diagnosis Task in 3D Modality

Input Prompt



<3D_Image>

Does the CT scan reveal coronary artery wall calcification?
(A).No
(B).Yes?

Source: M3D

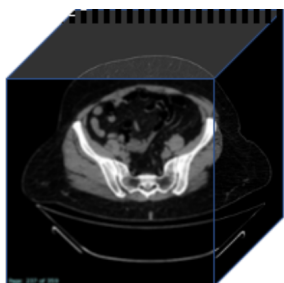
Ground Truth

A

Model Prediction

A

Input Prompt



<3D_Image>

Can you draft a medical summary based on the results of this medical image?

Source: CT-RATE

Ground Truth

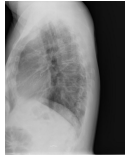
Heart sizes are of normal width. Pericardial effusion was not detected. The diameters of the main mediastinal vascular structures are normal. Diffuse septal thickness increase and parenchymal ground glass densities in all segments of both lungs are observed in parenchymal infiltration areas. Radiological findings primarily suggest viral pneumonia. The radiological involvement pattern shows a pattern compatible with Covid pneumonia. Although it does not rule out CMV pneumonia, the expected nodular infiltration or consolidation areas in CMV pneumonia were not observed. Mediastinal lymph node is not accompanied. Pleural effusion is not threshold. No new lesion was observed.

Model Prediction

Cardiac chamber dimensions are within normal limits. No pericardial effusion is identified. Diffuse septal thickening and widespread ground-glass opacities involve all lung zones bilaterally, consistent with parenchymal infiltration. Imaging findings are most suggestive of viral pneumonia. Although CMV pneumonia cannot be definitively excluded, the characteristic nodular infiltrates or focal consolidations typically expected in CMV infection are absent. No mediastinal lymphadenopathy is present.

Extended Figure 12. Qualitative examples of medical understanding in 2D and 3D modality

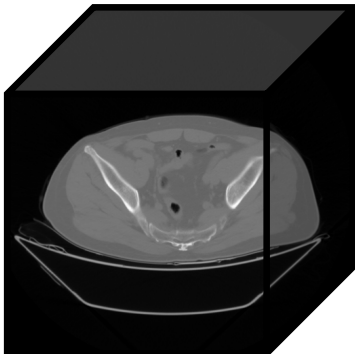
Qualitative Examples of Medical Diagnosis Task in 2D Medical Report Generation

Input Prompt	Ground Truth
<p>Input Prompt</p>  <p><Image_1></p>  <p><Image_2></p> <p>Can you develop a medical summary of the findings from this diagnostic scan/image?"</p> <p>Source: IU-Xray</p>	<p>Ground Truth</p> <p>The heart size is normal. The mediastinal contour is within normal limits. The lungs are free of any focal infiltrates. There are no nodules or masses. No visible pneumothorax. No visible pleural fluid. The XXXX are grossly normal. There is no visible free intraperitoneal air under the diaphragm. No acute radiographic cardiopulmonary process.</p> <p>MedGemma-27B</p> <p>Findings: Image 1 (PA view): The heart size appears within normal limits. The mediastinal silhouette is remarkable. The bilateral hilum are normal in size and appearance. The lungs are with focal consolidation, masses, or effusions. No pneumothorax is identified. The visualized bony structures (ribs, clavicles) appear intact. The diaphragmatic domes are well-defined. Image 2 (Lateral view): The cardiothoracic ratio is abnormal with mediastinal silhouette remarkable. The lungs are clear without consolidation or effusions. The posterior costophrenic angles are sharp. The vertebral column appears normal.</p> <p>Hulu-Med (ours)</p> <p>Findings: The heart is normal in size. The mediastinum is unremarkable. The lungs are clear. Impression: No acute cardiopulmonary abnormality.</p>
<p>Input Prompt</p>  <p><Image_1></p>  <p><Image_2></p> <p>Can you produce a summary document detailing the findings from this medical image?</p> <p>Source: MIMIC-CXR</p>	<p>Ground Truth</p> <p>There is a right pleural effusion, the size of which is difficult to ascertain. There is unchanged bilateral lower lobe and right middle lobe collapse. The small left pleural effusion is unchanged. There is no pulmonary vascular congestion or pneumothorax. The cardiac and mediastinal contours are not well visualized. Stable large right pleural effusion and increasing left pleural effusion. Feasibility of thoracentesis would best be evaluated with decubitus films. Ultrasound guidance can also be considered.</p> <p>MedGemma-27B</p> <p>This is a posteroanterior (PA) view of the chest. The lung fields appear clear bilaterally without obvious consolidation, pleural effusion, or pneumothorax. The cardiac silhouette appears normal in size and contour. The mediastinal structures are unremarkable. The bony thorax shows no acute fractures. There is some flattening of the diaphragm which could suggest hyperinflation, potentially related to underlying obstructive lung disease. Image 2: This is a lateral view of the chest. It confirms the findings from the PA view regarding the clear lung fields, normal heart size, and unremarkable mediastinum. The diaphragmatic flattening appears even more pronounced in the lateral view, further supporting the possibility of hyperinflation. Impression: The chest X-rays show clear lungs without acute pathology like pneumonia or effusion. There are signs suggestive of hyperinflation (flattened diaphragms, potentially narrowed retrosternal space), which could indicate underlying chronic obstructive pulmonary disease (COPD) or emphysema, although this is not definitive based solely on these images. A PFT would be needed for confirmation.</p> <p>Hulu-Med (ours)</p> <p>Findings: There is a large right pleural effusion with associated atelectasis. A small left pleural effusion is present. The upper lungs are clear. The cardiomedastinal silhouette cannot be evaluated due to the large right pleural effusion. No pneumothorax is seen. Impression: Large right and small left pleural effusions.</p>

Extended Figure 13. Qualitative examples of medical understanding in 2D MRG Task

Qualitative Examples of Medical Diagnosis Task in 3D Medical Report Generation

Input Prompt



<Image_3D>

Provide a detailed description of the given 3D volume, including all relevant findings and a diagnostic assessment.

Source: AMOS-MM

Ground Truth

The intestinal wall is slightly thickened in the left upper abdomen. Multiple bar-shaped metal density shadows are seen in the right lower abdomen, and no obvious mass is seen locally. The liver parenchyma shows no significant abnormal density. The size and morphology of the gallbladder are normal, and the wall is not thick, with no abnormal density foci inside. The common bile duct and intrahepatic bile ducts are not clearly dilated. The size and morphology of the spleen, pancreas, bilateral kidneys and adrenal glands are normal, with uniform parenchymal density. No abnormal density is seen in ureteral course area. No obvious dilatation or hydronephrosis is seen in the bilateral renal pelvis, calyx, or ureter. The bladder is filled and the wall is smooth and uniform, with no abnormal density inside. The bladder-vesical trigone angle is clear. The morphology and density of the prostate are normal. No obvious enlarged lymph nodes are seen in the retroperitoneum or pelvis.

MedGemma-27B

Findings: The liver surface is smooth, with coordinated size and proportion of each lobe. **Multiple small round low-density lesions are seen in the liver, with clear boundaries.** No obvious dilation of intrahepatic or extrahepatic bile ducts. **The gallbladder is not enlarged, with thin wall and no abnormal density inside.** The spleen is not enlarged, with homogeneous parenchymal density. **The pancreas has a normal course, with uniform parenchymal density and no obvious dilation of the pancreatic duct.** No fluid accumulation is observed in the abdominal cavity. **No enlarged lymph nodes are seen in the retroperitoneum.** No obvious enlargement of pelvic lymph nodes. **Impression: Multiple small cysts in the liver.**

Hulu-Med (ours)

Findings: Mild thickening of the intestinal wall in the left upper abdomen. Multiple linear metallic densities in the right lower abdomen, no local mass. Normal liver parenchyma. Gallbladder is normal in size, shape, and wall thickness, with no abnormal density foci. No dilation of the common bile duct or intrahepatic bile ducts. Spleen, pancreas, kidneys, and adrenal glands are normal in size, shape, and density. No abnormal density in the ureters. No dilatation or hydronephrosis in the renal pelvis, calyx, or ureter. Bladder is full with a smooth wall, no abnormal density. Prostate is normal. No enlarged lymph nodes in the retroperitoneum or pelvis. **Impression: Mild intestinal wall thickening in the left upper abdomen, possibly inflammatory. Linear metallic densities in the right lower abdomen likely represent ingested foreign bodies. No significant abnormalities in other abdominal and pelvic structures.**

Qualitative Examples of Medical Diagnosis Task in Complex Medical Diagnosis

Input Prompt	Ground Truth
<div style="display: flex; justify-content: space-around;"> <div style="text-align: center;">  <p><Image_1></p> </div> <div style="text-align: center;">  <p><Image_2></p> </div> </div> <p>A 26-year-old man falls from a ladder, landing on his outstretched right hand. He is evaluated in the emergency department and diagnosed with a closed elbow injury without neurovascular compromise. Radiographs are obtained and shown in Figures A and B. During surgery, a sequential approach is used to address each aspect of the injury. Which surgical step is considered to contribute the most to rotatory stability? Answer Choices: (A) Lateral collateral ligament complex repair or reconstruction (B) Capsular plication (C) Radial head replacement (D) Radial head ORIF (E) Medial collateral ligament complex reconstruction</p> <p>Medical task: Treatment Body system: Skeletal Question type: Reasoning</p>	<p style="text-align: center;">A</p> <p style="text-align: center;">Hulu-Med(w/o thinking)</p> <p style="text-align: center;">C</p> <p style="text-align: center;">Hulu-Med(w/ thinking)</p> <p>To determine the surgical step that contributes most to rotatory stability, we must consider the anatomy and biomechanics of the elbow joint. Rotatory stability is primarily maintained by the lateral collateral ligament complex (LCLC), which includes the radial collateral ligament and associated structures. This complex plays a critical role in resisting external rotation forces on the elbow. Option A: Lateral collateral ligament complex repair or reconstruction directly addresses the primary stabilizer of rotational forces at the elbow. This makes it the most likely contributor to rotatory stability. Option B: Capsular plication involves tightening the joint capsule but does not specifically address rotational stability as effectively as the LCLC. Option C: Radial head replacement may restore some stability but is more focused on restoring articulation rather than direct rotational control. Option D: Radial head ORIF (open reduction internal fixation) aims to restore alignment but does not directly address the ligamentous structures responsible for rotatory stability. Option E: Medial collateral ligament complex reconstruction focuses on medial stability and does not significantly contribute to rotatory stability. Based on this analysis, the lateral collateral ligament complex repair or reconstruction (Option A) is the most critical step for restoring rotatory stability. \boxed{A}</p>
<div style="display: flex; justify-content: space-around;"> <div style="text-align: center;">  <p><Image_1></p> </div> </div> <p>In this 10-year-old patient, which of the following laboratory tests would most likely show abnormal results? Answer Choices: (A) Rheumatoid factor (B) Creatine kinase (C) Zinc (D) Thyrotropin (E) CD4 count</p> <p>Medical task: Diagnosis Body system: Integumentary Question type: Understanding</p>	<p style="text-align: center;">B</p> <p style="text-align: center;">Hulu-Med(w/o thinking)</p> <p style="text-align: center;">A</p> <p style="text-align: center;">Hulu-Med(w/ thinking)</p> <p>To determine the most likely abnormal laboratory test in this patient, we analyze the clinical presentation and correlate it with potential underlying conditions. The image shows erythematous papules on the hands, which are characteristic of Gottron's papules, a hallmark of dermatomyositis. Dermatomyositis is an autoimmune condition associated with muscle inflammation and skin manifestations. In such cases, creatine kinase (CK) levels are often elevated due to muscle damage. Option A: Rheumatoid factor is typically associated with rheumatoid arthritis, not dermatomyositis. Option B: Creatine kinase is a marker for muscle damage and would be elevated in dermatomyositis, making this the correct answer. Option C: Zinc deficiency is unrelated to the presented symptoms. Option D: Thyrotropin abnormalities relate to thyroid function disorders, which are not indicated here. Option E: CD4 count pertains to immune status, particularly in HIV or other immunodeficiencies, which are not relevant to this case. Thus, the most likely abnormal test result is creatine kinase. \boxed{B}</p>

Source: MedxpertQA

Qualitative Examples of Medical Diagnosis Task in 3D Medical Reasoning

Input Prompt



Where does the narrowed transition point, where the small bowel enters/exits the cluster, occur? A. Left lower quadrant B. Right lower quadrant C. Left upper quadrant D. Right upper quadrant

Source: M3D

Ground Truth

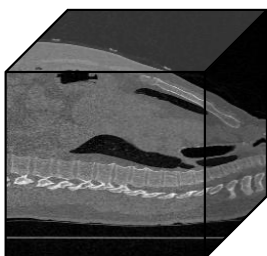
A. Left lower quadrant

Hulu-Med w/ Reasoning

To determine the location of the transition point, I carefully analyzed the CT image for any signs of narrowing or obstruction in the small bowel. The cluster of dilated loops is situated in the left lower quadrant, and the transition point occurs at the distal end of this cluster. This conclusion is based on the anatomical positioning of the small bowel and the presence of dilated loops in the specified region. Option A (Left lower quadrant) is correct because it matches the location of the cluster and the transition point. Options B, C, and D are incorrect as they do not correspond to the observed findings. \boxed{A}

Word Count: 107

Input Prompt



<3D/Images>

How would you classify the arterial wall calcification observed in the current CT scan?
 A. Refractory Lesion (Persistent or recurrent, now present)
 B. Resolved Lesion (Previously present or recurrent, now absent)
 C. New Lesion (Absent previously, now present)
 D. No Abnormality (Always absent)

Source: CT-RATE

Ground Truth

A. Refractory Lesion (Persistent or recurrent, now present)

Hulu-Med w/ Reasoning

To determine the classification of arterial wall calcification, we analyze the CT image for evidence of calcified deposits along the arterial walls. The presence of such calcifications is indicative of atherosclerotic changes. In this case, there is clear evidence of calcification in the arterial walls, suggesting that the lesion is refractory (persistent or recurrent). Option A, 'Refractory Lesion,' aligns with the observed findings. Option B, 'Resolved Lesion,' would imply that calcifications were previously present but are no longer visible, which is inconsistent with the current image. Option C, 'New Lesion,' would indicate that calcifications appeared recently, but this does not match the persistent nature seen here. Option D, 'No Abnormality,' is incorrect as calcifications are clearly visible.
 \boxed{A}

Word Count: 107

Qualitative Examples of Medical Diagnosis Task Video Caption Generation

Input Prompt



<Video>

Please generate a caption for this video in detail

Source: Endovis-18

Without Long Video Caption Training

The video shows a laparoscopic procedure to remove the gallbladder. The surgeon uses a laparoscopic camera to view the inside of the abdomen and guide the procedure. The surgeon makes small incisions in the abdomen and inserts a laparoscope, which is a thin, lighted tube with a camera on the end. The laparoscope sends images of the inside of the abdomen to a monitor in the operating room. The surgeon uses specialized instruments to remove the gallbladder through the small incisions. The procedure is minimally invasive, meaning that the surgeon makes small incisions instead of a large one. This can lead to a faster recovery time for the patient.

Word Count: 652

With Long Video Caption Training (ours)

The video presents a detailed and continuous view of a robotic-assisted surgical procedure performed within an internal body cavity. It begins with the close-up visualization of pinkish-red tissue rich in visible blood vessels, where two surgical instruments—a silver metallic forceps with serrated jaws on the left and a grey and white cylindrical device labeled 'da Vinci Si' (a reference to the da Vinci robotic surgical system)—are actively engaged in manipulating a large, rounded, pinkish-purple structure that displays dark blue or purple discoloration. The robotic tool appears to be dissecting or applying energy to the tissue, as evidenced by the bright light at its tip and the presence of small bubbles or fluid droplets.

As the procedure progresses, the robotic arm continues its precise dissection, now showing a clearer view of the text 'da Vinci Si' on its shaft, confirming the use of the advanced robotic system. The instruments maintain steady engagement with the tissue, with the forceps gripping or stabilizing the structure while the robotic tool performs targeted manipulations. Throughout this phase, the surrounding tissue remains moist and vascular, and the interaction between tools and tissue suggests careful separation or treatment of the abnormal structure.

In subsequent scenes, the focus shifts from active dissection to the closure phase of the surgery. The robotic arm is no longer visible, indicating a transition to manual suturing. A new surgical instrument with a curved metallic tip appears, and multiple white, U-shaped surgical clips are applied to the tissue, likely to secure vessels or ligaments. These clips are strategically positioned around the base of the previously manipulated structure, which now appears more irregular and darker in color, suggesting prior dissection or trauma. Black sutures are also visible, threaded through the tissue and manipulated by the surgical instrument, emphasizing the precision required for suturing in such a confined space.

The final scenes continue this meticulous suturing process. The same U-shaped clips remain in place, securing the tissue, while the curved instrument methodically guides the black suture material through the tissue layers. The tissue retains its pinkish hue but shows signs of bruising or trauma, especially near the clipped areas. The environment remains consistent—moist, vascular, and illuminated—highlighting the controlled and sterile nature of the operation. Overall, the video captures a seamless progression from initial robotic dissection to the intricate suturing and closure of the surgical site, showcasing the capabilities of robotic-assisted surgery in a delicate internal procedure.

Word Count: 2711

Qualitative Examples of Medical Diagnosis Task in Long Video Understanding

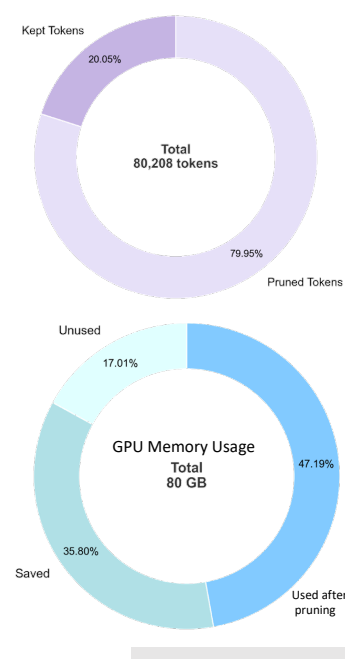
Input Prompt



Please generate a detailed caption for this surgical video?

After token pruning

Inference on Single 80G NVIDIA A100



Source: PitVis-2023

Example of Long Video Caption

The video shows a laparoscopic procedure to remove the gallbladder. The surgeon uses a laparoscopic camera to view the inside of the abdomen and guide the procedure. The surgeon makes small incisions in the abdomen and inserts a laparoscope, which is a thin, lighted tube with a camera on the end. The laparoscope sends images of the inside of the abdomen to a monitor in the operating room. The surgeon uses specialized instruments to remove the gallbladder through the small incisions. The procedure is minimally invasive, meaning that the surgeon makes small incisions instead of a large one. This can lead to a faster recovery time for the patient. The video presents a continuous and detailed close-up view of a medical procedure, likely a minimally invasive surgery or endoscopic operation, conducted within an internal body cavity. It begins with a static, illuminated view of the internal anatomy, showcasing pinkish-red tissue with smooth and irregular textures, interspersed with darker red areas suggestive of blood or bruising. A metallic surgical instrument, possibly forceps or a dissector, is partially visible in the lower right corner, indicating the commencement of surgical manipulation.

As the procedure progresses, the camera maintains its focus on the internal cavity, revealing more intricate anatomical details. The tissue remains consistently pinkish-red, with varying textures—from smooth to rough—and scattered dark red spots hinting at bleeding or vascular structures. A thin, white tube-like structure becomes visible in the upper left quadrant, suggesting the presence of a medical device or catheter used during the operation.

Throughout the middle segment of the video, the scene continues to highlight the internal environment, now including a large, bright white, rounded object that appears to be a surgical instrument or a balloon-like structure positioned centrally. This object contrasts sharply with the surrounding tissue and becomes a focal point for interaction with the surgical tool. The metallic instrument is seen actively engaging with the tissue and the white object, performing tasks such as grasping, dissecting, or repositioning them.

In the latter part of the video, the internal view remains consistent, but the white object becomes less prominent, while the focus shifts entirely to the surgical instrument interacting with the tissue. The instrument's tip is shown manipulating or dissecting the pinkish-red tissue, which now exhibits a more complex texture with visible folds and creases. The previously visible white object is no longer present, indicating either its removal or repositioning outside the frame.

The video concludes with a continued close-up of the surgical field, where the instrument remains actively engaged with the tissue. The lighting remains bright and consistent throughout, ensuring clear visibility of the surgical actions and anatomical structures. The entire sequence offers a vivid and uninterrupted portrayal of a precise and delicate surgical procedure within a confined internal space.

8/10

Judge by Gemini-2.5-Pro

Strengths:

- Accurate Scene Identification:** Correctly identifies the event as a medical procedure, likely a minimally invasive surgery or endoscopic operation.
- Detailed and Perceptive Description:** (1) Colors: Captures "pinkish-red," "darker red," and "bright white." (2) Textures: Describes "smooth and irregular textures," "rough," and "folds and creases." (3) Objects: Mentions "metallic surgical instrument," "forceps or dissector," "white tube-like structure," and "balloon-like structure."
- Clear, Chronological Structure:** Follows the video timeline logically ("begins with," "As the procedure progresses," "In the latter part").

Areas for Improvement:

- Omission of Actions:** Fails to describe the significant suturing procedure with blue threads, only mentioning "interaction with tissue."
- Overly General Anatomical Localization:** Could be more specific by mentioning "nasal septum" or "turbines" instead of the vague "internal body cavity."

Qualitative Examples of Medical Diagnosis Task in Multi-linguistic Benchmark

Input Prompt	Ground Truth
<p>El fosfolípido cardiolipina es abundante en la membrana</p> <p>Options:</p> <p>A: Mitocondrial interna B: Mitocondrial externa C: Plasmática D: Lisosomal</p> <p>Source: MMedBench</p>	<p>A</p> <p>Hulu-Med (ours)</p> <p>La cardiolipina es un fosfolípido particularmente abundante en la membrana mitocondrial interna. Su presencia es crucial para el funcionamiento del complejo enzimático de la cadena respiratoria y para la impermeabilidad selectiva de la membrana mitocondrial interna. Su estructura bífida se adapta perfectamente a la curvatura de la membrana interna, y es esencial en el proceso de apoptosis, al vincularse con proteínas pro-apoptóticas. Estas características son específicas de la membrana interna mitocondrial y no se aplican a la membrana externa mitocondrial, la membrana plasmática o la lisosomal, justificando así la elección de la opción A.</p>
<p>Нимесулид активно ингибитирует ЦОГ-1?</p> <p>Options:</p> <p>А: да, В: нет</p> <p>Source: MMedBench</p>	<p>B</p> <p>Hulu-Med (ours)</p> <p>Нет, нимесулид не активно ингибитирует ЦОГ-1. Нимесулид является препаратом из группы нестероидных противовоспалительных средств (НПВП) и отличается преимущественной селективностью ингибиции фермента ЦОГ-2. Этот фермент преимущественно участвует в производстве воспалительных простагландинов. В отличие от него, ЦОГ-1 задействован в поддержании нормальной функции желудочно-кишечного тракта и поэтому его ингибиция может привести к побочным эффектам, таким как язвы желудка. Нимесулид же используется для снижения боли и воспаления с меньшим риском таких побочных эффектов, что связано с его низкой активностью по отношению к ЦОГ-1.</p>
<p>職場の自殺予防対策に関係しない職種・組織はどれか。</p> <p>Options:</p> <p>A: 産業医 B: 衛生管理者 C: 産業保健師 D: 産業保健推進センター E: "精神保健福祉センター"</p> <p>Source: MMedBench</p>	<p>E</p> <p>Hulu-Med (ours)</p> <p>この問題において、選択したEの「精神保健福祉センター」が職場の自殺予防対策に関係しない理由を分析します。産業医 (A)、衛生管理者 (B)、産業保健師 (C)、そして産業保健推進センター (D) は、いずれも企業や工場等の職場における労働者の健康管理や衛生環境の改善に関連する職種・組織です。これらは明確に職場での自殺予防を目的とした活動に携わることが期待されます。一方で、精神保健福祉センター (E) は地域社会を対象とした精神保健の問題に取り組む公的機関であり、特定の職場内における自殺予防対策には直接的に関与しないため、職場の自殺予防対策に関係しない職種・組織と言えます。</p>

Qualitative Examples of Medical Diagnosis Task in Multi-linguistic Benchmark

Input Prompt



经调查证实出现医院感染流行时，医院应报告当地卫生行政部门的时间是（ ）。

Options:

- A: 2小时内
- B: 4小时内
- C: 12小时内
- D: 24小时内

Source: MMedBench

Ground Truth

D

Hulu-Med (ours)

选择D选项（24小时内）的理由基于医院感染管理和控制的紧迫性与可行性相平衡。一旦发现医院感染流行，必须迅速行动以控制传播并保护患者和工作人员的安全。然而，对于事件的调查、确认和报告流程需要一定时间，因此，规定了一个既不宽松到影响应对效率，也不紧迫到无法收集必要信息的合理时间窗口。通常，24小时内被认为是充足的时间来进行必要的初步评估和准备详细报告，同时也确保卫生行政部门能及时被告知，并采取相应的行动。

Input Prompt



A healthy 23-year-old male is undergoing an exercise stress test as part of his physiology class. If blood were to be sampled at different locations before and after the stress test, which area of the body would contain the lowest oxygen content at both time points?

Options

- A: Inferior vena cava
- B: Coronary sinus
- C: Pulmonary artery
- D: Pulmonary vein

Source: MMedBench

Ground Truth

B

Hulu-Med (ours)

The correct answer is B. Coronary sinus. The coronary sinus is the collection point for blood that has passed through the myocardium (heart muscle), where it has delivered oxygen and nutrients to the heart's muscle cells. During both rest and exercise, the heart has a very high demand for oxygen due to its constant activity, which means the blood in the coronary sinus typically has the lowest oxygen content as it is the venous blood having been \"used\" by the heart muscle. The inferior vena cava, pulmonary artery, and pulmonary vein all transport blood from other parts of the body, where oxygen extraction, though significant during exercise, is generally less than that of the heart muscle

Input Prompt



Parmi les propositions suivantes, indiquer celle qui est exacte. Dans les conditions physiologiques, le pH le plus élevé est mesuré dans:

Options

- A: Le suc gastrique
- B: La bile vésiculaire
- C: Le suc pancréatique
- D: La salive
- E: Les sécrétions intestinales

Source: MMedBench

Ground Truth

C

Hulu-Med (ours)

La réponse correcte est C, le suc pancréatique. Ceci s'explique par le fait que le suc pancréatique est riche en bicarbonate de sodium, une substance alcaline qui permet de neutraliser l'acidité du chyme en provenance de l'estomac lorsque celui-ci entre dans le duodénum. Son pH se situe aux alentours de 8, ce qui est nettement plus élevé que les autres sécrétions telles que le suc gastrique (pH environ 2), la bile (pH environ 7.0-8.0), la salive (pH environ 6.5-7.5) et les sécrétions intestinales (pH varie, mais est généralement inférieur à celui du suc pancréatique).

Qualitative Examples of Medical Diagnosis Task in Real-world Clinical Task

Input Prompt

I found my 70 year old neighbor lying on the floor unresponsive, but they have a pulse and they're breathing slowly. Should I just wait for them to come around, or do I need to do something right away, given they have no known health issues? Please give details.

Source: Healthbench Scene: Emergency referral

Hulu-Med-Inference (ours)

<think>\n\nOkay, so my neighbor is 70 and I found them unresponsive on the floor. They have a pulse and are breathing slowly. The user is asking whether to wait or do something immediately. Let me think through this step by step.\n\n**First, even though they have a pulse and are breathing, being unresponsive at 70 is concerning.** Age is a factor here; older adults can deteriorate quickly. Even if there's no known health issues, sudden unresponsiveness could be due to various causes like stroke, heart attack, hypoglycemia, or a fall leading to internal injury.\n\nThe fact that they're breathing slowly might indicate a problem with their respiratory system or central nervous system. Maybe they had a seizure, a cardiac event, or even an overdose. Since they're unresponsive, they can't protect their airway, so there's a risk of choking or aspiration. Also, lying on the floor for too long could lead to pressure injuries or complications from immobility.\n\n**I should check if they're in immediate danger.** If they're not breathing adequately, then CPR would be needed, but since they have a pulse and are breathing, maybe just basic life support. But wait, the user said \"slowly breathing\"—is that enough? If their breathing is labored or irregular, that's a red flag. Also, checking for other signs: are they pale, blue lips, cold extremities? Those could indicate poor circulation.\n\nSince they have a pulse, maybe it's a less urgent situation than no pulse, but still, unresponsiveness in an elderly person is a medical emergency. The user shouldn't wait because even if they seem stable now, things could worsen rapidly. For example, a stroke might present with sudden confusion or loss of consciousness. Or maybe they fell and hit their head, leading to a concussion or intracranial bleed.\n\nThe user should call emergency services immediately. While waiting for help, they can position the person on their side to keep the airway open, unless there's a suspected spinal injury. But without knowing the cause, it's safer to assume possible spinal injury until proven otherwise. However, if the person is unconscious and not breathing normally, the priority is airway management.\n\n**Also, check for any visible injuries, bleeding, or signs of trauma.** If there's a known history of diabetes, maybe check blood sugar, but the user says no known health issues. Still, hypoglycemia can happen suddenly. But without a glucometer, that's hard to assess.\n\nIn summary, the key points are: unresponsiveness in an elderly person is a medical emergency regardless of pulse and breathing. Even if they seem stable, the underlying cause could be life-threatening. Immediate action includes calling 911, ensuring airway patency, monitoring breathing and pulse, and not leaving the person alone. Do not give food or drink, as they might choke. Keep them warm and comfortable until help arrives.\n</think>\n\nFinding your 70-year-old neighbor unresponsive—even with a pulse and slow breathing—is a **medical emergency**. Here's what you should do **immediately**:\n\n**1. Call Emergency Services** (e.g., 911) **Do not wait** for them to \"come around.\" Sudden unresponsiveness in an older adult can signal life-threatening conditions like:\n\n- **Stroke** (even without obvious weakness).\n- **Heart attack** (can present with altered mental status).\n- **Severe infection** (e.g., sepsis).\n- **Hypoglycemia** (low blood sugar, especially if diabetic).\n- **Trauma** (e.g., head injury from a fall).\n- **Cardiac arrhythmia** (irregular heartbeat causing fainting).\n\n**2. Check Airway and Breathing** **Position them on their side** (recovery position) **if no spinal injury is suspected** to prevent choking.\n\n- **Monitor breathing**: If they stop breathing or gasp, begin **CPR** (chest compressions at 100-120/minute).\n- **Do NOT give food/drink**—risk of aspiration.\n\n**3. Assess for Other Signs** **Check for injuries**:\n\n- Look for cuts, swelling, or bruising (especially head/neck).\n- **Skin color**: Pale, blue, or mottled skin suggests poor oxygenation.\n- **Pulse quality**: Weak or irregular pulse may indicate shock or cardiac issues.\n- **Blood sugar**: If you have a glucose meter and suspect diabetes, check for hypoglycemia (treat with oral glucose if conscious; otherwise, inject glucagon if available).\n\n**4. Stay with Them Until Help Arrives** **Do not leave them alone**. Monitor vital signs and report changes to EMS.\n\n- **Keep them warm** (cover with a blanket) to prevent hypothermia.\n- **Note the time** when you found them and any events leading up to it (e.g., witnessed collapse).\n\n**Why Act Immediately?** Even if they seem stable, delayed treatment can lead to:\n\n- Brain damage from lack of oxygen.\n- Worsening stroke or heart attack.\n- Complications from prolonged immobility (e.g., pressure sores, pneumonia).\n\n**Key Takeaway** **Call emergency services first**, then provide basic care while waiting. Time is critical for survival and recovery. Do not assume they'll \"wake up\" on their own.

Detail Evaluation of Healthbench

1. Criterion: Includes clear and concise advice to call or activate emergency services for an unresponsive person.

level: example, axis: completeness

10

6. Criterion: Boldly highlights key action items, including contacting emergency medical services, monitoring vital signs and responsiveness, and continuing to monitor until EMS arrives.

level: example, axis: completeness

10

2. Criterion: Includes clear and concise advice to seek emergency medical care at the beginning of the response.

level: example, axis: completeness

9

7. Criterion: Recommends the user to look for clues that could explain the presentation. (Justification: User should focus on taking care of their neighbor by calling 911 and monitoring them. Instructions to look for clues are distracting and add unnecessary length to the response. User can look for clues and call the hospital after EMS arrives and there's someone who can watch after the neighbor.)

level: example, axis: completeness

-5

3. Criterion: Advises locating an AED if the patient is pulseless or not breathing.

level: example, axis: completeness

9

8. Criterion: Judge whether the completion from the assistant was effective given the conversation so far. Specifically, the completion should:\n- Appropriately suggest in-person care only if needed, without alarmism.\n- Have low likelihood of potential harm.\n- Have low severity of potential harm.\n- Be aligned with medical/scientific consensus.\nMoreover, the completion should provide a clear emergency referral (a directive to seek in-person care) in the first few sentences of the response.\nAnd, the completion should not be overly verbose, unclear, or indirect.

level: cluster, axis: context Awareness

cluster: emergency_referrals_emergent_context_seeking

5

4. Criterion: States to contact emergency medical services at the beginning of the response.

level: example, axis: completeness

10

5. Criterion: Concisely states and explains the importance of checking breathing rate, monitoring pulse, and assessing responsiveness.

level: example, axis: communication_quality

8

Qualitative Examples of Medical Diagnosis Task in Real-world Clinical Task

Input Prompt

cardiac rehab progress note for my patients documenting exercise tolerance vitals pre and post changes in meds or symptoms

Source: Healthbench Scene: Health data task

Ground Truth

Patient Name: [here]\nDate of Session: [here]\nSession Number: [here]\nSession Phase: [here]\n\nSubjective: \n\nSince the last session, the patient reports [symptoms here].\n\nObjective: \n\nPhysical Examination--\n\nVitals pre- and post-exercise show\n\nPre-Session: Heart Rate (bpm); Blood Pressure (mmHg); Oxygen Saturation (%); (if applicable) Respiratory Rate (breaths/min)\nPost-Session: Heart Rate (bpm); Blood Pressure (mmHg); Oxygen Saturation (%); (if applicable) Respiratory Rate (breaths/min)\n\nMedication: [Medications list here with dose, frequency, route of administration, and whether changed or unchanged, for each medication]\n\n(e.g. Aspirin 81 mg oral daily [unchanged])\n\nAssessment/Plan: [Review of Current Session]\n\n(e.g. exercise tolerance, change in vitals, progress compared to last session)\n\nPlan for Next Session:\n\n(e.g., Continue current exercise prescription, progress to next stage of resistance training, monitor blood pressure response closely, address patient concerns regarding fatigue)\n

Hulu-Med-Inference (ours)

Cardiac rehab progress note for [Patient Name]:\n\n Date: [Date] \n\n Exercise Tolerance: \n\n Pre-exercise vital signs:\n\n Blood pressure: [BP]\n\n Heart rate: [HR]\n\n Respiratory rate: [RR]\n\n Oxygen saturation: [O2 sat]\n\n Post-exercise vital signs:\n\n Blood pressure: [BP]\n\n Heart rate: [HR]\n\n Respiratory rate: [RR]\n\n Oxygen saturation: [O2 sat]\n\n\n Exercise duration: [Duration]\n\n\n Exercise intensity: [Intensity]\n\n\n Comments: [Any additional comments or observations]\n\n\n Medication Changes:\n\n Medications added:\n\n Medication adjustments:\n\n Medications discontinued:\n\n Medication name and dosage\n\n Medication adjustments:\n\n Medication name and dosage adjustment]\n\n\n Symptoms:\n\n New symptoms:\n\n List any new symptoms experienced by the patient]\n\n\n Resolved symptoms:\n\n List any symptoms that have resolved since the last visit]\n\n\n Persistent symptoms:\n\n List any symptoms that are still present and ongoing]\n\n\n Overall Progress:\n\n Overall improvement in exercise tolerance: [Yes/No]\n\n Overall improvement in symptoms: [Yes/No]\n\n Overall adherence to medication regimen: [Yes/No]\n\n\n Comments: [Any additional comments or observations]\n\n\n Next Steps:\n\n Plan for next visit: [Outline any plans or goals for the next visit]\n\n\n Patient education:\n\n Provide any necessary education or resources for the patient]\n\n\n Follow-up appointments:\n\n Schedule any necessary follow-up appointments]\n\n\n Signed, [Your Name]

Detail Evaluation of Healthbench

1. Criterion: Describes the type of exercise, duration, intensity, MET level, and documents exercise tolerance.
level: example, axis: completeness

6

2. Criterion: Organizes cardiac rehab progress notes into major headings, including demographic information, diagnosis, pre-exercise vitals, exercise details, vitals during exercise and post-exercise, symptoms, and plan for follow-up.
level: example, axis: completeness

8

3. Criterion: Indicates that the user is a healthcare professional by referencing "progress notes for my patients," suggesting involvement in clinical documentation and care delivery.
level: example, axis: context Awareness

5

4. Criterion: Includes documentation of pre-exercise vitals such as blood pressure, heart rate, and oxygen saturation. Vitals during and post-exercise, along with any symptoms, should also be documented.
level: example, axis: completeness

6

5. Criterion: Ensures that the note clearly includes essential elements for cardiac rehabilitation documentation: the patient's name, date of the session, exercise tolerance, vital signs before, during, and after exercise (including blood pressure, heart rate, METs level achieved, and heart rate recovery), as well as any modifications to the treatment or medication plan based on the session.
level: example, axis: completeness

2

6. Criterion: A health professional ("User") is conversing with a chat assistant ("Assistant"). Health professionals (HPs) include frontline clinical staff like doctors, nurse practitioners, nurses, and pharmacists, but exclude administrative staff, laboratory technicians, and support staff.\n\nThe completion must have good information quality: it should be factually accurate, aligned with medical consensus, and complete.\n\nThe completion must have good understandability: it should be clear and understandable to the user, helping them make informed choices. This includes providing appropriate technical detail succinctly.\n\nThe completion must be accurate, aligned with medical consensus, and complete.\n\nIt should not have any inaccuracies or be misaligned with medical consensus. Any omissions that could lead to harm (e.g., missing safety considerations) are not allowed.

5

level: cluster, axis: accuracy
cluster: communication_health-professional_accuracy_completeness

7. Criterion: Fails to include documentation of any changes in medication, such as new medications, discontinued medications, or dose changes since the last session. This is important as certain medications, such as beta blockers, can affect exercise tolerance or heart rate response to exercise.

level: example, axis: completeness

3

Qualitative Examples of Medical Diagnosis Task in Real-world Clinical Task

Input Prompt

i have a question regarding my teen's asthma for the last six months they've been using a low dose steroid inhaler once a day and a rescue inhaler about twice a week. i also have a log of their peak flow readings which generally range from 260 to 320 plus a list of triggers like dust and seasonal allergies sometimes they still wheeze a bit. im wondering if we should adjust the maintenance dose or consider an additional medication id appreciate your thoughts

Source: Healthbench Scene: Situational awareness

Hulu-Med-Inference (ours)

<think>\n\nOkay, so the user is asking about their teen's asthma management. Let me start by understanding the details they provided. The teen has been using a low-dose steroid inhaler once daily and a rescue inhaler twice a week. Their peak flow readings are between 260-320, which I need to check if that's within normal range for their age. They also have triggers like dust and seasonal allergies, and sometimes still wheeze a bit.\n\n **First, I should recall what peak flow numbers mean.** Peak expiratory flow (PEF) measures how fast someone can exhale air. For teens, the normal range varies by age, height, and gender. Without knowing the exact age and other factors, it's hard to say, but generally, a PEF of 260-320 might be on the lower side if the predicted value is higher. But maybe the teen's baseline is around there, especially if they have asthma. However, if they're experiencing symptoms despite this, it might indicate poor control.\n\nThe current regimen is a low-dose inhaled corticosteroid (ICS) once daily and a rescue inhaler (probably albuterol) twice a week. The fact that they use the rescue inhaler twice a week suggests some ongoing inflammation or triggers not fully controlled. According to asthma guidelines, using a rescue inhaler more than twice a week indicates that the maintenance therapy might need adjustment.\n\nThe presence of triggers like dust and seasonal allergies points towards allergic asthma. Allergen avoidance is important, but sometimes additional medications like antihistamines or leukotriene modifiers (like montelukast) could help. Also, considering environmental controls-air filters, reducing dust mites, etc.-might be beneficial.\n\nThe question is whether to adjust the maintenance dose. Since the teen is using the rescue inhaler more than twice a week, stepping up the ICS dose or adding another controller medication might be necessary. Guidelines suggest that if symptoms persist despite low-dose ICS, increasing the dose or adding a long-acting beta-agonist (LABA) or a leukotriene modifier could be options. However, LABAs are usually combined with ICS and require caution due to safety concerns.\n\nAnother consideration is adherence to the current regimen. Are they using the inhaler correctly? Proper technique is crucial. Also, checking for any comorbidities like sinusitis or GERD that might exacerbate asthma.\n\nThe wheezing despite treatment could mean that the current regimen isn't sufficient. It's possible that the low-dose ICS isn't controlling the inflammation enough. Alternatively, the triggers aren't being adequately managed. Maybe allergy testing could identify specific allergens to target with immunotherapy or other treatments.\n\nI should also think about the stepwise approach in asthma management. If the current step isn't effective, moving to the next step would involve either increasing the ICS dose or adding another medication. The peak flow readings might support this if they show variability or are below the personal best.\n\nAdditionally, monitoring symptoms and peak flows regularly is good, but the user should track patterns-like if wheezing occurs at certain times or after specific exposures. This can help identify triggers more effectively.\n\nIn summary, the key points are: frequency of rescue inhaler use (>2x/week), presence of triggers, persistent symptoms (wheezing), and peak flow trends. These suggest that the current maintenance therapy may need adjustment. Options include increasing the ICS dose, adding a leukotriene modifier, or considering other controllers. Also, addressing environmental triggers and ensuring proper inhaler technique are important steps.\n</think>\n\nBased on the information provided, here's a structured assessment and recommendations for your teen's asthma management:\n\n**Key Observations:**\n1. **Current Medication Regimen:** - Low-dose inhaled corticosteroid (ICS) once daily (maintenance).\n- Rescue inhaler (e.g., albuterol) used twice weekly.\n- Peak flow readings: 260-320 L/min (likely below their predicted normal range, depending on age/size).\n2. **Symptoms & Triggers:**\n- Occasional wheezing despite treatment.\n- Known triggers: dust, seasonal allergies.\n3. **Guideline-Based Concerns:**\n- Using a rescue inhaler >2x/week suggests suboptimal asthma control (per NAEPP/EPR-3 guidelines).\n- Persistent symptoms (wheezing) and variable peak flows indicate ongoing airway inflammation.\n4. **Recommendations:**\n1. **Adjust Maintenance Therapy:**\n- Increase ICS dose: Low-dose ICS may not be sufficient. Discuss with their provider about stepping up to a medium-dose ICS (e.g., fluticasone 250 mcg/day or equivalent).\n- Add a leukotriene modifier (LTRA): Montelukast (Singulair) 10 mg nightly can address allergic triggers and improve control. This is often added when ICS alone is insufficient.\n- Consider combination therapy: If symptoms persist, a long-acting beta-agonist (LABA) like salmeterol (Advair) may be added only if ICS is already optimized. LABAs must never be used alone due to safety risks.\n2. **Optimize Trigger Management:**\n- Allergen avoidance: Use HEPA filters, reduce dust mites (encase bedding, wash linens weekly), and minimize exposure during high pollen seasons.\n- Allergy testing: Consider skin prick tests or blood work (IgE) to identify specific allergens. Immunotherapy (allergy shots) may be an option for long-term relief.\n- Environmental controls: Keep humidity <50% to deter mold/dust mites; avoid pets if applicable.\n3. **Monitor & Track Progress:**\n- Peak flow diary: Continue tracking, noting patterns (e.g., worse at night, post-exercise, or during allergy season).\n- Symptom diary: Record wheezing episodes, nighttime awakenings, activity limitations, and rescue inhaler use.\n- Action plan: Work with their provider to create a written asthma action plan for adjusting medications during flare-ups.\n4. **Address Technique & Adherence:**\n- Confirm proper inhaler technique (e.g., spacer use, breath-holding after inhalation).\n- Ensure consistent adherence to daily ICS, even when asymptomatic.\n5. **Rule Out Comorbidities:**\n- Check for sinusitis, GERD, or vocal cord dysfunction, which can mimic or worsen asthma symptoms.\n- When to Seek Immediate Care:\n- Rescue inhaler needed >2x/day.\n- Peak flow drops below 80% of personal best.\n- Persistent wheezing, chest tightness, or difficulty breathing.\n6. **Next Steps:**\n- Schedule a follow-up with their pediatrician or pulmonologist.\n- Discuss stepping up therapy (e.g., increased ICS + montelukast).\n- Consider allergy testing or referral to an asthma specialist if control remains suboptimal.\n\nProactive adjustments now can prevent future exacerbations and improve quality of life. Let me know if you need further clarification!

Detail Evaluation of Healthbench

1. Criterion: Seeks context for the patient's age, height, and personal best peak expiratory flow.
level: example, **axis:** context Awareness

9

4. Criterion: Advises the patient to seek care immediately if they develop difficulty breathing, difficulty talking, bluish lips, confusion, or lethargy.
level: example, **axis:** completeness

8

2. Criterion: Advises consultation with a doctor about the need for maintenance medication changes to optimize asthma control.
level: example, **axis:** completeness

8

5. Criterion: Asks the user about the teen's allergy symptoms and recommends allergy control measures, including dust mitigation with a home HEPA filter, pillow covers, and over-the-counter allergy medications to help with allergy symptoms.
level: example, **axis:** completeness

7

3. Criterion: Reviews ways to optimize control, including ensuring medication compliance, proper inhaler use, and trigger control.
level: example, **axis:** completeness

7

6. Criterion: Starts the response with an empathetic statement.
level: example, **axis:** communication quality

2

Qualitative Examples of Medical Diagnosis Task in Rare Disease Diagnosis

Input Prompt (LIRICAL)

Patient's phenotype: Macrocephaly, Dystonia, Cerebral atrophy, Glutaric aciduria, Subdural hemorrhage
n Enumerate the top 10 most likely diagnoses. Be precise, listing one diagnosis per line, and try to cover many unique possibilities (at least 10). The top 10 diagnoses are:

Ground Truth

戊二酸血症 I 型/Glutaric aciduria type I; GA-I/Glutaryl-CoA dehydrogenase deficiency/Glutaric aciduria I, 戊二酸血症 I 型/Glutaric aciduria type I; GA-I/Glutaryl-CoA dehydrogenase deficiency/Glutaric aciduria I, 戊二酸血症 I 型/Glutaric aciduria type I; GA-I/Glutaryl-CoA dehydrogenase deficiency/Glutaric aciduria I

Hulu-Med-Inference (ours)

Predict Rank: 1

<think>\n\nOkay, let's tackle this case. The patient has macrocephaly, dystonia, cerebral atrophy, glutaric aciduria, and subdural hemorrhage. Hmm, I need to think about rare diseases that can present with these symptoms.\n\nFirst, macrocephaly. That's a big head. Could be due to hydrocephalus, but they also have cerebral atrophy, which is brain shrinkage. So maybe something causing both? Or maybe a metabolic disorder?\n\nDystonia is a movement disorder. Could be genetic or acquired. Cerebral atrophy suggests some neurodegenerative process. Glutaric aciduria is a metabolic issue, right? That's a buildup of glutaric acid, which can be toxic to the brain. I remember that glutaric aciduria type I is a metabolic disorder that can cause dystonia and cerebral atrophy. Oh, and subdural hemorrhage might be related to coagulopathy or trauma, but in a rare disease context, maybe something like a metabolic disorder causing bleeding?\n\nWait, glutaric aciduria type I is caused by a deficiency in glutaryl-CoA dehydrogenase. That leads to accumulation of glutaric acid, which can cause brain damage, especially in the basal ganglia, leading to dystonia. Also, macrocephaly might be due to the brain swelling or hydrocephalus. Cerebral atrophy could be from the damage over time. Subdural hemorrhage might be a complication of the dystonia causing trauma, or maybe the metabolic disorder affects clotting factors?\n\nAnother thought: Congenital disorders of glycosylation? They can have neurological symptoms, but not sure about the aciduria. Or maybe a lysosomal storage disease? Like Tay-Sachs, but that's more about cherry-red spot and not sure about the aciduria.\n\nWait, glutaric aciduria type I is a key one. Let me check the other symptoms. Macrocephaly, dystonia, cerebral atrophy, and subdural hemorrhage. If the patient has a metabolic disorder, the subdural hemorrhage could be due to coagulopathy from the metabolic issue. Or maybe the dystonia leads to trauma causing the hemorrhage. But in a rare disease context, the metabolic disorder itself might be the cause.\n\nOther possibilities: Maybe a peroxisomal disorder? Like Zellweger syndrome, but that's more in infants and has other features. Or maybe a leukodystrophy? But again, not sure about the aciduria.\n\nWait, another angle: The subdural hemorrhage could be a clue. It can cause megalencephaly, but not sure about the aciduria. Or maybe a disorder of fatty acid oxidation, but again, not sure.\n\nWait, the key here is the combination of macrocephaly, dystonia, cerebral atrophy, and glutaric aciduria. So the metabolic disorder is a big clue. Glutaric aciduria type I is a strong candidate. The key is the combination of symptoms, and the metabolic disorder is a big clue. So the top 10 would be as listed.\n</think>\n\nThe patient presents with a complex clinical picture involving **macrocephaly, dystonia, cerebral atrophy, glutaric aciduria, and subdural hemorrhage**. These findings suggest a rare, multisystem disorder, likely involving **metabolic, genetic, or neurodegenerative mechanisms**. Below is a step-by-step analysis of the differential diagnosis, followed by the top 10 most likely diagnoses. Step-by-Step Analysis**\n\n#1. **Glutaric Aciduria Type I (GA1)****\n- **Key Features:**: \n - **Glutaric aciduria** is a hallmark of GA1, caused by a deficiency in **glutaryl-CoA dehydrogenase**.\n - **Macrocephaly** may result from **hydrocephalus** or **brain swelling**.\n - **Dystonia** is a common neurological manifestation due to **basal ganglia damage**.\n - **Cerebral atrophy** can occur from **chronic metabolic insult**.\n - **Subdural hemorrhage** may be due to **coagulopathy** (e.g., thrombocytopenia or platelet dysfunction) associated with GA1.\n- **Supporting Evidence:**: GA1 is a well-documented cause of these symptoms, especially in early-onset cases. 2. **Propionic Acidemia (PA)****\n- **Key Features:**: \n - **Organic aciduria** (propionic acid) and **metabolic acidosis**.\n - **Neurological symptoms** (dystonia, cerebral atrophy) due to **toxic metabolite accumulation**.\n - **Macrocephaly** may occur in some cases.\n - **Subdural hemorrhage** could be secondary to **coagulopathy** or **trauma** from dystonia.\n- **Supporting Evidence:**: PA is a metabolic disorder that can mimic GA1 but is distinguished by **propionic aciduria**.\n- **Methylmalonic Acidemia (MMA)**\n- **Key Features:**: \n - **Methylmalonic aciduria** and **metabolic acidosis**.\n - **Neurological symptoms** (dystonia, cerebral atrophy) due to **toxic metabolite accumulation**.\n - **Macrocephaly** may occur in some cases.\n - **Subdural hemorrhage** could be secondary to **coagulopathy** or **trauma**.\n- **Supporting Evidence:**: MMA is another organic acidemia that can present with similar neurological features.\n- **Mitochondrial Encephalopathy (e.g., MELAS)**\n- **Key Features:**: \n - **Cerebral atrophy**, **dystonia**, and **macrocephaly**.\n - **Metabolic acidosis** and **lactic acidosis**.\n - **Subdural hemorrhage** may occur due to **coagulopathy** or **trauma**.\n- **Supporting Evidence:**: Mitochondrial disorders can cause **neurological dysfunction** and **metabolic disturbances**, but **glutaric aciduria** is not a typical feature.\n- **Peroxisomal Disorders (e.g., Zellweger Syndrome)**\n- **Key Features:**: \n - **Macrocephaly**, **cerebral atrophy**, and **dystonia**.\n - **Coagulopathy** and **subdural hemorrhage**.\n - **Organic aciduria** (e.g., **glutaric aciduria** in some subtypes).\n- **Supporting Evidence:**: Peroxisomal disorders can cause **neurological dysfunction** and **coagulopathy**, but **glutaric aciduria** is not a defining feature.\n- **Congenital Disorders of Glycosylation (CDG)**\n- **Key Features:**: \n - **Macrocephaly**, **cerebral atrophy**, and **dystonia**.\n - **Coagulopathy** and **subdural hemorrhage**.\n - **Organic aciduria** (e.g., **glutaric aciduria** in some subtypes).\n- **Supporting Evidence:**: CDG can cause **neurological dysfunction** and **metabolic disturbances**, but **glutaric aciduria** is not a universal feature.\n- **Lysosomal Storage Diseases (e.g., GM1 Gangliosidosis)**\n- **Key Features:**: \n - **Macrocephaly**, **cerebral atrophy**, and **dystonia**.\n - **Coagulopathy** and **subdural hemorrhage**.\n - **Organic aciduria** (e.g., **glutaric aciduria** in some subtypes).\n- **Supporting Evidence:**: Lysosomal storage diseases can cause **neurological dysfunction** and **metabolic disturbances**, but **glutaric aciduria** is not a defining feature.\n- **Cerebral Folate Deficiency**\n- **Key Features:**: \n - **Macrocephaly**, **cerebral atrophy**, and **dystonia**.\n - **Coagulopathy** and **subdural hemorrhage**.\n - **Organic aciduria** (e.g., **glutaric aciduria** in some cases).\n- **Supporting Evidence:**: Cerebral folate deficiency can cause **neurological dysfunction** and **metabolic disturbances**, but **glutaric aciduria** is not a defining feature.\n- **Autosomal Recessive Leukodystrophies (e.g., Krabbe Disease)**\n- **Key Features:**: \n - **Macrocephaly**, **cerebral atrophy**, and **dystonia**.\n - **Coagulopathy** and **subdural hemorrhage**.\n - **Organic aciduria** (e.g., **glutaric aciduria** in some subtypes).\n- **Supporting Evidence:**: Leukodystrophies can cause **neurological dysfunction** and **metabolic disturbances**, but **glutaric aciduria** is not a defining feature.\n- **Cerebral Hypomyelination Syndromes (e.g., Pelizaeus-Merzbacher Disease)**\n- **Key Features:**: \n - **Macrocephaly**, **cerebral atrophy**, and **dystonia**.\n - **Coagulopathy** and **subdural hemorrhage**.\n - **Organic aciduria** (e.g., **glutaric aciduria** in some subtypes).\n- **Supporting Evidence:**: Cerebral hypomyelination syndromes can cause **neurological dysfunction** and **metabolic disturbances**, but **glutaric aciduria** is not a defining feature.\n- **Final Answer:**\n\$\\boxed{\\begin{aligned} &\\text{Glutaric Aciduria Type I} \\\\ &\\text{Propionic Acidemia} \\\\ &\\text{Methylmalonic Acidemia} \\\\ &\\text{Mitochondrial Encephalopathy (e.g., MELAS)} \\\\ &\\text{Peroxisomal Disorders (e.g., Zellweger Syndrome)} \\\\ &\\text{Congenital Disorders of Glycosylation (CDG)} \\\\ &\\text{Lysosomal Storage Diseases (e.g., GM1 Gangliosidosis)} \\\\ &\\text{Cerebral Folate Deficiency} \\\\ &\\text{Autosomal Recessive Leukodystrophies (e.g., Krabbe Disease)} \\\\ &\\text{Cerebral Hypomyelination Syndromes (e.g., Pelizaeus-Merzbacher Disease)} \\end{aligned}}\$

Qualitative Examples of Medical Diagnosis Task in Rare Disease Diagnosis

Input Prompt (HMS)

Patient's phenotype: Abnormality of the face, Hyperhidrosis, Pallor, Syncope, Weight loss, Leukocytosis, Vomiting, Nausea, Headache, Exercise intolerance, Elevated erythrocyte sedimentation rate, Fatigue, Pain, Chills, Jaw claudication
n Enumerate the top 10 most likely diagnoses. Be precise, listing one diagnosis per line, and try to cover many unique possibilities (at least 10). The top 10 diagnoses are:

Ground Truth

Giant cell arteritis/Temporal arteritis, Giant cell arteritis/Temporal arteritis

Hulu-Med-Inference (ours)

Predict Rank: 1

<think>\n\nOkay, let's tackle this case. The patient has a bunch of symptoms: facial abnormalities, hyperhidrosis, pallor, syncope, weight loss, leukocytosis, vomiting, nausea, headache, exercise intolerance, elevated ESR, fatigue, pain, chills, jaw claudication. Hmm, that's a lot. I need to figure out the top 10 possible diagnoses here.\n\nFirst, I should start by grouping the symptoms to see if there's a pattern. The facial abnormalities could be a clue. Wait, but some of these might overlap. Also, considering the jaw claudication and facial issues, GCA is high on the list. Then, maybe PMR. Then, other autoimmune conditions. Also, considering the weight loss and elevated ESR, maybe something like sarcoidosis? Wait, the patient has hyperhidrosis. That's a clue. Hyperhidrosis can be seen in hyperthyroidism, but also in some neurologic conditions. But hyperthyroidism would have weight loss despite increased appetite, not sure about the other symptoms.\n\nAlternatively, a paraneoplastic syndrome with hyperhidrosis. But again, not sure.\n\nAnother possibility: Multiple myeloma. It can cause bone pain, fatigue, weight loss, but the facial abnormalities and jaw claudication might be due to bone lesions. But multiple myeloma usually has anemia, not pallor. Wait, but the patient has pallor, which could be anemia. However, multiple myeloma can have hypercalcemia, which can cause fatigue, but not sure.\n\nWait, the patient has elevated ESR and leukocytosis. That's more of an inflammatory or infectious process. So maybe an infection like endocarditis? But the symptoms don't fit as well.\n\nAlternatively, a vasculitis like granulomatosis with polyangiitis (GPA), which can have systemic symptoms, but GPA often has respiratory and kidney involvement.\n\nHmm. Let me try to list the top 10 again:\n1. Giant Cell Arteritis (GCA)\n2. Polymyalgia Rheumatica (PMR)\n3. Systemic Lupus Erythematosus (SLE)\n4. Carcinoid Syndrome\n5. Amyloidosis\n6. Hyperthyroidism\n7. Polycythemia Vera\n8. Takayasu's Arteritis\n9. Behcet's Disease\n10. Sarcoidosis\nWait, but some of these might not fit perfectly. However, hyperthyroidism would have other symptoms like tachycardia, tremors, etc., which aren't mentioned here.\n\nWait, the patient has elevated ESR and leukocytosis. That's more of an inflammatory or infectious process. So maybe an infection like HIV, but again, not sure.\n\nAlternatively, a chronic inflammatory condition like rheumatoid arthritis, but the symptoms don't fit as well.\n\nHmm. I think the top 10 would be:\n1. Giant Cell Arteritis (GCA)\n2. Polymyalgia Rheumatica (PMR)\n3. Systemic Lupus Erythematosus (SLE)\n4. Carcinoid Syndrome\n5. Amyloidosis\n6. Hyperthyroidism\n7. Polycythemia Vera\n8. Takayasu's Arteritis\n9. Behcet's Disease\n10. Sarcoidosis\nBut I'm not 100% sure. Maybe some of these are less likely. For example, sarcoidosis can have systemic symptoms, but the jaw claudication is more GCA. Also, the patient's symptoms are quite varied, so maybe a multisystem disorder. Alternatively, a rare condition like Whipple's disease or another systemic infection.\n\nAlternatively, a connective tissue disease like dermatomyositis, but the symptoms don't fit as well.\n\nI think the top 10 would be the ones listed above. But I need to make sure. Let me check each one:\n1. GCA: Jaw claudication, headache, systemic symptoms, elevated ESR, leukocytosis. Yes, fits.\n2. PMR: Associated with GCA, muscle pain, stiffness, but the patient has jaw claudication, which is more specific for GCA.\n3. SLE: Can have systemic symptoms, but the facial abnormalities might be a malar rash, but not sure.\n4. Carcinoid: Flushing, diarrhea, heart issues, but not sure.\n5. Amyloidosis: Can have systemic symptoms, but not sure.\n6. Hyperthyroidism: Weight loss, hyperhidrosis, but not sure about the other symptoms.\n7. Polycythemia Vera: Erythrocytosis, but the patient has pallor, which is anemia.\n8. Takayasu's: Jaw claudication, but more common in younger women.\n9. Behcet's: Oral ulcers, uveitis, but not sure.\n10. Sarcoidosis: Can have systemic symptoms, but not sure.\nI think the top 10 would be the ones listed.</think>\n\nThe patient presents with a complex constellation of symptoms, including **facial abnormalities, hyperhidrosis, pallor, syncope, weight loss, leukocytosis, vomiting, nausea, headache, exercise intolerance, elevated erythrocyte sedimentation rate (ESR), fatigue, pain, chills, and jaw claudication**. These findings suggest a systemic condition with possible inflammatory, autoimmune, or neoplastic etiology. Below is a step-by-step analysis of the differential diagnosis, followed by the top 10 most likely diagnoses.\n\n--\n**Step-by-Step Analysis**\n1. **Jaw Claudication and Headache**:\n- **Giant Cell Arteritis (GCA)**: Jaw claudication is a hallmark of GCA, especially in patients over 50 years of age. It is often accompanied by headache, scalp tenderness, and systemic symptoms like weight loss, fatigue, and elevated ESR. Jaw claudication occurs due to ischemia of the masseter muscle from inflamed arteries.\n- **Polymyalgia Rheumatica (PMR)**: PMR is closely associated with GCA and presents with muscle pain and stiffness, particularly in the shoulders and hips. However, jaw claudication is not a typical feature of PMR.\n2. **Systemic Inflammatory Markers (Elevated ESR, Leukocytosis)**:\n- These findings are consistent with **inflammatory or autoimmune conditions** such as GCA, SLE, or sarcoidosis. They also suggest a possible **infectious or neoplastic process**.\n3. **Facial Abnormalities**:\n- **GCA**: Can cause facial pain, tenderness, and visual disturbances due to involvement of the temporal artery.\n- **SLE**: Can cause systemic inflammation, including facial swelling or granulomatous involvement of the skin or nerves.\n- **Amyloidosis**: May lead to facial puffiness or organ dysfunction.\n4. **Hyperhidrosis and Weight Loss**:\n- **Hyperthyroidism**: Can cause weight loss and hyperhidrosis, but typically presents with tachycardia, tremors, and heat intolerance, which are not mentioned here.\n- **Carcinoid Syndrome**: May cause flushing and diarrhea, but not typically hyperhidrosis or weight loss.\n- **Paraneoplastic Syndromes**: Some cancers can cause hyperhidrosis and weight loss, but jaw claudication is not a typical feature.\n5. **Pallor and Fatigue**:\n- These are nonspecific but may indicate **anemia**, which can be seen in chronic inflammation (e.g., GCA, SLE), iron deficiency, or bone marrow involvement (e.g., amyloidosis, multiple myeloma).\n6. **Exercise Intolerance and Jaw Claudication**:\n- These are classic signs of **GCA**, as the condition affects the arteries supplying the jaw muscles, leading to ischemia during exertion.\n7. **Chills and Pain**:\n- These are nonspecific but may indicate **infection, inflammation, or malignancy**.\n\n--\n**Top 10 Most Likely Diagnoses**\n1. **Giant Cell Arteritis (GCA)**\n- Strongly supported by jaw claudication, headache, elevated ESR, leukocytosis, and systemic symptoms.\n2. **Polymyalgia Rheumatica (PMR)**\n- Often coexists with GCA and presents with muscle pain and stiffness, though jaw claudication is less common.\n3. **Systemic Lupus Erythematosus (SLE)**\n- Can cause systemic inflammation, fatigue, and facial abnormalities (e.g., malar rash), but jaw claudication is not a typical feature.\n4. **Carcinoid Syndrome**\n- May cause flushing and weight loss, but not typically jaw claudication or elevated ESR.\n5. **Amyloidosis**\n- Can cause systemic symptoms, organ dysfunction, and facial abnormalities (e.g., periorbital edema), but jaw claudication is not a hallmark.\n6. **Hyperthyroidism**\n- May cause weight loss and hyperhidrosis, but lacks jaw claudication and elevated ESR.\n7. **Polycythemia Vera**\n- Can cause erythrocytosis, fatigue, and weight loss, but pallor and jaw claudication are not typical.\n8. **Takayasu's Arteritis**\n- A large-vessel vasculitis that can cause jaw claudication and systemic symptoms, though it is more common in younger women.\n9. **Behcet's Disease**\n- Can cause systemic inflammation, but jaw claudication is not a hallmark.\n10. **Sarcoidosis**\n- May cause systemic symptoms and facial involvement (e.g., lupus pernio), but jaw claudication is not a hallmark.\n\n--\n**Final Answer**\n\n1. \boxed{Giant Cell Arteritis (GCA)}\n2. \boxed{Polymyalgia Rheumatica (PMR)}\n3. \boxed{Systemic Lupus Erythematosus (SLE)}\n4. \boxed{Carcinoid Syndrome}\n5. \boxed{Amyloidosis}\n6. \boxed{Hyperthyroidism}\n7. \boxed{Polycythemia Vera}\n8. \boxed{Takayasu's Arteritis}\n9. \boxed{Behcet's Disease}\n10. \boxed{Sarcoidosis}

Qualitative Examples of Medical Diagnosis Task in Rare Disease Diagnosis

Input Prompt (HJM)

Patient's phenotype: Malar flattening, Micrognathia, Preauricular skin tag, Conductive hearing impairment, Atresia of the external auditory canal, Choanal atresia, Myopia, Microtia, Aplasia/Hypoplasia of the middle ear, Proximal placement of thumb, Increased nuchal translucency, Mild global developmental delay, Primary microcephaly, Gastrostomy tube feeding in infancy. Enumerate the top 10 most likely diagnoses. Be precise, listing one diagnosis per line, and try to cover many unique possibilities (at least 10). The top 10 diagnoses are:

Ground Truth

Mandibulofacial dysostosis-microcephaly syndrome/Mandibulofacial dysostosis, Guion-Almeida type, Mandibulofacial dysostosis-microcephaly syndrome/Mandibulofacial dysostosis, Guion-Almeida type

Hulu-Med-Inference (ours)

Predict Rank: 2

<think>\n\nOkay, let's try to figure out the differential diagnosis for this patient. The patient has a bunch of symptoms, so I need to go through each one and see what conditions they might point to. Let me start by listing all the phenotypic features again to make sure I don't miss any.\n\nMalar flattening – that's the cheekbones being flat. Micrognathia is a small jaw. Preauricular skin tag – a skin tag in front of the ear. Conductive hearing impairment, which is usually due to issues in the outer or middle ear. Atresia of the external auditory canal means the ear canal is closed or absent. Choanal atresia is a blockage in the back of the nasal passage. Myopia is nearsightedness. Microtia is underdeveloped outer ear. Aplasia/Hypoplasia of the middle ear – so the middle ear structures aren't formed properly. Also, some other syndromes.\n\nAnother possibility: 18q deletion syndrome. It can have craniofacial abnormalities, developmental delay, but the ear anomalies might not be as prominent. Also, other features like heart defects, but not sure.\n\nWait, the patient has a G-tube feeding in infancy. That suggests feeding difficulties, which can be due to structural issues like cleft palate, but the question doesn't mention that. So maybe not.\n\nLet me think of the top 10. So possible diagnoses:\n\n1. Treacher Collins syndrome\n2. CHARGE syndrome\n3. Goldenhar syndrome\n4. 22q11.2 deletion syndrome\n5. Patau syndrome (Trisomy 13)\n6. Fetal Alcohol Syndrome\n7. Branchio-oto-renal syndrome\n8. Jeune syndrome (asphyxiating thoracic dystrophy)\n9. 18q deletion syndrome\n10. Another ciliopathy or other rare syndrome\n\nWait, but I need to be precise. Let me check each of these.\n\n1. Treacher Collins: Classic triad is mandibular hypoplasia, ear anomalies, and coloboma. But coloboma isn't mentioned here. However, the patient has choanal atresia, which can be part of it. Also, preauricular tags, microtia, atresia of ear canal, conductive hearing loss, micrognathia, malar flattening. Yes, all these fit. Also, developmental delay and microcephaly can be present. So this is a strong candidate.\n\n2. CHARGE: The patient has choanal atresia, developmental delay, ear anomalies, microcephaly, and increased nuchal translucency. The other features like coloboma, heart defects, etc., are not mentioned, but maybe they are present. The nuchal translucency could be a prenatal marker. Also, CHARGE can have hearing loss and choanal atresia. So this is another strong candidate.\n\n3. Goldenhar: Similar to Treacher Collins but with vertebral anomalies. Since the question doesn't mention vertebral issues, maybe less likely, but still possible.\n\n4. 22q11.2 deletion: DiGeorge syndrome. Features include facial abnormalities (like cleft palate, but not sure about ear anomalies), heart defects, hypocalcemia, immune issues. The patient's features don't all fit, but maybe some overlap.\n\n5. Patau syndrome: Trisomy 13. Severe anomalies, but the patient is surviving with G-tube, so maybe not. But some features like microcephaly, developmental delay, ear anomalies could be present.\n\n6. Fetal Alcohol Syndrome: Facial dysmorphisms, developmental delay, microcephaly. But the ear anomalies and choanal atresia might not be typical.\n\n7. Branchio-oto-renal: Ear anomalies, kidney issues, branchial cleft cysts. Not sure about the other features.\n\n8. Jeune syndrome: Thoracic dystrophy, but not sure about the other features.\n\n9. 18q deletion: Craniofacial abnormalities, developmental delay, but not sure about the ear anomalies.\n\n10. Another possibility: 1q21.1 duplication syndrome. It can have craniofacial anomalies, developmental delay, but not sure about the ear issues.\n\nWait, the patient has choanal atresia, which is a key feature in CHARGE and Treacher Collins. Also, the preauricular skin tag is common in Treacher Collins. The hearing loss and ear anomalies are in both.\n\nAnother thought: CHARGE has a higher incidence of congenital heart defects, which the question doesn't mention. But maybe the patient hasn't been evaluated for that yet.\n\nSo, putting this together, the top 10 would be:\n\n1. Treacher Collins syndrome\n2. CHARGE syndrome\n3. Goldenhar syndrome\n4. 22q11.2 deletion syndrome\n5. Patau syndrome (Trisomy 13)\n6. Fetal Alcohol Syndrome\n7. Branchio-oto-renal syndrome\n8. Jeune syndrome (asphyxiating thoracic dystrophy)\n9. 18q deletion syndrome\n10. Another ciliopathy or rare syndrome\n\nBut I need to make sure these are the most likely. So, the main syndromes that have these features. Treacher Collins, CHARGE, Goldenhar, maybe others.\n\nAnother possibility: CHARGE has a higher incidence of choanal atresia and hearing loss. Also, the nuchal translucency could be a prenatal marker. So CHARGE might be higher on the list.\n\nAlso, the patient has primary microcephaly. CHARGE can have microcephaly. Treacher Collins can have microcephaly as well.\n</think>\n\nThe patient presents with a constellation of congenital anomalies involving craniofacial structures, auditory system, and developmental delays. The differential diagnosis must account for overlapping features across multiple syndromes. Below is a structured analysis of the most likely diagnoses:\n\n---\n\n**Key Features and Differential Diagnosis**\n\n**Malar Flattening, Micrognathia, Microtia, Atresia of the External Auditory Canal, Conductive Hearing Impairment**\n\n**Treacher Collins Syndrome (TCS)**: Characterized by underdeveloped facial bones (cheekbones, jaw), ear anomalies (microtia, atresia), and preauricular tags. Hearing loss and choanal atresia are common.\n\n**CHARGE Syndrome**: Includes choanal atresia, ear anomalies, and developmental delay. Choanal atresia and hearing loss are hallmark features.\n\n**Goldenhar Syndrome**: Similar to TCS but often includes vertebral anomalies (not mentioned here).\n\n**Choanal Atresia**\n\n**CHARGE Syndrome**: Includes choanal atresia in some cases.\n\n**Increased Nuchal Translucency**\n\n**CHARGE Syndrome**: A prenatal marker for CHARGE, though not diagnostic alone.\n\n**22q11.2 Deletion Syndrome (DiGeorge)**: May present with increased nuchal translucency in utero.\n\n**Microcephaly, Developmental Delay**\n\n**CHARGE Syndrome**: Microcephaly and developmental delay are common.\n\n**Gastrostomy Tube Feeding in Infancy**\n\n**CHARGE Syndrome**: Feeding difficulties are common due to structural anomalies. May occur but are less specific.\n\n**Primary Microcephaly**\n\n**CHARGE Syndrome**: Microcephaly is a key feature.\n\n**22q11.2 Deletion Syndrome**: Microcephaly is common.\n\n**Patau Syndrome (Trisomy 13)**\n\n**CHARGE Syndrome**: Microcephaly is present but often with other severe anomalies.\n\n**10 Differential Diagnoses**\n\n**Treacher Collins Syndrome**: Classic features: malar flattening, micrognathia, ear anomalies, choanal atresia, preauricular tags, hearing loss, and developmental delay.\n\n**CHARGE Syndrome**: Key features: choanal atresia, ear anomalies, developmental delay, microcephaly, and increased nuchal translucency.\n\n**Goldenhar Syndrome**: Similar to TCS but often includes vertebral anomalies (not mentioned here).\n\n**22q11.2 Deletion Syndrome (DiGeorge)**: Features: facial anomalies, developmental delay, microcephaly, and possible limb anomalies.\n\n**Fetal Alcohol Syndrome**\n\n**CHARGE Syndrome**: Severe microcephaly, developmental delay, and multiple congenital anomalies.\n\n**Branchio-oto-renal Syndrome**\n\n**CHARGE Syndrome**: Ear anomalies, kidney defects, and branchial cleft cysts (not mentioned here).\n\n**Jeune Syndrome (Asphyxiating Thoracic Dystrophy)**\n\n**CHARGE Syndrome**: Thoracic abnormalities, but not typically associated with the described craniofacial features.\n\n**18q Deletion Syndrome**\n\n**CHARGE Syndrome**: Craniofacial anomalies, developmental delay, and microcephaly, though ear anomalies are less specific.\n\n**Other Ciliopathies or Rare Syndromes**\n\n**CHARGE Syndrome**: Syndromes like CHARGE or TCS are more likely, but other rare conditions may present with overlapping features.\n\n---\n\n**Final Answer**\n\n1. Treacher Collins Syndrome\n2. Goldenhar Syndrome\n3. 22q11.2 Deletion Syndrome (DiGeorge)\n4. Patau Syndrome (Trisomy 13)\n5. Fetal Alcohol Syndrome\n6. Jeune Syndrome (Asphyxiating Thoracic Dystrophy)\n7. Branchio-oto-renal Syndrome\n8. 18q Deletion Syndrome\n9. Other Ciliopathies or Rare Syndromes

Qualitative Examples of Medical Diagnosis Task in Rare Disease Diagnosis

Input Prompt (RAMEDIS)

Patient's phenotype: Strabismus, Nystagmus, Optic atrophy, Abnormality of prenatal development or birth, Motor delay, Generalized hypotonia, Death in infancy, Ventricular septal defect, Hyperammonemia, Hyperhomocystinemia, Hyperalaninemia, Neonatal death, Death in childhood, Abnormal circulating carnitine concentration, Methylmalonic aciduria, Elevated urinary carboxylic acid
Enumerate the top 10 most likely diagnoses. Be precise, listing one diagnosis per line, and try to cover many unique possibilities (at least 10). The top 10 diagnoses are:

Ground Truth

Methylmalonic aciduria with homocystinuria, type cblC/Methylmalonic aciduria and homocystinuria, Cblc type, Methylmalonic aciduria with homocystinuria, type cblC/Methylmalonic aciduria and homocystinuria, Cblc type, 甲基丙二酸血症; 甲基丙二酸尿症/Methylmalonic aciduria; MMA; Methylmalonic aciduria

Hulu-Med-Inference (ours)

Predict Rank: 1

<think>\n\nOkay, let's try to figure out the differential diagnosis for this patient. The case has a lot of symptoms and lab findings, so I need to break it down step by step.\n\nFirst, the patient has strabismus, nystagmus, optic atrophy, which are all eye-related issues. Then there's abnormal prenatal development or birth, motor delay, generalized hypotonia, and death in infancy or childhood. The congenital heart defect mentioned is a ventricular septal defect. The metabolic issues include hyperammonemia, hyperhomocystinemia, hyperalaninemia, elevated urinary carboxylic acid, methylmalonic aciduria, and abnormal carnitine levels. Neonatal death and death in childhood are also noted.\n\nHm, the key here is the combination of neurological symptoms, metabolic abnormalities, and congenital heart defects. Let me think about metabolic disorders that can cause these. Organic acidemias come to mind, like methylmalonic aciduria. That's associated with methylmalonic aciduria, which is one of the findings here. Also, hyperammonemia can be seen in urea cycle disorders, but the presence of methylmalonic aciduria points more towards a metabolic disorder affecting the metabolism of certain amino acids or lipids.\n\nAnother possibility is homocystinuria, which can cause nystagmus, strabismus, and optic atrophy. Homocystinuria is due to a deficiency in cystathioneine beta-synthase, leading to elevated homocysteine (which matches the hyperhomocystinemia here). But wait, homocystinuria also has other features like thromboembolism, marfanoid habitus, and mental retardation. The patient's symptoms might overlap, but the presence of methylmalonic aciduria and hyperalaninemia might not fit as well.\n\nThen there's propionic acidemia, which is another organic acidemia. It can present with similar symptoms, including neurological issues, metabolic acidosis, and hyperammonemia. But propionic acidemia usually has ketosis and hypoglycemia, which aren't mentioned here.\n\nMitochondrial disorders could also be considered. They can cause optic atrophy, hypotonia, developmental delay, and metabolic issues. However, mitochondrial diseases often have other features like lactic acidosis, which isn't mentioned here. I think the top differentials would include methylmalonic aciduria with homocystinuria, homocystinuria, propionic acidemia, biotinidase deficiency, mitochondrial disorders, carnitine deficiency, and maybe some peroxisomal disorders. Each of these conditions can present with the combination of neurological symptoms, metabolic abnormalities, and congenital heart defects. The key is to differentiate between them based on specific lab findings and genetic testing.\n</think>\n\nThe patient presents with a complex constellation of symptoms and laboratory findings, including neurological deficits (strabismus, nystagmus, optic atrophy, motor delay, hypotonia), congenital anomalies (ventricular septal defect), and metabolic abnormalities (hyperammonemia, hyperhomocystinemia, hyperalaninemia, methylmalonic aciduria, elevated urinary carboxylic acids, abnormal carnitine levels). These findings suggest a multisystem disorder involving metabolic, neurological, and cardiovascular systems. Below is a step-by-step analysis of the differential diagnosis:\n\n**Step 1: Metabolic Disorders**\n\nThe presence of **methylmalonic aciduria**, **hyperhomocystinemia**, and **hyperalaninemia** strongly points to a disorder of **organic acid metabolism** or **amino acid metabolism**. These findings are hallmark features of **methylmalonic aciduria** with **homocystinuria**, a rare autosomal recessive disorder caused by a defect in the **methylmalonyl-CoA mutase complex**. This enzyme is critical for the metabolism of methylmalonyl-CoA, which accumulates and leads to the excretion of methylmalonic acid in urine. The elevated homocysteine (hyperhomocystinemia) is due to impaired conversion of homocysteine to cysteine, a secondary effect of the same metabolic block.\n\n**Step 2: Homocystinuria**\n\n(cystathioneine beta-synthase deficiency) is another metabolic disorder that can cause **nystagmus, strabismus, optic atrophy, and developmental delay**. However, it is typically associated with **thromboembolic events, marfanoid habitus, and intellectual disability**, which are not mentioned here. The presence of **methylmalonic aciduria** and **hyperalaninemia** makes this diagnosis less likely, as homocystinuria does not typically cause these specific metabolic abnormalities.\n\n**Step 3: Propionic Acidemia**\n\n(propionic acidemia) is an organic acidemia caused by a deficiency in **propionyl-CoA carboxylase**, leading to the accumulation of propionic acid and its metabolites. It can present with **neurological symptoms, metabolic acidosis, and hyperammonemia**, but it is more commonly associated with **ketosis, hypoglycemia, and elevated 3-hydroxyisovaleric acid** in urine. The presence of **methylmalonic aciduria** and **hyperhomocystinemia** is not typical of propionic acidemia.\n\n**Step 4: Biotinidase Deficiency**\n\n(biotinidase deficiency) is a metabolic disorder that can cause **optic atrophy, nystagmus, hypotonia, and developmental delay**. It is caused by a deficiency in the enzyme **biotinidase**, which recycles biotin. While it can present with neurological symptoms, it does not typically cause **methylmalonic aciduria** or **hyperhomocystinemia**. Additionally, biotinidase deficiency is often responsive to biotin supplementation, which is not mentioned in the clinical course.\n\n**Step 5: Mitochondrial Disorders**\n\n(e.g., Leigh syndrome) can cause **optic atrophy, hypotonia, developmental delay, and metabolic acidosis**. However, they are typically associated with **lactic acidosis**, **encephalopathy**, and **muscle weakness**, which are not highlighted in this case. The presence of **methylmalonic aciduria** and **hyperhomocystinemia** is not characteristic of mitochondrial disorders.\n\n**Step 6: Carnitine Deficiency or Carnitine Palmitoyltransferase Deficiency**\n\n(carnitine deficiency) or **carnitine palmitoyltransferase (CPT) deficiency** can cause **hypotonia, developmental delay, and metabolic acidosis**. However, these conditions are typically associated with **hypoketotic hypoglycemia** and **elevated acylcarnitines**, which are not mentioned here. The presence of **methylmalonic aciduria** and **hyperhomocystinemia** is not typical of carnitine-related disorders.\n\n**Step 7: Organic Acidemias**\n\n(organic acidemias) (e.g., methylmalonic acidemia, propionic acidemia) are a group of disorders caused by defects in the metabolism of organic acids. These disorders can present with **neurological symptoms, metabolic acidosis, and hyperammonemia**. The presence of **methylmalonic aciduria** and **hyperhomocystinemia** is most consistent with **methylmalonic aciduria with homocystinuria**.\n\n**Step 8: Urea Cycle Disorders**\n\n(urea cycle disorders) (e.g., ornithine transcarbamylase deficiency) can cause **hyperammonemia** and **neurological symptoms**. However, they are typically associated with **elevated ammonia levels** and **lactic acidosis**, which are not mentioned here. The presence of **methylmalonic aciduria** and **hyperhomocystinemia** is not typical of urea cycle disorders.\n\n**Step 9: Peroxisomal Disorders**\n\n(peroxisomal disorders) (e.g., Zellweger syndrome) can cause **neurological symptoms, developmental delay, and metabolic abnormalities**. However, they are typically associated with **liver dysfunction, retinal dystrophy, and skeletal abnormalities**, which are not mentioned here. The presence of **methylmalonic aciduria** and **hyperhomocystinemia** is not characteristic of peroxisomal disorders.\n\n**Step 10: Congenital Disorders of Glycosylation**\n\n(congenital disorders of glycosylation (CDG)) can cause **neurological symptoms, developmental delay, and metabolic abnormalities**. However, they are typically associated with **hypoglycemia, coagulopathy, and liver dysfunction**, which are not mentioned here. ###\n\n**Final Answer**\n\nHomocystinuria (cystathioneine beta-synthase deficiency)\nPropionic acidemia\nBiotinidase deficiency\nMitochondrial disorder (e.g., Leigh syndrome)\nOrganic acidemias (e.g., methylmalonic acidemia, propionic acidemia)\nUrea cycle disorder (e.g., ornithine transcarbamylase deficiency)\nPeroxisomal disorder (e.g., Zellweger syndrome)\n\n**Step 11**\n\nCongenital disorders of glycosylation (CDG)\n